AFRL-HE-WP-TR-2007-0085

An Analysis of Vertebral Stress and BMD During +Gz Impact Accelerations

Hilary L. Gallagher

Oak Ridge Institute for Science and Education (ORISE)
1299 Bethel Valley Road
Oak Ridge TN 37830

John R. Buhrman
Chris E. Perry

Biosciences and Protection Division
Biomechanics Branch

Stephen E. Mosher

General Dynamics, AIS
5200 Springfield Pike, Suite 200
Dayton OH 45431-1289

Delano D. Wilson

88th Medical Group
Wright-Patterson AFB OH

April 2007
Final Report for May 2004 to April 2007

Air Force Research Laboratory
Human Effectiveness Directorate
Biosciences and Protection Division
Biomechanics Branch
Wright-Patterson AFB OH 45433-7947

NOTICE AND SIGNATURE PAGE

THIS REPORT HAS BEEN REVIEWED AND IS APPROVED FOR PUBLICATION IN ACCORDANCE WITH ASSIGNED DISTRIBUTION STATEMENT.

AFRL-HE-WP-TR-2007-0085

//SIGNED//	//SIGNED//
JOHN BUHRMAN, Work Unit Manager Biomechanics Branch	MARK M. HOFFMAN Biosciences & Protection Division Human Effectiveness Directorate Air Force Research Laboratory

REPORT DOCUMENTATION PAGE

Form Approved OMB No. 074-0188

1. REPORT DATE (DD-MMM-YYYY)	2. REPORT TYPE	3. DATES COVERED (From – To)
APRIL 2007	Final Report	May 2004 – April 2007

4. TITLE AND SUBTITLE

An Analysis of Vertebral Stress and BMD During +Gz Impact Accelerations

5a. CONTRACT NUMBER FA8650-04-D-6472

5b. GRANT NUMBER

5c. PROGRAM ELEMENT NUMBER 62202F

5d. PROJECT NUMBER 7184

5e. TASK NUMBER 02

5f. WORKUNIT NUMBER 12

6. AUTHOR(S)

Hilary L. Gallagher * John R. Buhrman **
Stephen E. Mosher *** Chris E. Perry **
Delano D. Wilson ****

7. PERFORMING ORGANIZATION NAME(S) AND ADDRESS(ES)

*ORISE
1299 Bethel Valley Road
Oak Ridge TN 37830

*** General Dynamics, AIS
5200 Springfield Pike, Ste 200
Dayton OH 45431-1289

****88th Medical Group
Air Force Material Command
Wright-Patterson AFB OH 45433

8. PERFORMING ORGANIZATION REPORT NUMBER

9. SPONSORING / MONITORING AGENCY NAME(S) AND ADDRESS(ES)

**Air Force Materiel Command
Air Force Research Laboratory
Human Effectiveness Directorate
Biosciences & Protection Division
Biomechanics Branch
Wright-Patterson AFB OH 45433

10. SPONSOR / MONITOR'S ACRONYM AFRL/HEPA

11. SPONSOR/MONITOR'S REPORT NUMBER(S) AFRL-HE-WP-TR-2007-0085

12. DISTRIBUTION / AVAILABILITY STATEMENT

Approved for public release; distribution is unlimited.

13. SUPPLEMENTARY NOTES

AFRL/WS-07-1792 approved by AFRL/PA on 3 Aug 07

14. ABSTRACT

The U.S. Air Force pilot population includes both males and females with an expanded range of anthropometric measurements. To address concerns that females and/or small and large individuals may be more at risk during ejections, a series of tests were conducted at the Air Force Research Laboratory (AFRL) to identify the effects of gender and size on vertebral stress and BMD. Twenty-two males and twenty-four females were tested at acceleration levels up to 10G on a vertical deceleration tower. The subjects' bone mineral density (BMD) and vertebral size at C2, C5, T12, L1, and L2 were measured by quantitative computed tomography (QCT). Vertebral loads and stresses were calculated at the five selected vertebrae for all subjects. As expected, vertebral sizes were significantly smaller for the female subjects when compared to the male subjects. No significant gender differences were found for BMD values except C2 which was 10% lower in females. Females have significantly higher vertebral stresses in the cervical vertebrae while no significant gender differences were found in the thoracic and lumbar vertebrae. Relationships between stress and weight, height, and sitting height were investigated for the five vertebrae. Correlations were found between stress and weight at T12, L1, and L2.

15. SUBJECT TERMS

Vertebral Stress, BMD, CSA, Vertebral Load

16. SECURITY CLASSIFICATION OF: a. REPORT	b. ABSTRACT	c. THIS PAGE	17. LIMITATION OF ABSTRACT	18. NUMBER OF PAGES	19a. NAME OF RESPONSIBLE PERSON:
U	U	U	SAR	114	John R. Buhrman
					19b. TELEPHONE NUMBER (Include area code)

Standard Form 298 (Rev. 8/98)
Prescribed by ANSI Std. Z39-18

THIS PAGE IS INTENTIONALLY LEFT BLANK

TABLE OF CONTENTS

LIST OF FIGURES

LIST OF TABLES

PREFACE

The impact tests and data analysis described in this report were accomplished by the Biomechanics Branch, Human Effectiveness Directorate of the Air Force Research Laboratory (AFRL/HEPA) at Wright-Patterson Air Force Base, Ohio. The test facility for this study was the Vertical Deceleration Tower (VDT). Testing support at AFRL/HEPA was provided by Dyncorp under contract F33601-96-DJ001. Engineering support was provided by General Dynamics under contract FA8650-04-D-6472 and the Oak Ridge Institute for Science and Education (ORISE) under contract AFRLHE9981MISC.

THIS PAGE IS INTENTIONALLY LEFT BLANK

.

INTRODUCTION

With the expanded weight and height requirements of the US Air Force pilot population and the integration of helmet mounted devices (HMD), Air Force researchers are concerned that females and individuals at the outer size extremes may be at increased risk of spinal injury during the abrupt accelerations experienced during aircraft ejections. Nearly 17% of current aviators are beyond previously set standards for weight and height [26]. These concerns are founded in part on studies showing that vertebral breaking strength, which has been shown to be a good indicator of human tolerance limits in acceleration environments [28], is significantly different for males and females [21]. These differences need to be investigated when establishing gender and body size differences as related to impact injury thresholds, particularly since the acceleration responses of males and females have been shown to be very similar [7,8]. Vertebral breaking strength and associated vertebral stress therefore would appear to be primary predictors of spinal injury, particularly in an ejection environment where large compressive spinal loading can occur during the catapult phase.

BACKGROUND

Vertebral breaking strength has been shown to be directly proportional to both bone mineral density (BMD) and vertebral size [4,14,31]. Also, the mechanical stress within a vertebra during axial compression has been shown to be inversely proportional to the cross-sectional area (CSA) of the bone, and directly proportional to the applied load [17], which is determined in part by the weight of the upper torso and head. It has also been demonstrated that the CSA of vertebral bodies may be as much as 25% smaller in females than in males when matched for age, vertebral body height, and vertebral bone density for a given vertebral level [17]. Although males have been shown to have larger vertebral CSA than females, the advantage of greater stability of the larger vertebral bodies in males is at least partially offset by increased loads due to their generally higher body weight [10,24]. The large upper-torso mass of large males and/or the small CSA of small females, when coupled with the high-g impact accelerations experienced in an ejection environment, could lead to increased vertebral stress and associated increased spinal injury risk for some of these individuals.

Since vertebral fractures have been shown to be a primary mode of serious ejection injury [22], any increase in vertebral stress due to the large impact accelerations experienced during the catapult phase could lead to a significant increase in injury potential. This can be observed in the frequency of compression fractures of the upper lumbar and lower thoracic vertebral bodies of individuals using aircraft ejection seats [33], as well as injuries to the cervical spine occurring between the C3-C7 segments, with compression fractures well documented at the C5-C7 levels [13]. During the catapult phase of aircraft ejections, spinal loads increase non-linearly with the applied seat acceleration resulting in the crewmember experiencing large amounts of vertebral stress during this period.

While a plethora of literature is available on the topic of vertebral bone strength, the literature weighs heavily towards the identification, prevention, and clinical management of osteoporosis. A small number of studies have previously measured height, weight, and vertebral body size. These measurements are typically performed on cadavers of older individuals [20]. Detailed anthropometric measurements and vertebral body parameters continue to be lacking in the young healthy pilot population. Furthermore, existing injury risk criteria were established with ejection data and experimental research using mostly average-size male subjects [5]. Little quantitative data is therefore available for the current expanded pilot population.

This study investigates the relative differences in the vertebral stress and BMD among males, females, and small and large individuals following exposure to a simulated ejection environment. The results will be used to identify anthropometric and gender risk factors, and to modify ejection models and injury criteria in order to ensure the deployment of safe ejection systems for the full aircrew population.

METHODS

CT Scans

Forty-six subjects (22 male and 24 female) were exposed to a series of vertical impact acceleration tests as well as quantitative computed tomography (QCT) scans. All subjects were volunteer members of the AFRL Impact Acceleration Test Panel at Wright-Patterson AFB, Ohio and provided written informed consent before participating. All subjects were active-duty military and were medically qualified through the completion of a medical screening process. Sixty anthropometric measurements were recorded for each subject by Anthrotech (Yellow Springs, Ohio) and made available through the AFRL Biodynamics Data Bank [6,9]. This study was reviewed and approved for human testing by the Wright Site Institutional Review Board (IRB) at Wright-Patterson AFB, Ohio.

Vertebral body slices and trabecular bone mineral density (BMD) measurements were obtained from the subjects using QCT. The scans were accomplished at the Wright-Patterson AFB Medical Center (74th Medical Group) using a GE HiSpeed Advantage CT scanning system. The measurements were obtained at mid-level C2, C5, T12, L1, and L2 using technique factors of 80 kVp, 140 mA, 10 mm slice thickness, and 1 second scan time. Lateral scan projection radiographs were obtained to accurately prescribe the slices through the aforementioned vertebral bodies (Figure 1). Anterior-posterior diameter (depth) and transverse diameter (width) measurements were obtained from the scans using the GE PACS Pathspeed Workstation, excluding the pedicles and posterior elements of the vertebrae from the measurements. Anterior, mid, and posterior height measurements of the vertebra were also obtained. The BMD measurements were made by QCT using a calibration reference phantom (Radiation Oncology Data Systems).

The measured diameters were used to calculate the vertebral CSA, assuming the CSA to approximate an ellipse (area = π * width/2 * depth/2) [32]. Use of the mid-vertebral CSA as the load-bearing area for calculation of vertebral stress is well documented [18,31]. The stress values were expressed as the vertebral load divided by the CSA. The mean vertebral height was calculated for each vertebral level by averaging the anterior, mid, and posterior location on the lateral plain radiographs of the subjects [27]. Vertebral Volume was obtained using the calculated CSA and the mean vertebral height (Volume = CSA * Mean Vertebral Height).

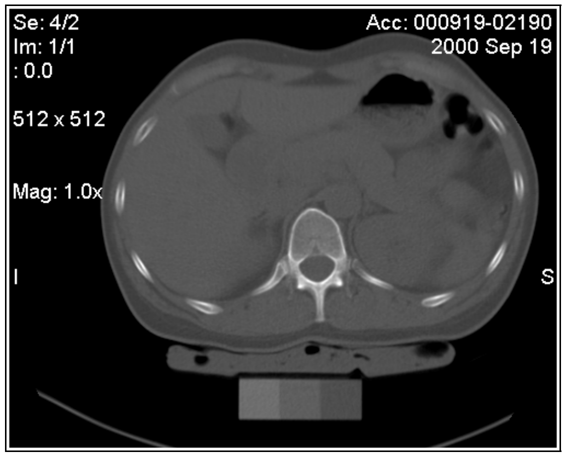

Figure 1. CT image showing cross-section of lumbar vertebra

VDT Impact Testing

A series of vertical impact acceleration tests were performed on the Vertical Deceleration Tower (VDT) (Figure 2) at Wright-Patterson Air Force Base, OH. The VDT is comprised of a carriage-mounted seat, guided by two vertical rails, which is released to a free-fall state from a predetermined height. The +Gz acceleration pulse is applied to the carriage when the plunger, mounted on the back of the carriage, is guided into a hydraulic decelerator between the two rails. When the water is displaced from the cylinder, the acceleration pulse is produced. The profile generated by the VDT is approximately a half-sine wave acceleration pulse with duration of 150 ms and a rise-time of 75 ms. Tests were conducted in a sequential manner with the order of acceleration level increasing as shown in Table 1, to ensure subject accommodation and safety.

Table 1. +Gz impact test matrix

Test Cell	**Acceleration Level (G)**	**Helmet**	**Plunger No.**	**Headrest Position**
A	6	HGU-55/P	102	0”
B	8	HGU-55/P	102	0”
C	10	HGU-55/P	102	0”
G	10	VWI	102	1” Aft

Figure 2. Air Force Research Laboratory VDT

The subjects were positioned in a generic seat mounted to the VDT carriage in an upright position. The seat back was parallel with the vertical rails while the seat pan was perpendicular to the seat back. The headrest was mounted in-line with the seat back for all cells with the exception of Cell G, which had a 1" aft shift. The subjects' were restrained using a standard MB-6 double shoulder harness and HBU lap belt. All restraint points were pre-tensioned to 20 ± 5 lbs. The subjects' thighs and wrists were loosely restrained by additional single straps. Each subject wore cut-off long underwear and a standard HGU-55/P flight helmet weighing approximately 2.2 pounds for the first three test conditions (Figure 3). A variable weighted impact (VWI) helmet was donned for the last test condition (Cell G). This helmet had no extra weights added and weighed approximately 3.0 pounds.

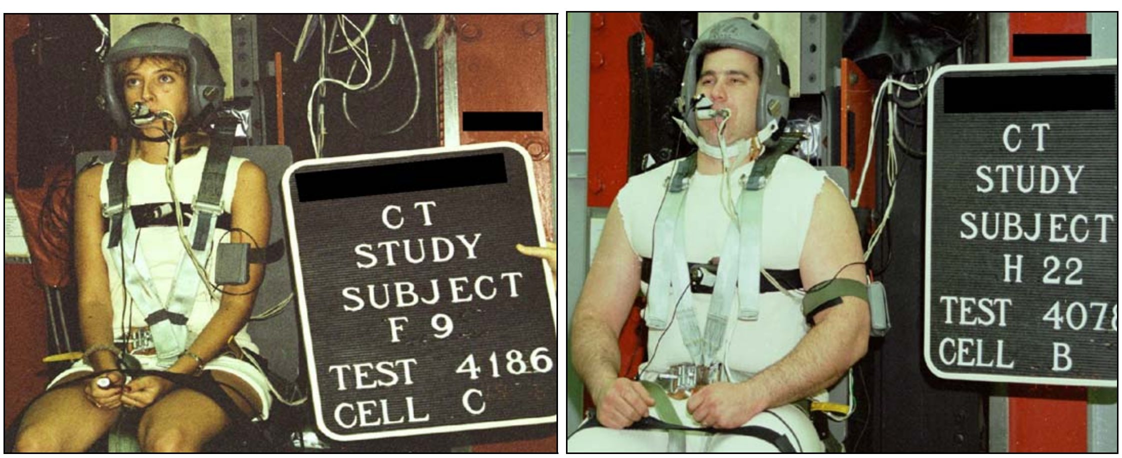

Figure 3. Subjects prior to impact test on VDT

Dynamic response data were collected at 1,000 samples per second by a Pacific Instruments on-board automatic data acquisition system that provided digitization and anti-aliasing filtering at 120 Hz using a low-pass 8-pole Butterworth filter. Seat accelerations and head and chest linear and angular accelerations were collected, with the head and chest z-axis linear accelerations being used to estimate the load on the cervical, thoracic, and lumbar sections of the spine.

Accelerations and Loads on Thoracic/Lumbar Spine

The subjects' chest acceleration responses were measured using a linear tri-axial accelerometer package that was firmly mounted to the chest using a Velcro strap. The use of chest acceleration to approximate thoracic vertebral compressive response has previously been demonstrated by Perry [25]. The z-axis chest accelerations (Chest Z) were corrected for small variations in the subjects' chest angle (Cell C only, Table 1) by combining the x and z components of the accelerometer output using $z(\cos\theta) + x(\sin\theta)$, where θ was the mean angle of the chest at the surface measured with respect to the vertical plane for each subject. The effect of small variations in the carriage input accelerations on chest acceleration response were normalized using the formula [(10G – Carriage Accel)/10G +1] * Chest Z Accel. The chest accelerations were combined with estimates of upper-torso mass obtained for each subject through the Generator of Body Data (GEBOD) computer model [19] to estimate the vertebral loading. This model uses thirty-two anthropometry measurements to calculate the mass of fifteen body segments. Seven of the fifteen body segments (head, neck, left/right upper arms, left/right lower arms, upper torso) were combined along with the mass of the helmet to estimate the upper-torso mass. The upper leg circumference measurement required by the GEBOD model was not recorded for a majority of the subjects; therefore the average between the thigh circumference and the knee circumference was used to estimate this parameter. The vertebral loading was then divided by the subjects' CSA to obtain the magnitude of thoracic and lumbar vertebral stress experienced during the impact tests.

Accelerations and Loads on Cervical Spine

The subjects' head acceleration responses (Head Z and Head X) were measured with a tri-axial accelerometer and angular accelerometer rigidly affixed to a bite bar. The head accelerations were normalized with respect to a constant carriage input acceleration as explained in the previous paragraph before being used to calculate the vertebral stress at the surface of C2 and C5 (again for Cell C only). An in-house software program (Neckload4) used the measured normalized linear accelerations and angular head accelerations and inertial properties of the helmet, head, and neck to estimate the resultant forces and moments experienced during vertical impact accelerations (See Appendix A). This program estimates the mass and center of mass of the helmet, head and neck and then combines them to find the total mass and the total center of mass of the system as a whole at both the C1/C2 junction and the C4/C5 junction of the cervical spine. The inertial properties of the helmet were previously measured using the methods described in a report by Albery *et al.*[1] and within the accuracies stated in AL-TR-1992-0137 [30]. The head mass was estimated using head circumference and body weight [12] while the segmented neck mass used neck circumference, body weight, and height depending on the gender [11,15,23,35,37]. The measured linear and angular head accelerations were used to compute the acceleration at the center of mass of the combined helmet, head and neck system [2,3]. The neck force was estimated based on the total mass, the acceleration at the center of mass, and on the equations of motion for rigid bodies. The measured head accelerations and calculated neck forces were reported in the head coordinate system (Figure 4). This neck force was divided by the vertebral CSA to estimate the cervical vertebral stress experienced during +Gz accelerations.

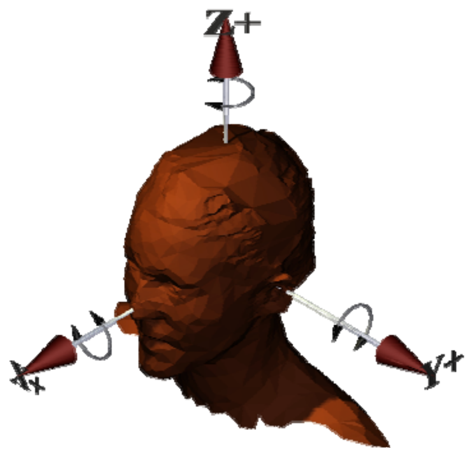

Figure 4. Anatomical axis system of the human head

Statistical Analysis

Bone mineral density (BMD), cross-sectional area (CSA), height, and volume were obtained from the QCT scans for C2, C5, T12, L1, and L2 of the vertebral spine. A comparison of genders was performed for each of these four factors at all five vertebral levels using a two-tailed, two-sample t-test. One-way ANOVA tests were also conducted to compare vertebral differences for both male and female subjects combined. The percent differences were calculated using the male subjects as the baseline gender. The vertebral properties, head and chest accelerations, loads, and vertebral stresses were examined for significant differences among varying parameters, including acceleration magnitudes, vertebral level, and gender. Linear regression modeling was also conducted to examine relationships between vertebral properties and factors such as weight, height, and sitting height.

RESULTS

A total of 253 vertical deceleration tests were evaluated for this study for Cells A, B and C. QCT scans and anthropometric measurements were taken for all subjects, 22 males and 24 females. Table 2 displays sample descriptive statistics for all 46 subjects.

Table 2. Descriptive statistics of subjects' anthropometry

	Male (n=22)			**Female (n=24)**		
	Min	**Max**	**Mean ± Std**	**Min**	**Max**	**Mean ± Std**
Age (years)	23	45	33.2 ± 6.0	20	39	26.1 ± 5.7
Height (mm)	1660	1903	1774 ± 67	1464	1789	1636 ± 72
Cervicale Height (mm)	1413	1649	1530 ± 62	1231	1559	1408 ± 70
Waist Height (mm)	975	1135	1065 ± 47	846	1090	980 ± 57
Sitting Height (mm)	867	1027	929 ± 37	793	925	869 ± 28
Weight (kg)	62	128	88.2 ± 16.2	49	79	62.3 ± 9.2
Head Circumference (mm)	538	600	574 ± 15	520	565	545 ± 14
Head Breadth (mm)	145	163	155 ± 5	135	157	147 ± 5
Head Length (mm)	188	212	200 ± 7	167	201	186 ± 8
Neck Circumference (mm)	354	450	395 ± 27	285	353	316 ± 20
Buttock Depth (mm)	214	311	261 ± 24	185	265	224 ± 21
Chest Circumference (mm)	911	1280	1067 ± 99	789	1063	917 ± 75
Chest Breadth (mm)	295	393	345 ± 31	247	340	288 ± 23
Waist Circumference (mm)	737	1157	957 ± 103	649	893	784 ± 65
Calf Circumference (mm)	342	458	393 ± 33	310	416	356 ± 26
Foot Length (mm)	250	290	269 ± 13	223	267	238 ± 11

Vertebral Properties

Bone Mineral Density (BMD)

Table 3 shows the mean BMD and standard deviations for male and female subjects along with the calculated percent difference between the genders and the t-test results. The BMD is also plotted in Figure 5. The female BMD was not significantly different from the male BMD at all vertebral levels except C2 where the males had significantly higher BMD ($\alpha = 0.05$). As expected, the cervical vertebrae demonstrated significantly higher BMD than the thoracic and lumbar vertebrae (≤ 0.001).

Table 3. Mean vertebral BMD (mg/cm^3)

Vertebra	**Males**	**Females**	**% Diff**	***p*-value**
C2	339.7 +/- 63.5	303.4 +/- 39.2	- 10.7 %	0.023
C5	339.8 +/- 46.2	350.2 +/- 51.2	+ 3.1 %	0.472
T12	192.2 +/- 21.1	197.2 +/- 28.8	+ 2.5 %	0.509
L1	186.3 +/- 25.1	194.0 +/- 27.7	+ 4.0 %	0.329
L2	183.4 +/- 24.4	188.8 +/- 27.1	+ 2.9 %	0.480

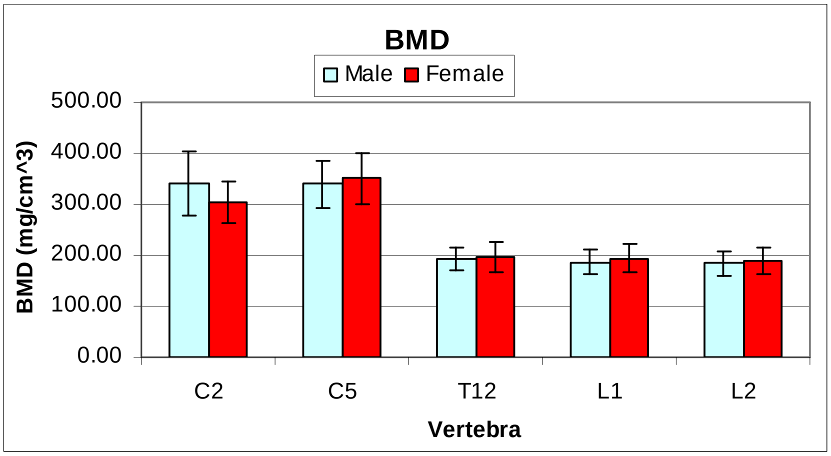

Figure 5. BMD of five vertebrae for males and females

BMD for the five selected vertebrae demonstrated weak correlations (< 0.45) as a function of weight, height, and sitting height. These were inconsistent across all vertebrae and across both genders and were therefore of limited value.

Cross-Sectional Area (CSA)

Mean values for vertebral CSA are shown in Table 4 and plotted in Figure 6. The male subjects had significantly larger CSA than the female subjects by approximately 20-25% for the five vertebrae examined. As expected, the CSA increased with descending vertebral levels for both males and females. The CSA of the thoracic and lumbar vertebrae was significantly larger than for the cervical vertebrae (≤ 0.001).

Table 4. Mean vertebral CSA (cm^2)

Vertebra	Males	Females	% Diff	*p*-value
C2	2.97 +/- 0.4	2.41 +/- 0.4	- 18.9 %	≤ 0.001
C5	3.35 +/- 0.5	2.55 +/- 0.3	- 23.9 %	≤ 0.001
T12	9.53 +/- 1.2	7.29 +/- 0.9	- 23.5 %	≤ 0.001
L1	9.92 +/- 1.1	7.33 +/- 0.8	- 26.1 %	≤ 0.001
L2	10.44 +/- 1.1	7.81 +/- 1.0	- 25.2 %	≤ 0.001

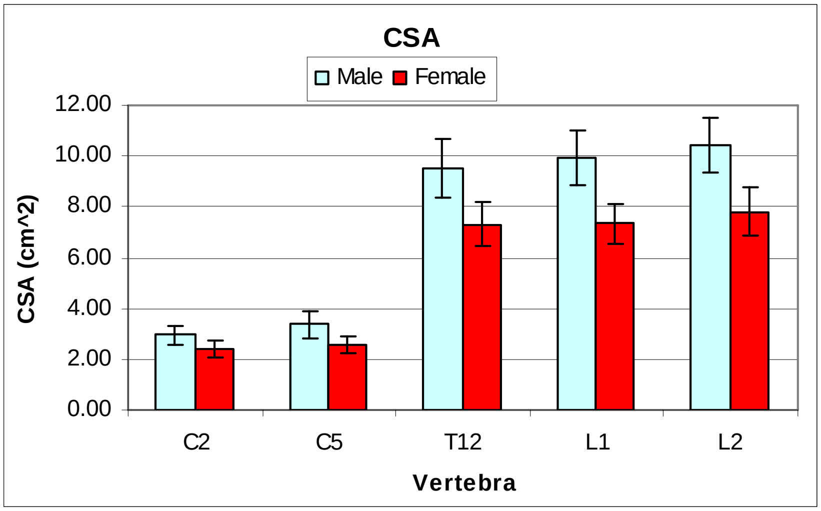

Figure 6. CSA of five vertebrae for males and females

The CSA at all vertebral levels demonstrated positive correlations with weight, height, and sitting height for all five vertebrae as shown in Table 5. In addition, the CSA of both cervical vertebrae showed positive correlations with head and neck circumferences. In general, the sitting height correlations were the most moderately consistent over all vertebrae (followed closely by height) and are plotted for C5 and L2, as shown in Figure 7. The results were similar for the other three vertebrae in the correlations with sitting height except for C2 CSA in females which revealed only a weak correlation. Moderate correlations were also found for male cervical CSA and for female thoracic and lumbar CSA as a function of weight. Also, moderate correlations were found for male cervical CSA as a function of neck circumference, and for female C2 CSA as a function of head circumference. When CSAs were recorded using the male and female regression lines at common sitting height (90 cm), height (170 cm), and weight (70 kg), the female CSA was found to be 12-15% lower at C5, and 15-20% lower at L2 than the males. The female CSA was also found to be 17% lower for common head circumference (56 cm) and 8% lower for common neck circumference (36 cm).

Table 5. Correlations of subject size versus CSA for five vertebrae

	Vertebrae									
	Male (r-value)					**Female (r-value)**				
Subject Size	**C2**	**C5**	**T12**	**L1**	**L2**	**C2**	**C5**	**T12**	**L1**	**L2**
Head Circumference (cm)	0.35	0.21	N/A	N/A	N/A	0.43	0.33	N/A	N/A	N/A
Neck Circumference (cm)	0.58	0.42	N/A	N/A	N/A	0.12	0.31	N/A	N/A	N/A
Weight (kg)	0.44	0.43	0.18	0.25	0.12	0.18	0.39	0.41	0.51	0.51
Height (cm)	0.33	0.46	0.51	0.52	0.51	0.21	0.48	0.56	0.60	0.58
Sitting Height (cm)	0.51	0.54	0.40	0.47	0.51	0.23	0.53	0.55	0.60	0.67

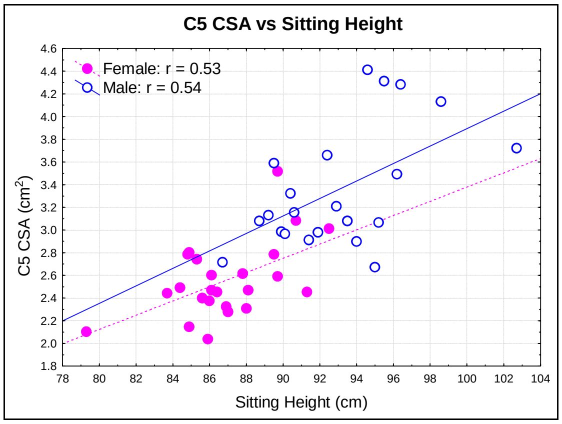

(a)

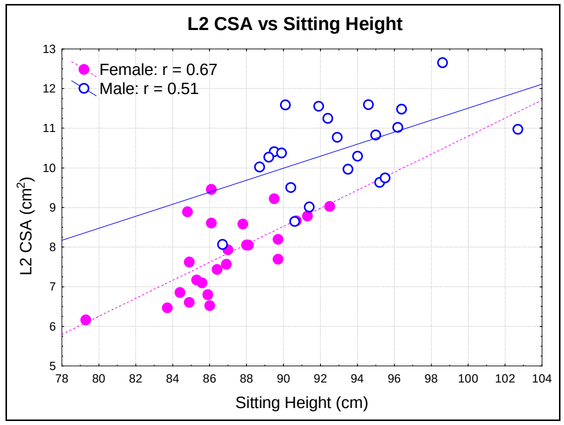

(b)

Figure 7. Scatterplot of (a) C5 CSA and (b) L2 CSA versus sitting height

Mean Vertebral Height

Mean vertebral height was calculated for C5, T12, L1, and L2 (no accurate height measurements for C2 could be obtained from the lateral radiographs). The male subjects were found to have significantly greater vertebral heights when compared to the female subjects (Table 6, Figure 8). As expected, the thoracic and lumbar vertebrae had significantly greater vertebral heights than the cervical vertebrae (≤ 0.001).

Table 6. Mean vertebral height (cm)

Vertebra	Males	Females	% Diff	*p*-value
C5	1.35 +/- 0.1	1.20 +/- 0.1	- 11.1 %	≤ 0.001
T12	2.56 +/- 0.2	2.42 +/- 0.2	- 5.5 %	0.004
L1	2.71 +/- 0.2	2.60 +/- 0.2	- 4.1 %	0.031
L2	2.79 +/- 0.2	2.68 +/- 0.2	- 3.9 %	0.021

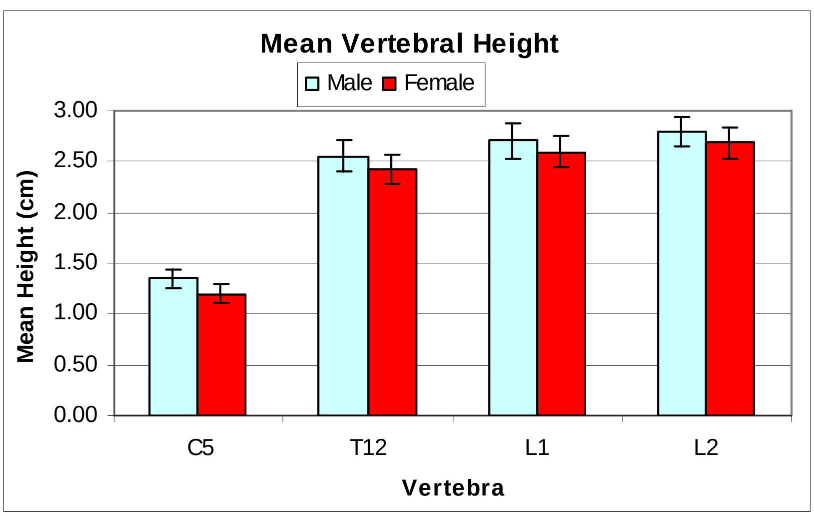

Figure 8. Mean vertebral height of four vertebrae for males and females

Vertebral Volume

Vertebral volume for each subject was estimated by multiplying the CSA (Table 4) by the average of the anterior, mid, and posterior heights as measured on the lateral plain radiograph (Table 6). Again there are no values calculated for C2 volume as explained above. The mean and standard deviations of the male and female vertebral volumes are listed in Table 7 and plotted in Figure 9. Males had significantly larger vertebral volumes than the females in this study (≤ 0.001), while the cervical vertebrae had significantly lower volumes than the thoracic and lumbar vertebrae for all subjects (≤ 0.001).

Table 7. Mean vertebral volume (cm^3)

Vertebra	Males	Females	% Diff	*p*-value
C5	4.54 +/- 0.9	3.06 +/- 0.5	- 32.6 %	≤ 0.001
T12	24.4 +/- 3.8	17.7 +/- 2.9	- 27.8 %	≤ 0.001
L1	26.9 +/- 3.8	19.1 +/- 2.9	- 29.0 %	≤ 0.001
L2	29.2 +/- 3.9	21.1 +/- 3.5	- 27.7 %	≤ 0.001

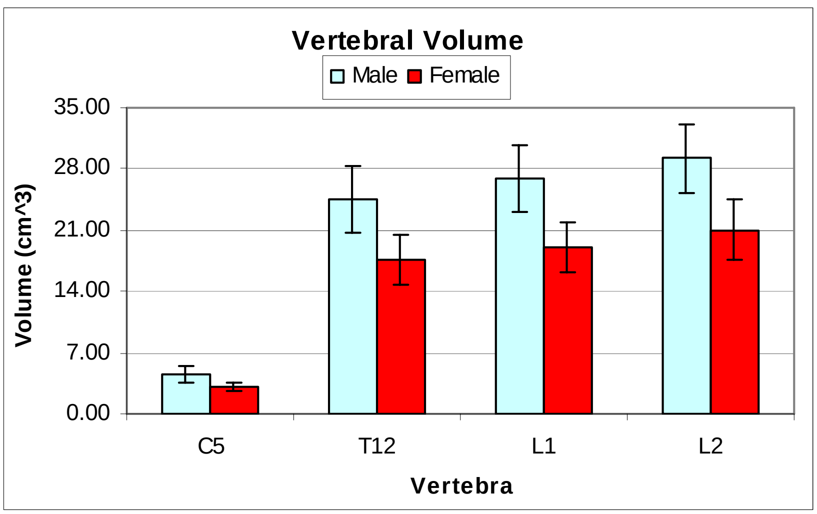

Figure 9. Mean vertebral volume of four vertebrae for males and females

Dynamic Response and Loading

Head Z Acceleration

Mean peak Head Z accelerations and standard deviations for male and female subjects are listed in Table 8, including the percent difference between genders and t-test results. The results are also plotted in Figure 10. Female subjects experienced higher Head Z accelerations than the male subjects, although a statistically significant difference was present for Cell C only. As expected, the head accelerations increased with increasing input (seat) acceleration level.

Table 8. Mean Head Z Acceleration (G)

Test Cell	Male	Female	% Diff	p-value
A (6 G)	8.1 +/- 1.5	8.6 +/- 1.4	+ 5.8 %	0.202
B (8 G)	10.9 +/- 1.8	11.5 +/- 1.2	+ 5.2 %	0.141
C (10 G)	13.7 +/- 1.4	14.4 +/- 1.6	+ 4.9 %	0.003

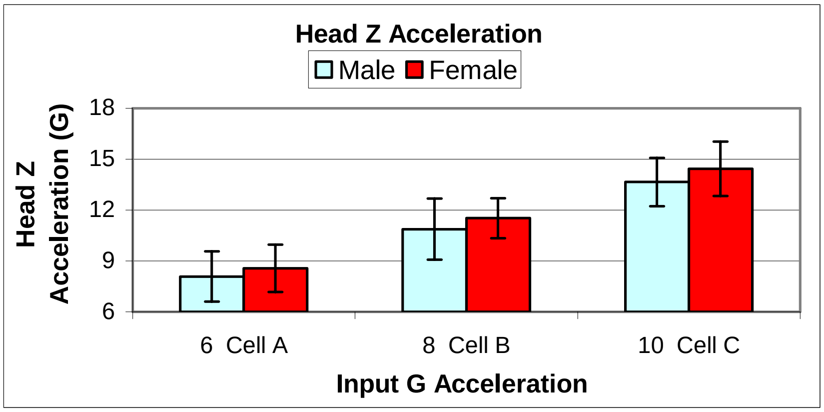

Figure 10. Head Z Acceleration of male and female subjects at 6-10 G

Chest Z Acceleration

Chest Z accelerations were also collected from the VDT and are shown in Table 9. The means and standard deviations as well as the percent differences and t-test results are included. Males had slightly higher Chest Z accelerations than females at both the 8 G and 10 G levels, although significant ($\alpha = 0.10$) for Cell C only. The chest accelerations increased as the input acceleration level increased (Figure 11).

Table 9. Mean Chest Z Acceleration (G)

Test Cell	Male	Female	% Diff	p-value
A (6 G)	7.69 +/- 0.9	8.02 +/- 1.3	+ 4.1 %	0.275
B (8 G)	11.3 +/- 1.4	11.0 +/- 1.1	- 2.7 %	0.347
C (10 G)	14.5 +/- 1.8	13.7 +/- 1.2	- 5.5 %	0.092

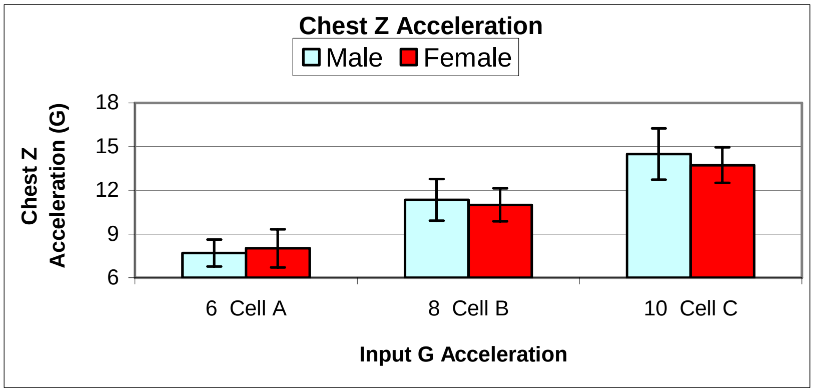

Figure 11. Chest Z Acceleration of male and female subjects at 6-10 G

Total Estimated Neck Supported Mass

The total neck supported mass at C2 and above and C5 and above was calculated and used to estimate the vertebral loads on C2 and C5 respectively (See Appendix A). Females were found to have significantly lower total neck supported mass for both C2 and above and C5 and above (Table 10, Figure 12).

Table 10. Mean estimated total neck supported mass (kg)

Vertebra	Male	Female	% Diff	p-value
C2	6.22 +/- 0.4	5.43 +/- 0.3	- 12.6 %	$\leq$ 0.001
C5	6.69 +/- 0.4	5.74 +/- 0.3	- 14.3 %	$\leq$ 0.001

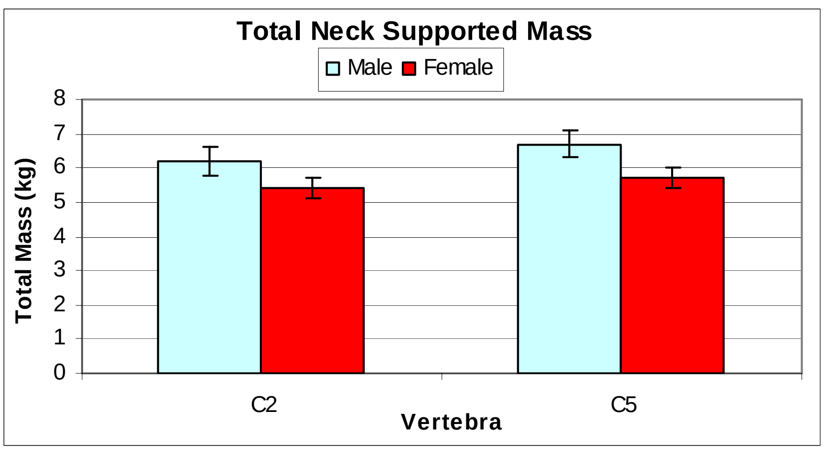

Figure 12. Total neck supported mass at C2 and C5 for males and females

Total Upper-Torso Mass

The total mass of the upper-torso and above (including upper torso, arms, neck, head, and helmet), was estimated using the subjects' anthropometric measurements in conjunction with the GEBOD computer model (see Methods section), in order to calculate vertebral loading. The means and standard deviations for males and females were 38.9 ± 7.5 kg and 25.5 ± 3.9 kg respectively. The female subjects had 34.5% lower upper-torso mass than male subjects ($\leq$ 0.001).

Vertebral Loads

The mean peak estimated loads and standard deviations for 10 G tests are listed in Table 11 and plotted in Figure 13. The loads on the cervical spine were estimated using the Neckload4 program (Appendix A) including the data from Tables 8 and 10. The loads for the thoracic and lumbar vertebrae were calculated by multiplying the Chest Z acceleration (Table 9) and the estimated total upper-torso mass for each subject. Significant gender differences were found for all vertebrae except C2, with the males experiencing higher vertebral loads than the females. As expected, the loads on the thoracic and lumbar vertebrae were significantly higher than the loads on the cervical vertebrae.

Table 11. Mean vertebral load (N)

Vertebra	Male	Female	% Diff	p-value
C2	930 +/- 153	865 +/- 113	- 6.9 %	0.110
C5	1004 +/- 156	914 +/- 120	- 9.0 %	0.032
T12, L1, L2	5534 +/- 1291	3452 +/- 748	- 37.6 %	$\leq$ 0.001

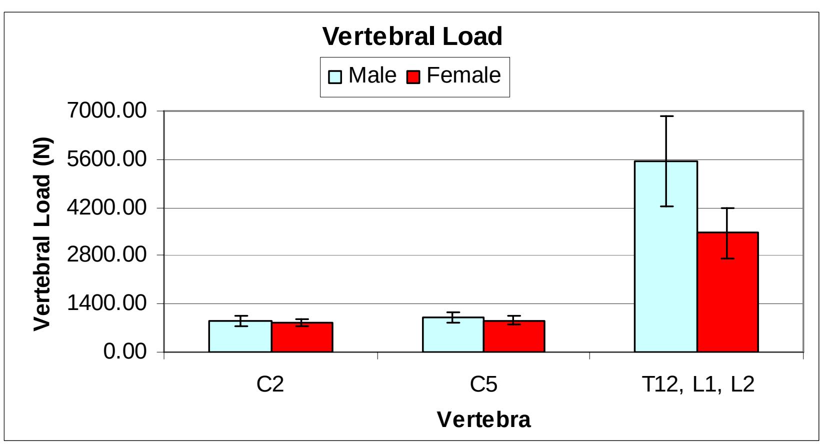

Figure 13. Vertebral loads at five vertebrae for males and females

Vertebral Stress

Mechanical stresses were estimated by dividing the subject's vertebral load (Table 11) by the vertebral CSA (Table 4) as explained in the methods section. The mean stresses and standard deviations for both male and female subjects are listed in Table 12 and plotted in Figure 14. The female subjects experienced statistically larger cervical stresses when compared to the male subjects, while the thoracic and lumbar stresses for females were smaller than the males, although not significant. The thoracic and lumbar vertebrae experienced significantly larger stresses than the cervical vertebrae.

Table 12. Mean estimated vertebral stress (MPa)

Vertebra	Males	Females	% Diff	*p*-value
C2	3.19 +/- 0.7	3.64 +/- 0.6	+ 12.4 %	0.023
C5	3.05 +/- 0.6	3.63 +/- 0.6	+ 16.0 %	0.002
T12	5.87 +/- 1.5	4.78 +/- 1.1	- 18.6 %	0.169
L1	5.62 +/- 1.4	4.74 +/- 1.0	- 15.7 %	0.160
L2	5.36 +/- 1.4	4.46 +/- 1.1	- 16.8 %	0.170

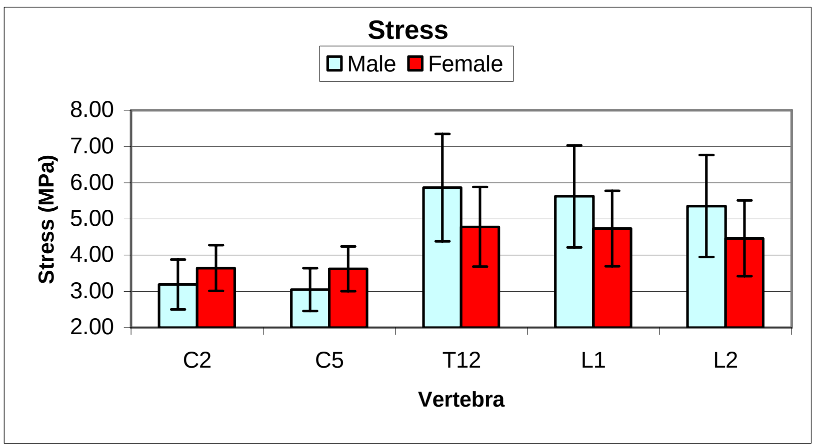

Figure 14. Vertebral stress at five vertebrae for males and females

Relationships between stress and weight, height, and sitting height were investigated for the five vertebrae. The influence of head and neck circumference were also investigated for the cervical vertebrae only. As shown in Table 13, weak negative correlations ($r < 0.34$) were found for all factors for both C2 and C5 stress with the exclusion of negligible positive correlations for C2 height and C5 head circumference for males. C5 stress versus sitting height is plotted in Figure 15(a). For the thoracic/lumbar vertebrae, the males demonstrated generally positive correlations for all three vertebrae for each of the three factors, although only weight was strongly correlated (≈ 0.7). The females showed moderate positive correlations (≈ 0.5) for weight, and weak negative correlations ($r < 0.26$) for both height and sitting height. Figures 15(b) displays the strong correlation with weight for L2 only, but the trends were similar for T12 and L1. When thoracic/lumbar stresses were recorded using the male and female regression lines at a common weight (70 kg), the female stress was found to be 14% greater at L2 than the males.

Table 13. Correlations of subject size versus stress for all five vertebrae

	Vertebrae									
	Male (r-value)					Female (r-value)				
Subject Size	**C2**	**C5**	**T12**	**L1**	**L2**	**C2**	**C5**	**T12**	**L1**	**L2**
Head Circumference (cm)	-0.08	0.12	N/A	N/A	N/A	-0.12	-0.04	N/A	N/A	N/A
Neck Circumference (cm)	-0.32	-0.19	N/A	N/A	N/A	-0.01	-0.16	N/A	N/A	N/A
Weight (kg)	-0.06	-0.03	0.70	0.71	0.74	-0.05	-0.20	0.50	0.51	0.45
Height (cm)	0.03	-0.04	0.17	0.23	0.23	-0.08	-0.26	-0.23	-0.23	-0.26
Sitting Height (cm)	-0.22	-0.27	0.00	0.01	0.00	-0.13	-0.34	-0.16	-0.18	-0.24

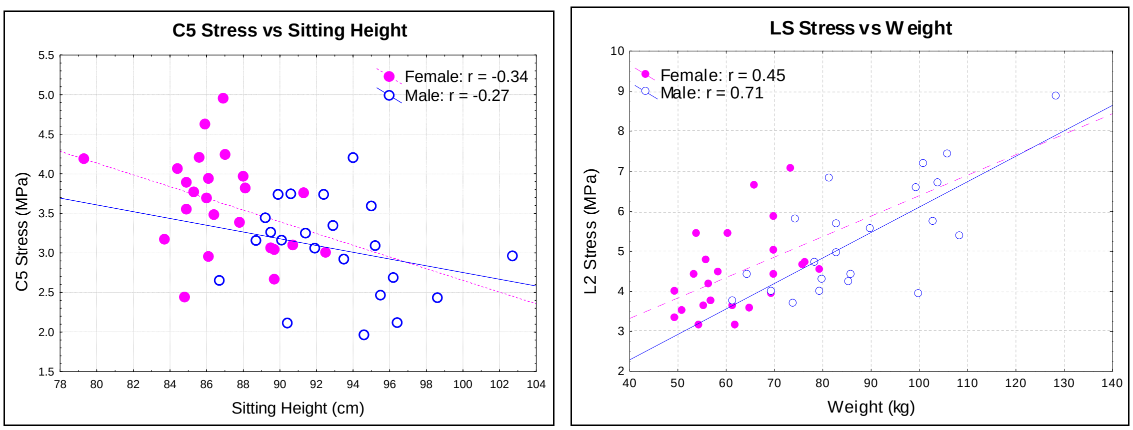

(a) (b)

Figure 15. Scatterplot of (a) C5 stress versus sitting height and (b) L2 stress versus weight at 10G acceleration input

Effect of Headrest Shift (Cell G)

A total of 26 tests were conducted on the VDT to examine the effect of an aft-shifted headrest (Cell G, Table 1). Cell G tests were conducted after the subjects completed all tests in cells A-C, and employed a 10 G seat acceleration input with the headrest shifted approximately 1” aft of the seat back. The subjects wore a Variable Weighted Impact (VWI) helmet that was slightly heavier than the standard HGU-55/P used in cells A-C (see Methods section). Input accelerations were statistically the same for both cell C and G tests. There were no significant differences in the acceleration responses between the in-line (Cell C) and aft (Cell G) headrest conditions, as shown in Table 14 and Figure 17. There were also no gender differences found within any of the conditions.

Table 14. Acceleration summary comparing in-line and aft headrest conditions

Measured Response Parameter	**Cell C** Headrest in-line	**Cell G** Headrest aft	**% Diff**	***p*-value**
Chest Z Acceleration (G)	14.1 +/- 1.5	13.6 +/- 1.4	- 3.5 %	0.169
Head Z Acceleration (G)	14.0 +/- 1.6	14.0 +/- 1.5	0 %	0.666
Head Ry Acceleration (Rad/s^2)	380.3 +/- 243	461.5 +/- 249	+ 17.6 %	0.120

DISCUSSION

Vertebral Properties Summary

This study investigated the gender differences of vertebral properties in young, healthy subjects, and the effects of accelerations and forces experienced by both males and females during vertical impacts. Vertebral breaking strength has been shown to be a good indicator of human tolerance limits in acceleration environments [28] and is directly related to the vertebral stress [17] and bone density of the vertebral body [4,14,31]. Our study used non-invasive techniques to estimate the amount of vertebral stress experienced by human subjects during impact acceleration exposures, including the use of measured accelerations, CT scans, and estimated body segment weights based on subject anthropometric measurements. These estimates are primarily intended to help establish trends for relative comparisons among males and females and large and small individuals within our subject pool, and are not intended to mimic results that might be seen in instrumented cadaver tests. As expected, the vertebral cross-sectional areas, vertebral heights and volumes were significantly smaller in the female subjects when compared with the male subjects for all five measured vertebrae. This is in agreement with other clinical studies of the spine [17,24]. The smaller vertebral size is a mechanical disadvantage that increases the stress on the vertebrae and limits the load capacity on the spine.

Bone Mineral Density (BMD)

The measurements demonstrated no significant differences in BMD between males and females at all measured vertebrae except C2, which was 10% lower in females. As expected, the cervical vertebrae had significantly higher BMD when compared to the thoracic and lumbar vertebrae, but it was surprising to find that there was no difference between C2 and C5 for the male subjects. This was an unexpected result when compared to other studies that generally show an increase from C2 to C5 [34,36], as was the case with our female subjects. This discrepancy could have been due in part to our relatively small number of subjects and their diversity of body size and fitness. It has been shown that spinal BMD can be affected by the subject's fitness level; more specifically, weight lifting can increase the density of bone [18,29]. Another surprising result was that the cervical BMD for this study had generally higher values when compared to the bone density of other studies [16,34,36]. This could be the effect of our subject pool consisting of active duty military volunteers who are required to maintain relatively stringent Air Force fitness standards.

CSA and Vertebral Stress

Vertebral stress in this study was significantly higher for females at the cervical vertebral levels, despite males experiencing larger dynamic loads and having larger head mass. Female subjects experienced 14-18% greater estimated cervical stresses than male subjects, due primarily to their smaller vertebral CSA. The smaller amount of neck-supported mass in females was not enough to balance out their smaller CSA when combined with their higher head accelerations. The higher neck loads and smaller cervical stresses experienced by the males are in agreement with findings by Coakwell *et al*.[13], who collected data from cadaver and human studies and determined that males have 25% greater compressive load tolerance than females. Vertebral stresses on the thoracic and lumbar vertebrae however, were slightly higher for males than females, although the differences were not significant. Our findings show that although males have significantly larger lumbar/thoracic CSA than the females, they also have significantly larger upper torso mass and estimated loads when compared to the female subjects. The smaller upper torso mass and correspondingly smaller lumbar/thoracic loads of the females were able to mitigate the stress incurred on their smaller vertebral CSA during the accelerations, which was not the case with their cervical vertebrae.

Vertebral stress was found to be affected by subject size (weight, height, and sitting height), although moderate to strong correlations were determined only in the lumbar/thoracic region for body weight In general, the heavier individuals tended to experience greater lumbar/thoracic stress under the dynamic loading conditions. Although most of the heavier individuals were males, it was shown that when the regressions were interpolated to the same weight for both genders, the females would actually experience 14% greater stress than the males. These results are similar, although not as pronounced, as the findings by Gilsanz [17], who used male and female subjects matched for height and weight, and determined that females would experience 33% greater lumbar stress in axial compression in a static environment. In addition, interpolation of the regressions in our study show that females have 15-19% smaller lumbar/thoracic CSA than males for the same size individuals with respect to their height, sitting height, and weight. This would cause higher lumbar/thoracic stress for females, assuming equivalent upper torso mass and chest accelerations. In general, the gender differences in lumbar/thoracic CSA indicate lesser compressive strength of the female vertebrae, which is in concurrence with the findings by Brinckmann *et al*.[4].

For the cervical vertebrae, the mechanical stress generally decreased with increasing body size, although the correlations were weak or negligible for all factors. However, the CSA data gave more definitive correlations, with regression interpolations indicating that the female CSAs were 12-15% smaller than males for the same size individuals with respect to their height, sitting height, and weight, 17% smaller for the same head circumference and 8% smaller for the same neck circumference. This would again appear to indicate a gender effect since the female CSA was found to be smaller when these measured size factors are normalized. The smaller CSA would be expected to lead to greater cervical stress for individuals with the same head/neck mass and same head accelerations under dynamic conditions.

Our study also found that the thoracic and lumbar vertebrae had significantly higher stresses than the cervical vertebrae under dynamic conditions. The upper torso mass was obviously much larger than the weight of the head, while there was little difference between the measured torso (chest) and head accelerations. The CSA of the lumbar/thoracic vertebrae was approximately three times larger than the cervical vertebrae while the loads were almost 4-5 times greater, therefore producing a higher stress on the lumbar/thoracic regions. In addition to the greater mechanical stress, the lumbar/thoracic vertebrae had significantly lower BMD than the cervical vertebrae. The greater stress and lower BMD of the lumbar/thoracic region would appear to explain the high incidence of lower back spinal injuries compared to cervical injuries occurring during pilot ejections prior to the advent of heavy helmet mounted systems, which can increase the head mass by as much as 50%.

Dynamic Neck Loads

It is interesting to note that the males experienced higher neck loads even though their head accelerations were lower than the females. Many variables can affect the estimate of compressive neck force including head acceleration, anthropometric measurements, and the mass of the combined helmet, head, and segment of the neck. The difference in head acceleration could be due to the position/bracing techniques of the subjects during testing, whereby individuals with greater neck strength were able to better stabilize their head and decrease their accelerations by bracing against the headrest just prior to impact. In addition, the total neck supported mass above the vertebrae at both C2 and C5 was significantly higher for the males than the females, thus contributing to higher neck forces for the males as a result, but as mentioned above, their greater neck strength tended to mitigate their head accelerations and when combined with their larger CSA, had the effect of reducing the vertebral stress as compared to females.

Headrest Shift

There was no effect found on the human dynamic response with a 1” aft shift of the headrest from the seat back. When comparing Cells C and G, which were both 10 G acceleration seat inputs, there were no statistical differences in the measured head or chest accelerations.

CONCLUSIONS

The risk of impact acceleration injury to the spine depends on both bone strength and dynamic vertebral stress. In this study, the bone mineral density, which is indicative of bone strength, demonstrated no conclusive gender differences for either cervical or lumbar/thoracic vertebrae. However, female subjects experienced significantly higher mechanical stresses on the cervical vertebrae under dynamic conditions, which were primarily due to their smaller vertebral cross-sectional areas. The greater cervical vertebral stresses indicate that females may be more at risk of cervical spinal injury during impact acceleration events, such as those occurring during aircraft ejections. Surprisingly, females demonstrated smaller thoracic and lumbar stresses during dynamic loading due to their lower upper torso mass. However, when the data were normalized for subject size, the females would actually experience greater lumbar/thoracic stress, again primarily due to their smaller vertebral size.

REFERENCES

1) Albery, C.B., Kaleps, I. (1997) A Procedure to Measure the Mass Properties of Helmet Systems. NDIA Design and Integration of Helmet Systems Symposium Proceedings. Framingham, MA.
2) Anthropometry and Mass Distribution for Human Analogues. Volume 1: Military Male Aviators. (1988) Harry G. Armstrong Aerospace Medical Research Laboratory, WPAFB, OH. AAMRL-TR-88-010.
3) Beier, G., Schuller, E., Schuck, M., Ewing, C.L., Becker, E.D., Thomas, D.J. (1980) Center of Gravity and Moments of Inertia of Human Heads. Scientific Report No. 1:218-228. Institute for Forensic Medicine, University of Munich. Naval Biodynamics Laboratory, New Orleans, LA.
4) Brinckmann, P., Biggeman, M., Hilweg, D. (1989) Prediction of the Compressive Strength of Human Lumbar Vertebrae. Clinical Biomechanics, Suppl 2:S1-S27.
5) Brinkley, J.W., Dearing, E.R., Rauterkus, L.T. (1969) Evaluation of the Effects of Selected Egress System Design. 40th Annual Aerospace Medical Association Meeting.
6) Buhrman, J.R. (1999) The AFRL Biodynamics Data Bank and Modeling Applications. Research and Technology Organization (RTO), Human Factors and Medicine Panel Meeting, Proceedings No. 20, "Models for Aircrew Safety Assessment: Uses, Limitations, and Requirements".
7) Buhrman, J.R., Mosher, S.E., (1999) A Comparison of Male and Female Acceleration Responses During Laboratory +Gz Impact Tests. Proceedings of the 37th Annual SAFE Symposium.
8) Buhrman J.R., Perry C.E., and Mosher S.E. (2001) A Comparison of Male and Female Acceleration Responses During Laboratory Frontal –Gx Axis Impact Tests. AFRL Technical Report AFRL-HE-WP-TR-2001-0022.
9) Buhrman, J.R., Plaga, J.A., Cheng, H., Mosher, S.E. (2001) The AFRL Biodynamics Data Bank on the Web: A Repository of Human Impact Acceleration Response Data. Proceedings of the 39th Annual SAFE Symposium.
10) Cann, C.E. Genant, H.K., Kolb, F.O., Ettinger, B. (1985) Quantitative Computed Tomography for Prediction of Vertebral Fracture Risk. Bone, 6:1-7.
11) Cheng, H., Obergefell, L., Rizer, A. (1994) Generator of Body Data (GEBOD) Manual. Armstrong Laboratory, Crew Systems Directorate. WPAFB, OH. AL/CF-TR-1994-0051.
12) Clauser, C.E., McConville, J.T., Young, JW. (1969) Weight, Volume, and Center of Mass of Segments of the Human Body. AMRL-TR-69-70.
13) Coakwell, M.R., Bloswick, D.S., Moser, Jr., R. (2004) High Risk Head and Neck Movements at High G and Interventions to Reduce Associated Neck Injury. Aviation, Space, and Environmental Medicine, 75(1): 68-80.
14) Cody, D.D., Goldstein, S.A., Flynn, M.J., Brown, E.B. (1991) Correlations between Vertebral Regional Bone Mineral Density (rBMD) and Whole Bone Fracture Load. Spine, 16(2):146-154.
15) Dempster, W.T. (1955) Space Requirements of the Seated Operator. Geometrical, Kinematic, and Mechanical Aspects of the Body with Special Reference to the Limbs. Human Mechanics: 215-328. AMRL-TDR-63-123.

16) Dicuccio, M., Paskoff, G., Whitley, P., Schweitzer, M. Comparison of Vertebral Strength Properties of Anthropometrically Similar Male and Female using Quantitative Computed Tomography.
17) Gilsanz, V., Boechat, M.I., Gilsanz, R., Loro, M.L., Roe, T.F. Goodman, W.G. (1994) Gender Differences in Vertebral Sizes in Adults: Biomechanical Implications. Radiology, 190:678-682.
18) Gleeson, P.B., Protas, E.J., LeBlanc, A.D., Schneider, V.S., Evans, H.J. (1990) Effects of Weight Lifting on Bone Mineral Density in Premenopausal Women. Journal of Bone and Mineral Research, 5(2): 153-158.
19) Gross, M.E. (1991) The GEBODIII Program User's Guide and Description. Air Force Research Laboratory, Technical Report. AL-TR-1991-0102.
20) Hansson, T., Roos, B., Nachemson, A. (1980) The Bone Mineral Content and Ultimate Compressive Strength of Lumbar Vertebrae. Spine, 5(1):46-55.
21) Jager, M., Luttman, A. (1991) Compressive Strength of Lumbar Spine Elements Related to Age, Gender, and Other Influencing Factors. 8th Congress of the International Society of Electrophysiological Kinesiology. 1990 Aug 12-16. Elsevier Science Publishers: 291-294.
22) Kazarian, L.E. (1978) Standardization and Interpretation of Spinal Injury Criteria. Aerospace Medical Research Laboratory, WPAFB, OH. AMRL-TR-75-85.
23) McConville, J.T., Churchill, T.D., Kaleps, I., Clauser, C.E., Cuzzi, J. (1980) Anthropometric Relationships of Body and Body Segment Moments of Inertia. Air Force Aerospace Medical Research Laboratory. AFAMRL-TR-80-119.
24) Mosekilde, L., Mosekilde, L. (1990) Sex Differences in Age-Related Changes in Vertebral Body Size, Density and Biomechanical Competence in Normal Individuals. Bone, 11:67-73.
25) Perry, C.E. (1994) Investigation of Biodynamic Characteristics of the Chest and Thoracic Spine During +Gz Impact. In-house test program at Air Force Research Laboratory.
26) Pilot Survey. (2000) AFMOA, Bolling Air Force Base, Washington, D.C.
27) Ross, P.D., Huang, C., Davis, J.W., Wasnich, R.D. (1995) Vertebral Dimension Measurements Improve Prediction of Vertebral Fracture Incidence. Bone, 16(4): 257-262.
28) Ruff, S. (1950) Brief Acceleration: Less than One Second. In: Surgeon General, U.S. Air Force, ed. German Aviation Medicine, World War II. 1. Washington D.C.: U.S. Government Printing Office: 584-597.
29) Ryan, A.S., Treuth, M.S., Rubin, M.A., Miller, J.P., Nicklas, B.J., Landis, D.M., Pratley, R.E., Libanati, C.R., Gundberg, C.M., Hurley, B.F. (1994) Effects of Strength Training on Bone Mineral Density: Hormonal and Bone Turnover Relationships. Journal of Applied Physiology, 77(4): 1678-1684.
30) Self, B.P., Spittle, E.K., Kaleps, I., Albery, C.B. (1992) Accuracy and Repeatability of the Standard Automated Mass Properties Measurement System. AL-TR-1992-0137.
31) Singer, K., Edmondston, S. Day, R., Breidahl, P., Price, R. (1995) Prediction of Thoracic and Lumbar Vertebral Body Compressive Strength: Correlations with Bone Mineral Density and Vertebral Region. Bone, 17(2): 167-174.
32) Tabensky, A.D., Williams, J., Deluca, V., Briganti, E., Seeman, E. (1996) Bone Mass, Areal, and Volumetric Bone Density are Equally Accurate, Sensitive, and Specific

Surrogates of the Breaking Strength of the Vertebral Body: An In Vitro Study. Journal of Bone and Mineral Research, 11(12):1981-1987.

33) Von Gierke, H.E., Brinkley, J.W. (1975) Impact Accelerations. In: Calvin, C., Gazenko, O.G. eds. Foundations of Space Biology and Medicine. 2(1). Washington D.C.: National Aeronautics and Space Administration: 214-246.
34) Weishaupt, D. Schweitzer, M.E., DiCucccio, M.N., Whitley, P.E. (2001) Relationships of Cervical, Thoracic, and Lumbar Bone Mineral Density by Quantitative CT. Journal of Computer Assisted Tomography, 25(1): 146-150.
35) Williams, J., Belytschko, T. (1981) A Dynamic Model of the Cervical Spine and Head. Air Force Aerospace Medical Research Laboratory, WPAFB, OH. AFAMRL-TR-81-5.
36) Yoganandan, N., Pintar, F.A., Stemper, B.D., Baisden, J.L., Aktay, R., Shender, B.S., Paskoff, G. (2006) Bone Mineral Density of Human Female Cervical and Lumbar Spines from Quantitative Computed Tomography. Spine, 31(1): 73-76.
37) Young, J.W., Chandler, R.F., Snow, C.C., Robinette, K.M., Zehner, G.F., Lofberg, M.S. (1983) Anthropometric and Mass Distribution Characteristics of the Adult Female. FAA-AM-83-16.

APPENDIX A: IN-HOUSE NECKLOAD PROGRAM

An in-house software program, “Neckload4”, was designed to calculate neck forces and moments using measured head linear and angular accelerations and inertial properties of the helmet, head, and neck. The user would have the choice to calculate the force and moment at four different junctions of the cervical neck. These junctions include the occipital condyles (OC or head-neck junction), C1/C2 junction, C4/C5 junction, and C7/T1 junction. The calculated forces and moments describe the force and moment (Figure 1) on the surface of C1, C2, C5, and T1. These calculated forces and moments are based on the equations of motion for rigid bodies or systems. This program separates the head, neck, and helmet into two systems: the head and neck are combined as the first system and the helmet is the second system.

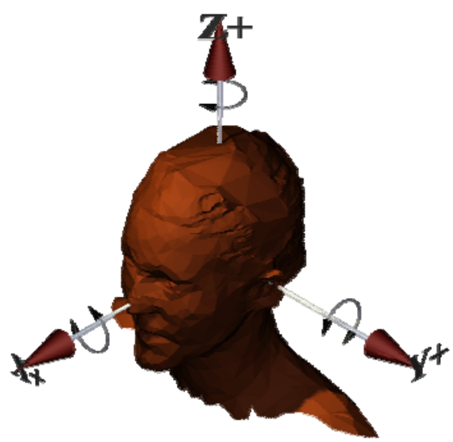

Figure 1: Anatomical Axis System of the Human Head and Neck.

<u>Neck Mass/Center of Mass.</u>
Total and partial neck lengths of the subjects are calculated to obtain dimensions needed for estimating the center of mass of the selected neck segments. The total neck length is calculated using the subject’s anthropometric measurements, by taking the difference between the height of the nuchale (the lowest point in the mid-sagittal plane of the occiput that can be palpated among the nuchal muscles[8]) and the height of the cervicale (the superior tip of the spine of the seventh cervical vertebra[8]) (Figure 2). This gives the effective distance between the superior surface of C1 and the inferior surface of C7.

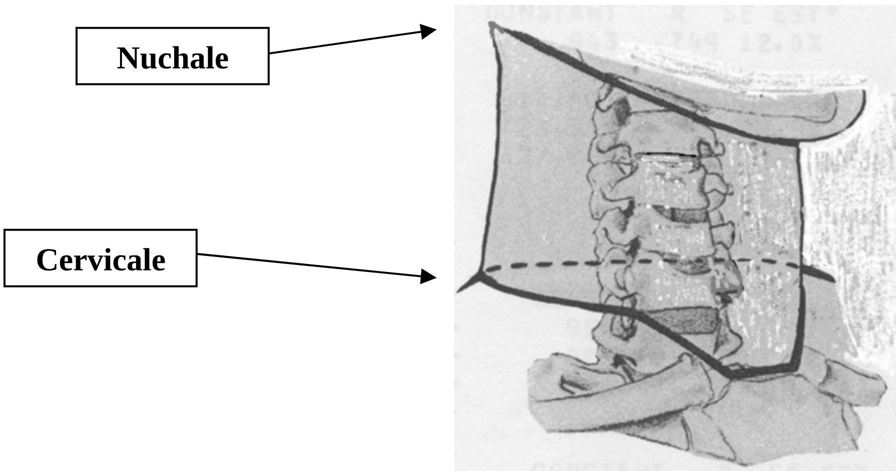

Figure 2: Human Head and Neck

Partial neck lengths as a proportion of total neck length were calculated using cadaveric data from a study by Williams and Belytschko[10], who determined the average vertical heights of the vertebral slices (including intervertebral discs) of the human neck (Table 1). Slices above the C2 and C5 surfaces (Figure 3) were then summed and divided by the total neck length to obtain the percentages for these two partial neck lengths. The percentages are multiplied by the measured total neck length of individual subjects (above) to find their specified neck segment lengths.

Table 1: Height of Vertebral Slices[10]

Vertebral Slice	Vertical Height (cm)
C1	0.8
C2	1.8
C3	1.1
C4	1.2
C5	0.9
C6	1.1
C7	1.3

- Total Average Vertical Height = 8.2 cm
- Superior Surface of C2 and Above = 0.80 / 8.2 = 10 % of Total Neck Length
- Superior Surface of C5 and Above = 4.90 / 8.2 = 60 % of Total Neck Length

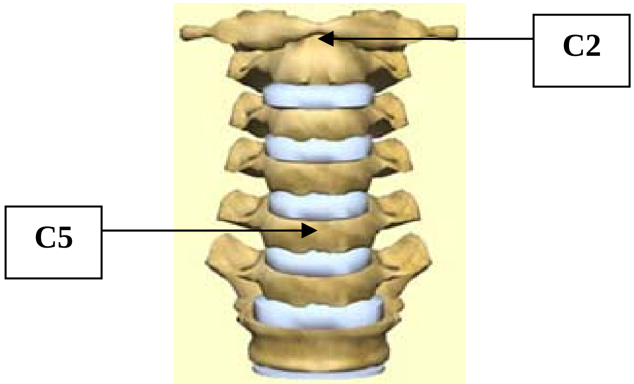

Figure 3: Human Cervical Spine (C1-C7)

To find the total neck mass of the subject, first an estimated neck volume is obtained and multiplied by the neck density. Separate regression equations for male[7, 8] and female[11] neck volumes are used. Each regression equation uses the subject's measured anthropometry to determine the neck volume in cubic centimeters.

Male Subject:

Neck Volume = 36.89 * Neck Circumference + 1.83 * Body Weight – 659.40[7,8]

Female Subject:

Neck Volume = 10.25 * Stature + 19.10 * Neck Circumference – 1543.33[11]

Total neck mass of the subject is then obtained by multiplying the calculated neck volume by a homogeneous density of 0.00112287 slugs per cubic inch[5]. This density was estimated from studies by Dempster[7], McConville[8], and Young[11].

Partial neck masses were determined by a neck segmented into vertebral slices, where the total neck mass was distributed to each slice according to the volume of the slice[10] (Table 2). Percentages of total neck mass for the C2 and C5 surfaces and above are calculated from these data. These percentages are then multiplied by the subject's total neck mass (above) to obtain estimates of these two neck segments for individual subjects.

Table 2: Mass of Vertebral Slices[10]

Vertebral Slice	Mass (g)
C1	815
C2	815
C3	815
C4	815
C5	815
C6	900
* A portion of C7 slice	900

* Estimated by AFRL/HEPA

- Total Average Mass = 5875 g
- Superior Surface of C2 and Above = 815 / 5875 = 14 % of Total Neck Mass
- Superior Surface of C5 and Above = 3260 / 5875 = 55 % of Total Neck Mass

Only a portion of the C7 vertebral slice was included in this program in order for it to correspond with the lower neck segmentation from the thorax performed and described by Dempster[7]. The head was segmented from the neck through the right and left gonial points and nuchale. The neck was segmented from the thorax with two connecting planes. The first plane originates at the cervicale and passes anteriorly parallel with the standing surface. The second plane originates at the lower of the two clavicale landmarks, rises 45 degrees from the horizontal and then passes diagonally superiorly-posteriorly until it intersects with the first plane (Figure 4) [7].

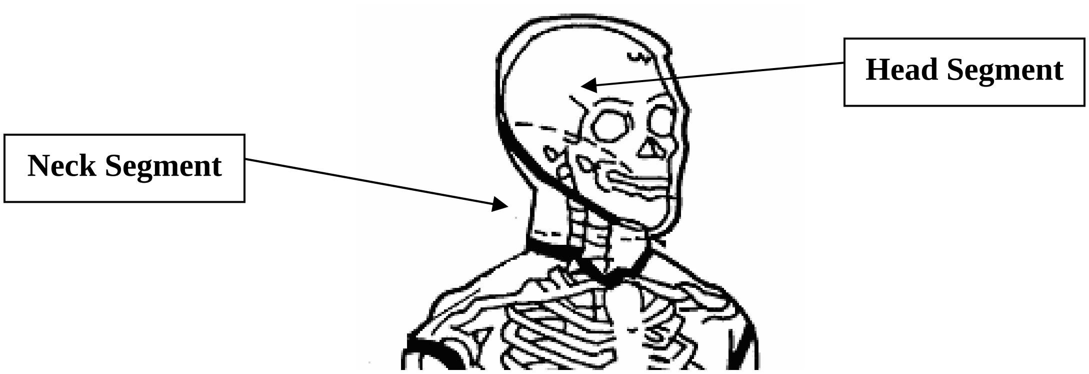

Figure 4: Head and Neck Segmentation

The mass of the neck can be calculated for four different junctions. The mass is calculated for the neck segment down to the C1/C2 junction, the neck segment from the C1/C2 junction down to the C4/C5 junction, and the neck segment for the C4/C5 junction down to the C7/T1 junction. The mass was distributed evenly for the C1-C5 vertebral slices[11], as seen from Table 2; therefore the center of mass is located in the center of each neck segment. The center of mass for the C7/T1 junction however is not located in the center of the neck. An average distance was calculated from nuchale to the center of mass of small, mid-size, and large male aviators[2]. The distance from nuchale to the center of mass was estimated to be 82% of the total neck length for the C7/T1 junction. Depending on the neck junction selected by the program user, the masses of the three neck segments and the centers of mass of the segments are combined in order to calculate the mass and center of mass of the segment of neck that is above the selected neck junction.

The user chooses the neck junction with a drop down menu (Figure 5). When the user chooses to calculate the force at the OC, the properties of the neck are not included. The force on the surface of T1 would include the total neck length and total neck mass. For C2, 10% of the total neck length will be incorporated along with 14% of the total neck mass. For C5, 60% of the total neck length will be included along with 55% of the total neck mass.

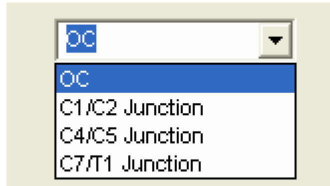

Figure 5: Drop Down Menu for Neck Junction Selection

Head Mass/Center of Mass.
The following regression equation is used to determine the subject's head mass. Clauser et al.[6] predicted the head mass in kilograms by using the subject's measured head circumference and body weight.

Head Mass = 0.104 * Head Circumference + 0.015 * Body Weight – 2.189[6]

The center of mass of the head is assumed to be at the average location for the head center of gravity determined by Beier[3]. The mean and standard deviation for the head center of gravity was calculated from twenty-one fresh cadavers. The three-dimensional location of the center of gravity of the head was related to the anatomically based coordinate reference system (Table 3).

Table 3: Head Center of Gravity[3]

Coordinates of Head Center of Gravity	Mean and Standard Deviation (cm)
X	0.83 +/- 0.25
Y	-0.05 +/- 0.13
Z	3.12 +/- 0.56

Total Neck Supported Mass/Center of Mass.
Biodynamic response data are collected by an on-board data acquisition system during testing on the Vertical Deceleration Tower (VDT) at Wright-Patterson AFB, Ohio. The subject is instrumented with accelerometers. Head linear and angular accelerations are measured by a tri-axial accelerometer and an angular accelerometer array mounted on a bite bar. The head acceleration is normalized to eliminate the variations in carriage acceleration.

The inertial properties of the helmet were previously measured by General Dynamics using the methods described in a report by Albery, et al.[1] and within the accuracies stated in AL-TR-1992-0137[9].

Force and Moment Calculation.
The bite bar acceleration and the bite bar angular acceleration are used to compute the acceleration at the center of mass of the combined helmet, head and neck system. A 1G vector in the vertical direction was added to the measured bite bar acceleration when the head is in its initial position. As the bite bar accelerometer rotated, the bite bar acceleration always contained 1G in the vertical direction due to the force of gravity. The 1G vector is carried over to the computed acceleration at the center of mass. The 1G vector represents the weight of the combined system in the calculation. The force is computed based on the total mass and the

acceleration at the center of mass. The torque is calculated based on the total mass, inertial tensor, acceleration at the center of mass, position relative to the center of mass, angular acceleration, and angular velocity.

The acceleration at the center of mass is[12]: $\vec{a}_{cm} = \vec{a} + \dot{\vec{\omega}} \times \vec{r} + \vec{\omega} \times (\vec{\omega} \times \vec{r})$, where a is the actual acceleration at the bite bar, ω is the angular velocity, $\dot{\omega}$ is the angular acceleration, and r is a vector from the bite bar accelerometer location to the center of mass. The angular velocity can be calculated by integrating the angular acceleration. However, the piezoresistive accelerometers measure a combination of the actual acceleration and the force of gravity: $\vec{a} = \vec{a}_M - \vec{g}_0 + \vec{g}$, where a_M is the measured acceleration at the bite bar as measured by the piezoresistive accelerometers, a is the actual acceleration at the bite bar and g_0 is the initial acceleration of gravity vector at the time before the impact when the accelerometer is zeroed. The input bite bar acceleration that is read in by the Neckload4 program is assumed to be $\vec{a}_M - \vec{g}_0$, a value that is normally stored in the Biodynamic Data Bank[4]. Combining the two equations, $\vec{a}_{cm} - \vec{g} = \vec{a}_M - \vec{g}_0 + \dot{\vec{\omega}} \times \vec{r} + \vec{\omega} \times (\vec{\omega} \times \vec{r})$.

Force Calculation.

The force is then calculated using $\vec{F} = m(\vec{a}_{cm} - \vec{g})$; where F is the force, m is the total mass of the combined helmet, head and neck, a_{cm} is the acceleration at the center of mass, and g is a vector in the direction of the acceleration of gravity.

Moment Calculation.

The moment (or torque) is calculated using[13]: $\vec{\tau} = \vec{R} \times m(\vec{a}_{cm} - \vec{g}) + I \cdot \dot{\vec{\omega}} + \vec{\omega} \times (I \cdot \vec{\omega})$. Where τ is the torque, R is a vector from the point at which the torque is calculated to the center of mass and I is the inertial tensor for the moments of inertia in the head anatomical coordinate system. The torque represents the torque as it would be measured at the corresponding location in the neck.

The total mass and the location of the center of mass of the combined helmet, head, and neck system are calculated based on the masses and center of masses of the helmet, head and neck. The inertial tensor of the combined system is calculated from the principal moments of inertia of the helmet, head and neck by finding the inertial tensors of the individual components using: $I = AI_pA^T$ where A is the direction cosine matrix, I is the inertial tensor in the anatomical coordinate system and I_p is the inertial tensor in the principle axis coordinate system. The inertial tensors of the individual components are then combined using the parallel-axis theorem.

Time histories and summary information about the calculated neck forces and moments are output and stored in an Excel workbook. The sign conventions use SAE J211 sign convention for the output which has the z-axis positive downward.

A source of error for the program is the use of regression equations. These equations do take into account some of the subject's true measurements, but the segment weights and inertial properties are still estimations. Also, the program calculates the acceleration at the center of mass based on the measured head linear and angular accelerations. Unfortunately, the angular accelerations are often noisy. The program gives the user the option to filter the angular acceleration, but the noise on the angular acceleration could cause the calculated acceleration at the center of mass to be higher than it should be.

A limitation of the Neckload4 program is that the program assumes that the linear and angular accelerations of the head are caused entirely by the neck forces. The forces due to the neck were assumed to be the only external force acting on the system. If external forces other than the neck (such as due to a headrest) were acting on the head, they would need to be subtracted out of the total force that is calculated by the program in order to find the neck force and moment. Consequently, the results from the program only accurately represent the neck force and moment for each axis direction during the time period when no other external forces are acting on the head in that direction.

REFERENCES

1) Albery, C.B., Kaleps, I. (1997) A Procedure to Measure the Mass Properties of Helmet Systems. NDIA Design and Integration of Helmet Systems Symposium Proceedings. Framingham, MA.
2) Anthropometry and Mass Distribution for Human Analogues. Volume 1: Military Male Aviators. (1988) Harry G. Armstrong Aerospace Medical Research Laboratory, WPAFB, OH. AAMRL-TR-88-010.
3) Beier, G., Schuller, E., Schuck, M., Ewing, C.L., Becker, E.D., Thomas, D.J. (1980) Center of Gravity and Moments of Inertia of Human Heads. Scientific Report No. 1:218-228. Institute for Forensic Medicine, University of Munich. Naval Biodynamics Laboratory, New Orleans, LA.
4) Buhrman, J.R., Plaga, J.A., Cheng, H., Mosher, S.E. (2001) The AFRL Biodynamics Data Bank on the web: A repository of human impact acceleration response data. Proceedings of the 39th Annual SAFE Symposium.
5) Cheng, H., Obergefell, L., Rizer, A. (1994) Generator of Body Data (GEBOD) Manual. Armstrong Laboratory, Crew Systems Directorate. WPAFB, OH. AL/CF-TR-1994-0051.
6) Clauser, C.E., McConville, J.T., Young, JW. (1969) Weight, Volume, and Center of Mass of Segments of the Human Body. AMRL-TR-69-70.
7) Dempster, W.T. (1955) Space Requirements of the Seated Operator. Geometrical, Kinematic, and Mechanical Aspects of the Body with Special Reference to the Limbs. Human Mechanics: 215-328. AMRL-TDR-63-123.
8) McConville, J.T., Churchill, T.D., Kaleps, I., Clauser, C.E., Cuzzi, J. (1980) Anthropometric Relationships of Body and Body Segment Moments of Inertia. Air Force Aerospace Medical Research Laboratory, WPAFB, OH. AFAMRL-TR-80-119.
9) Self, B.P., Spittle, E.K., Kaleps, I., Albery, C.B. (1992) Accuracy and Repeatability of the Standard Automated Mass Properties Measurement System. AL-TR-1992-0137.
10) Williams, J., Belytschko, T. (1981) A Dynamic Model of the Cervical Spine and Head. Air Force Aerospace Medical Research Laboratory, WPAFB, OH. AFAMRL-TR-81-5.
11) Young, J.W., Chandler, R.F., Snow, C.C., Robinette, K.M., Zehner, G.F., Lofberg, M.S. (1983) Anthropometric and Mass Distribution Characteristics of the Adult Female. FAA-AM-83-16.
12) Wells, D.A., (1967) Lagrangian Dynamics, Schaum's Outline Series, McGraw-Hill, p. 180.
13) Symon, K.R. (1960) Mechanics, Addison-Wesley, p. 451.

APPENDIX B: INDIVIDUAL SUBJECT DATA

Anthropometric Data

	Subj	Gender	Age	Height (cm)	Weight (kg)	Sitting Height (cm)	Head Circ (cm)	Neck Circ (cm)
1	A-10	F	20	167.6	50.8	88.1	52.6	28.9
2	A-12	F	23	153.1	56.2	85.6	55.6	31.5
3	B-16ab	F	34	165.7	64.9	89.5	55	33.2
4	B-25	F	22	162.8	66.2	85.9	54.8	31.6
5	C-22	F	23	168.8	69.9	89.7	55.3	31.3
6	C-23	F	30	178.9	76.7	90.7	55.7	33.9
7	C-25	F	39	156.5	54.4	84.8	52.8	30
8	C-26	F	29	172.8	79.4	92.5	55.5	35.3
9	C-27	F	23	157.1	53.3	84.4	52	30.6
10	F-9	F	20	168.9	49.4	86.9	52.7	29.5
11	G-16	F	21	158.8	60.6	86.4	55.2	32.1
12	K-10	F	20	164.3	69.9	87	56.1	33.1
13	L-14	F	24	158.8	73.3	85.3	55.5	34
14	L-16	F	20	163.3	61.7	86.1	55.5	31.5
15	M-32	F	25	162.9	55.3	84.9	53.7	29.1
16	M-33	F	30	155.6	58.5	86	53.8	31.2
17	M-35	F	20	167.4	70.1	88	53.9	33.9
18	M-36	F	30	166.5	69.6	87.8	56.4	33.5
19	M-38	F	36	166.5	49.4	84.9	56.5	29.2
20	P-12	F	31	163	76.2	86.1	55.8	35.1
21	R-23	F	26	174	57.2	89.7	52.5	31
22	S-24	F	23	158.5	56.5	83.7	53.6	30
23	S-26	F	34	168.3	61.9	91.3	55.7	31.1
24	T-11	F	24	146.4	54	79.3	52.5	28.5
25	B-9b	M	34	172.9	74.4	89.5	56.5	37.9
26	B-23	M	39	180.1	85.7	94.6	58.7	39.7
27	B-27	M	25	166	61.5	90.4	55.1	36.4
28	C-17b	M	33	176.5	79.4	96.2	57.7	41.3
29	D-11	M	33	179.5	108.4	96.4	58.1	43
30	D-13	M	36	186.9	99.8	98.6	56.5	41
31	F-8	M	23	170.6	89.8	91.4	60	41.8
32	G-14a	M	35	184.9	86.2	95	58.6	41.1
33	G-15	M	32	175.6	83.2	92.9	59.8	38.1
34	H-13	M	37	180.3	78.5	92.4	57.1	37.9
35	H-16	M	43	170.2	81.6	90.6	56	37
36	H-18	M	28	182.8	106.1	95.2	57	39
37	H-20	M	24	177.7	100.9	89.9	57.6	42.7
38	H-21	M	27	190.3	103.2	102.7	58.5	42.2
39	H-22	M	33	171.3	104.1	88.7	58.2	42.6
40	J-13	M	26	179	79.8	93.5	56.7	37.7
41	L-15	M	38	170.6	69.6	90.1	56.7	37.2
42	M-21b	M	40	167.4	64.4	86.7	53.8	36.9
43	M-34	M	33	187.8	128.4	95.5	58.4	45
44	M-37	M	32	177.7	73.9	91.9	56.3	36.7
45	S-11b	M	35	180.8	99.3	94	57.3	39.1
46	W-12	M	45	173.6	83	89.2	58	36.7

BMD (mg/cm^3) Measurement Data

	Subj	Gender	C2 BMD	C5 BMD	T12 BMD	L1 BMD	L2 BMD
1	A-10	F	335.4	401.34	204.76	201.51	197.13
2	A-12	F	313.74	364.76	264.11	248.98	240.88
3	B-16ab	F	394.62	378.01	179.74	181.83	174.79
4	B-25	F	330.74	312.27	224.84	215.04	211.21
5	C-22	F	292.57	341.64	190.52	182.74	173.37
6	C-23	F	338.81	514.1	233.47	237.1	237.05
7	C-25	F	240.81	304.2	152.7	157.71	155.62
8	C-26	F	294.71	370.83	181.07	167.21	154.81
9	C-27	F	229.58	276.06	152.69	153.72	160.58
10	F-9	F	346.25	343.11	205.62	209.44	202.86
11	G-16	F	352.36	351.5	188.82	184.25	181.47
12	K-10	F	315.69	356.58	200.99	195.51	193.53
13	L-14	F	291.36	310.67	206.78	207.18	206.96
14	L-16	F	304.49	425.27	208.56	212.96	186.59
15	M-32	F	254.15	368.21	220.33	216.44	215.72
16	M-33	F	296.07	383.13	237.44	238.29	231.77
17	M-35	F	243.29	264.96	172.63	164.29	163.2
18	M-36	F	325.04	324.03	170.44	173.24	178.06
19	M-38	F	329.15	334.35	206.14	205.42	204.27
20	P-12	F	307.74	345.5	176.24	176.51	165.03
21	R-23	F	287.57	296.79	150.73	151.11	148.15
22	S-24	F	307.18	358.31	201.87	192.24	185.21
23	S-26	F	294.7	348	227.14	217.69	207.2
24	T-11	F	255.59	331.98	174.81	166.02	156.32
25	B-9b	M	489.02	412.58	182.32	189.4	215.66
26	B-23	M	276.89	294.94	156.01	152.89	145.96
27	B-27	M	356.97	376.38	230.86	231.16	216.26
28	C-17b	M	334.63	350.14	182.19	178.13	168.24
29	D-11	M	268.88	302.32	194.39	188.66	179.2
30	D-13	M	386.79	318.29	192.04	167.28	170.86
31	F-8	M	353.69	369.19	203.4	196.7	188.86
32	G-14a	M	275.49	269.15	157.54	154.57	158.66
33	G-15	M	295.18	301.35	186.81	179.87	177.2
34	H-13	M	362.59	308.74	177.37	161.17	163.32
35	H-16	M	288.16	311.66	200.32	203.01	197.33
36	H-18	M	285.89	321.58	170.45	159.27	169.49
37	H-20	M	456.99	427.91	235.56	233.51	232.66
38	H-21	M	442.03	407.43	199.09	184.74	187.14
39	H-22	M	364.81	395.47	215.83	230.1	221.86
40	J-13	M	300.66	378.76	197.34	176.89	167.59
41	L-15	M	369.07	370.6	193.81	189.02	187.02
42	M-21b	M	272.5	279.65	170.2	166.26	167.38
43	M-34	M	317.61	297.97	221.74	225.47	220.78
44	M-37	M	363.53	326.83	185.98	182.06	178.84
45	S-11b	M	264.17	303.75	176.63	160.46	150.12
46	W-12	M	347.52	350.21	198.25	188.28	170.11

CSA (cm^2) Measurement Data

	Subj	Gender	C2 CSA	C5 CSA	T12 CSA	L1 CSA	L2 CSA
1	A-10	F	2.18	2.47	7.75	7.59	8.05
2	A-12	F	2.21	2.40	6.22	6.31	7.10
3	B-16ab	F	2.77	2.79	7.63	7.90	9.22
4	B-25	F	1.80	2.04	6.33	6.95	6.80
5	C-22	F	2.96	3.52	7.71	7.61	8.20
6	C-23	F	3.08	3.08	7.41	7.88	8.66
7	C-25	F	2.51	2.79	8.27	8.27	8.89
8	C-26	F	2.18	3.01	7.81	8.22	9.03
9	C-27	F	2.37	2.49	6.58	6.38	6.86
10	F-9	F	2.15	2.32	6.67	6.60	7.57
11	G-16	F	2.34	2.45	6.39	6.87	7.44
12	K-10	F	2.21	2.28	7.40	7.42	7.93
13	L-14	F	2.48	2.74	7.21	6.70	7.17
14	L-16	F	2.22	2.60	7.87	8.30	8.61
15	M-32	F	2.01	2.15	6.00	6.26	6.61
16	M-33	F	2.43	2.38	6.52	6.40	6.52
17	M-35	F	2.13	2.31	7.89	8.23	8.06
18	M-36	F	3.06	2.62	8.52	8.24	8.59
19	M-38	F	2.99	2.80	7.39	7.41	7.63
20	P-12	F	2.30	2.47	8.75	8.37	9.46
21	R-23	F	2.08	2.59	8.71	7.80	7.70
22	S-24	F	2.16	2.44	6.13	6.33	6.47
23	S-26	F	2.77	2.45	7.74	7.63	8.79
24	T-11	F	2.48	2.10	5.98	6.15	6.17
25	B-9b	M	3.33	3.59	11.31	10.24	10.41
26	B-23	M	3.02	4.41	10.40	11.00	11.60
27	B-27	M	3.16	3.32	8.46	9.23	9.50
28	C-17b	M	3.55	3.49	9.59	9.71	11.03
29	D-11	M	3.33	4.28	10.00	11.05	11.48
30	D-13	M	3.36	4.13	11.42	12.15	12.66
31	F-8	M	2.85	2.91	7.60	8.54	9.01
32	G-14a	M	2.70	2.67	10.35	10.42	10.83
33	G-15	M	3.14	3.21	9.59	10.20	10.77
34	H-13	M	2.69	3.66	10.55	10.68	11.25
35	H-16	M	2.48	3.16	7.11	7.87	8.65
36	H-18	M	3.08	3.07	9.28	9.81	9.64
37	H-20	M	3.23	2.99	9.01	9.98	10.38
38	H-21	M	3.29	3.72	10.10	10.29	10.97
39	H-22	M	3.23	3.08	9.87	10.47	10.03
40	J-13	M	3.11	3.08	9.15	9.44	9.97
41	L-15	M	2.76	2.96	10.88	10.82	11.59
42	M-21b	M	2.19	2.72	7.37	7.59	8.07
43	M-34	M	3.16	4.31	9.69	9.53	9.75
44	M-37	M	2.26	2.98	9.53	10.60	11.56
45	S-11b	M	2.90	2.90	9.18	9.35	10.30
46	W-12	M	2.40	3.13	9.31	9.29	10.27

Vertebral Height (cm) Measurement Data

	Subj	Gender	C5 Height	T12 Height	L1 Height	L2 Height
1	A-10	F	1.22	2.39	2.55	2.63
2	A-12	F	1.11	2.49	2.49	2.56
3	B-16ab	F	1.26	2.56	2.81	2.86
4	B-25	F	1.11	2.32	2.58	2.76
5	C-22	F	1.26	2.45	2.67	2.78
6	C-23	F	1.28	2.47	2.66	2.62
7	C-25	F	1.11	2.45	2.59	2.63
8	C-26	F	1.27	2.64	2.90	2.96
9	C-27	F	1.26	2.33	2.54	2.53
10	F-9	F	1.07	2.49	2.57	2.78
11	G-16	F	1.17	2.50	2.60	2.75
12	K-10	F	1.20	2.48	2.53	2.71
13	L-14	F	1.22	2.33	2.47	2.54
14	L-16	F	1.14	2.25	2.39	2.58
15	M-32	F	1.20	2.38	2.56	2.60
16	M-33	F	1.16	2.15	2.45	2.56
17	M-35	F	1.39	2.46	2.80	2.86
18	M-36	F	1.28	2.56	2.73	2.90
19	M-38	F	1.09	2.30	2.43	2.56
20	P-12	F	1.27	2.69	2.82	2.90
21	R-23	F	1.26	2.51	2.70	2.63
22	S-24	F	1.03	2.29	2.57	2.58
23	S-26	F	1.26	2.55	2.71	2.83
24	T-11	F	1.08	2.05	2.22	2.30
25	B-9b	M	1.27	2.55	2.78	2.87
26	B-23	M	1.23	2.60	2.54	2.78
27	B-27	M	1.32	2.53	2.67	2.82
28	C-17b	M	1.43	2.65	2.84	2.77
29	D-11	M	1.43	2.58	2.78	2.89
30	D-13	M	1.49	2.85	3.01	3.00
31	F-8	M	1.26	2.30	2.45	2.48
32	G-14a	M	1.38	2.54	2.87	2.92
33	G-15	M	1.40	2.56	2.65	2.74
34	H-13	M	1.39	2.50	2.64	2.70
35	H-16	M	1.29	2.65	2.74	2.76
36	H-18	M	1.23	2.53	2.75	2.77
37	H-20	M	1.46	2.21	2.41	2.70
38	H-21	M	1.55	2.88	3.05	3.14
39	H-22	M	1.27	2.39	2.46	2.85
40	J-13	M	1.37	2.71	2.91	2.98
41	L-15	M	1.33	2.57	2.59	2.67
42	M-21b	M	1.29	2.40	2.55	2.57
43	M-34	M	1.41	2.56	2.76	2.88
44	M-37	M	1.43	2.74	2.85	2.83
45	S-11b	M	1.26	2.50	2.61	2.64
46	W-12	M	1.23	2.47	2.61	2.67

Vertebral Volume (cm^3) Measurement Data

	Subj	Gender	C5 Volume	T12 Volume	L1 Volume	L2 Volume
1	A-10	F	3.00	18.53	19.38	21.20
2	A-12	F	2.67	15.47	15.70	18.20
3	B-16ab	F	3.52	19.51	22.16	26.38
4	B-25	F	2.26	14.67	17.91	18.75
5	C-22	F	4.43	18.92	20.32	22.77
6	C-23	F	3.94	18.28	20.94	22.73
7	C-25	F	3.08	20.25	21.38	23.42
8	C-26	F	3.83	20.64	23.86	26.75
9	C-27	F	3.14	15.35	16.17	17.32
10	F-9	F	2.48	16.60	16.95	21.07
11	G-16	F	2.86	15.96	17.85	20.47
12	K-10	F	2.73	18.32	18.80	21.49
13	L-14	F	3.36	16.80	16.52	18.21
14	L-16	F	2.96	17.67	19.85	22.19
15	M-32	F	2.58	14.29	16.03	17.16
16	M-33	F	2.76	14.03	15.68	16.72
17	M-35	F	3.21	19.44	23.03	23.01
18	M-36	F	3.35	21.81	22.53	24.87
19	M-38	F	3.04	17.03	18.01	19.55
20	P-12	F	3.14	23.54	23.57	27.44
21	R-23	F	3.27	21.89	21.10	20.24
22	S-24	F	2.52	14.04	16.28	16.66
23	S-26	F	3.08	19.76	20.69	24.85
24	T-11	F	2.27	12.28	13.65	14.18
25	B-9b	M	4.55	28.87	28.42	29.91
26	B-23	M	5.43	26.99	27.97	32.24
27	B-27	M	4.40	21.37	24.67	26.80
28	C-17b	M	4.99	25.41	27.60	30.51
29	D-11	M	6.12	25.81	30.77	33.14
30	D-13	M	6.16	32.58	36.52	37.93
31	F-8	M	3.67	17.46	20.93	22.32
32	G-14a	M	3.69	26.26	29.88	31.63
33	G-15	M	4.48	24.53	27.01	29.48
34	H-13	M	5.10	26.33	28.17	30.41
35	H-16	M	4.08	18.81	21.53	23.86
36	H-18	M	3.77	23.44	27.01	26.66
37	H-20	M	4.36	19.91	24.03	28.03
38	H-21	M	5.75	29.05	31.39	34.42
39	H-22	M	3.90	23.63	25.80	28.61
40	J-13	M	4.22	24.83	27.44	29.68
41	L-15	M	3.93	28.01	27.99	30.92
42	M-21b	M	3.51	17.67	19.38	20.74
43	M-34	M	6.06	24.84	26.34	28.10
44	M-37	M	4.25	26.15	30.17	32.67
45	S-11b	M	3.66	22.98	24.39	27.19
46	W-12	M	3.85	22.97	24.28	27.43

Average Measured Z-Axis Acceleration (G) and Calculated Load (N) Data

	Subj	Gender	Head Accel	Chest Accel	C2 Load	C5 Load	T12, L1, L2 Load
1	A-10	F	14.77	12.77	889.12	943.80	2808.34
2	A-12	F	15.57	14.69	962.59	1009.46	3401.41
3	B-16ab	F	13.57	12.81	805.77	853.85	3286.64
4	B-25	F	14.33	16.08	893.47	943.20	4531.60
5	C-22	F	15.81	13.88	1011.50	1070.87	3610.98
6	C-23	F	14.04	14.21	913.91	956.45	4078.90
7	C-25	F	12.08	12.82	647.12	680.62	2793.61
8	C-26	F	13.91	13.69	851.24	906.25	4092.92
9	C-27	F	16.10	14.29	960.46	1013.21	3028.27
10	F-9	F	17.46	13.32	1083.05	1151.51	2502.07
11	G-16	F	12.57	15.20	811.72	854.99	4039.92
12	K-10	F	14.93	13.91	915.06	966.77	3989.98
13	L-14	F	15.54	15.51	981.50	1034.62	5071.38
14	L-16	F	12.03	12.50	728.45	768.68	3100.43
15	M-32	F	12.89	11.28	723.05	762.83	2389.81
16	M-33	F	13.58	13.19	834.28	877.38	2907.93
17	M-35	F	14.20	15.16	862.93	916.78	4714.31
18	M-36	F	13.93	13.01	837.20	886.18	3376.95
19	M-38	F	16.08	14.32	1032.84	1090.68	3043.48
20	P-12	F	14.43	14.51	919.83	973.06	4419.14
21	R-23	F	12.37	12.87	651.21	691.50	2868.06
22	S-24	F	12.83	11.97	736.38	774.84	2683.42
23	S-26	F	14.13	12.19	870.35	921.43	2761.76
24	T-11	F	15.61	15.08	846.21	881.37	3340.31
25	B-9b	M	16.65	18.57	1090.93	1171.65	6019.44
26	B-23	M	12.47	12.42	806.91	867.86	4910.60
27	B-27	M	11.40	12.68	656.84	703.15	3543.77
28	C-17b	M	13.35	12.84	868.61	938.72	4376.22
29	D-11	M	13.12	12.91	837.51	907.91	6161.80
30	D-13	M	13.34	13.05	927.54	1005.65	4942.59
31	F-8	M	12.98	13.07	877.06	946.07	4998.21
32	G-14a	M	13.90	13.14	889.18	959.94	4794.49
33	G-15	M	15.44	14.99	854.89	1073.66	5334.15
34	H-13	M	14.58	16.38	1271.92	1368.77	5274.11
35	H-16	M	14.56	16.29	1100.68	1183.26	5875.10
36	H-18	M	13.07	15.95	878.89	947.54	7134.20
37	H-20	M	14.37	17.20	1028.29	1116.73	7456.85
38	H-21	M	13.61	14.06	1016.84	1103.10	6316.69
39	H-22	M	13.37	14.92	896.21	971.83	6692.89
40	J-13	M	12.96	12.84	838.89	900.32	4260.87
41	L-15	M	13.35	15.02	875.17	937.77	4649.16
42	M-21b	M	12.56	12.62	670.67	720.20	3562.50
43	M-34	M	12.22	14.69	974.38	1064.23	8623.34
44	M-37	M	12.87	13.29	849.90	911.09	4242.05
45	S-11b	M	16.87	15.26	1232.68	1218.23	6754.69
46	W-12	M	14.71	16.38	1008.29	1078.80	5831.53

Estimated Vertebral Stress (MPa) Data

	Subj	Gender	C2 Stress	C5 Stress	T12 Stress	L1 Stress	L2 Stress
1	A-10	F	4.07	3.82	3.62	3.70	3.49
2	A-12	F	4.36	4.21	5.47	5.39	4.79
3	B-16ab	F	2.91	3.06	4.31	4.16	3.56
4	B-25	F	4.96	4.63	7.16	6.52	6.66
5	C-22	F	3.42	3.05	4.68	4.75	4.40
6	C-23	F	2.97	3.10	5.50	5.17	4.71
7	C-25	F	2.58	2.44	3.38	3.38	3.14
8	C-26	F	3.90	3.01	5.24	4.98	4.53
9	C-27	F	4.05	4.07	4.60	4.75	4.42
10	F-9	F	5.03	4.95	3.75	3.79	3.30
11	G-16	F	3.47	3.49	6.32	5.88	5.43
12	K-10	F	4.14	4.24	5.39	5.38	5.03
13	L-14	F	3.96	3.77	7.04	7.57	7.07
14	L-16	F	3.27	2.96	3.94	3.73	3.60
15	M-32	F	3.60	3.55	3.98	3.82	3.62
16	M-33	F	3.43	3.69	4.46	4.54	4.46
17	M-35	F	4.06	3.97	5.97	5.73	5.85
18	M-36	F	2.73	3.39	3.96	4.10	3.93
19	M-38	F	3.45	3.89	4.12	4.11	3.99
20	P-12	F	3.99	3.94	5.05	5.28	4.67
21	R-23	F	3.13	2.67	3.29	3.68	3.73
22	S-24	F	3.41	3.17	4.38	4.24	4.15
23	S-26	F	3.14	3.76	3.57	3.62	3.14
24	T-11	F	3.42	4.19	5.58	5.43	5.42
25	B-9b	M	3.27	3.26	5.32	5.88	5.78
26	B-23	M	2.67	1.97	4.72	4.47	4.23
27	B-27	M	2.08	2.12	4.19	3.84	3.73
28	C-17b	M	2.45	2.69	4.56	4.51	3.97
29	D-11	M	2.51	2.12	6.16	5.57	5.37
30	D-13	M	2.76	2.43	4.33	4.07	3.90
31	F-8	M	3.08	3.25	6.58	5.85	5.55
32	G-14a	M	3.29	3.59	4.63	4.60	4.43
33	G-15	M	2.72	3.35	5.56	5.23	4.95
34	H-13	M	4.73	3.74	5.00	4.94	4.69
35	H-16	M	4.44	3.75	8.27	7.47	6.79
36	H-18	M	2.85	3.09	7.69	7.27	7.40
37	H-20	M	3.18	3.74	8.28	7.47	7.18
38	H-21	M	3.09	2.96	6.25	6.14	5.76
39	H-22	M	2.77	3.16	6.78	6.39	6.68
40	J-13	M	2.69	2.92	4.66	4.51	4.27
41	L-15	M	3.17	3.16	4.27	4.30	4.01
42	M-21b	M	3.06	2.65	4.83	4.69	4.41
43	M-34	M	3.09	2.47	8.90	9.05	8.85
44	M-37	M	3.76	3.06	4.45	4.00	3.67
45	S-11b	M	4.26	4.20	7.36	7.23	6.56
46	W-12	M	4.20	3.45	6.26	6.28	5.68

APPENDIX C: TEST CONFIGURATION AND DATA ACQUISITION SYSTEM

TEST CONFIGURATION AND

DATA ACQUISITION SYSTEM FOR THE

INVESTIGATION OF GENDER DIFFERENCES

IN VERTEBRAL BODY SIZE AND LUMBAR

LOADING DURING $+G_Z$ IMPACT ACCELERATION

(CT Study)

WITH ADDENDUM

INVESTIGATION OF EJECTION SEAT CUSHION

AND LUMBAR SUPPORT

(RSC Addendum)

Prepared under
Contract F3301-96-DJ001

March 2001

DynCorp
Human Effectiveness Division
Building 824, Area B
Wright-Patterson AFB, Ohio 45433

Table of Contents

List of Figures

List of Tables

INTRODUCTION

The DynCorp Human Effectiveness Division prepared this report for the Air Force Research Laboratory, Acceleration Effects and Escape Branch (AFRL/HEPA) under Air Force Contract F3301-96-DJ001. It describes the test facility, seat fixture, restraint configuration, test subjects, test configurations, data acquisition, and the instrumentation procedures that were used in The Investigation Of Gender Differences In Vertebral Body Size and Lumbar Loading During $+G_Z$ Impact Acceleration (CT Study). Three hundred ninety five tests were conducted between 13 SEP 1999 and 02 FEB 2001 on the Vertical Deceleration Tower.

This report also covers the addendum to the main study, Investigation of Ejection Seat Cushion and Lumbar Support (RSC Addendum). This short study caused a brief interruption in the CT Study on the VDT. Twenty-two tests were conducted between 29 February 2000 and 1 March 2000.

1. TEST FACILITY

The AFRL/HEPA Vertical Deceleration Tower (Figure A-1) was used for all of the tests. The facility consists of a 60-foot vertical steel tower, which supports a guide rail system, an impact carriage supporting a plunger, a hydraulic deceleration device and a test control and safety system. The impact carriage can be raised to a maximum height of 39 feet prior to release. After release, the carriage free falls until the plunger, attached to the undercarriage, enters a water filled cylinder mounted at the base of the tower.

The subject experiences a deceleration impulse as the plunger displaces water in the cylinder. The deceleration profile is determined by the free fall distance, the carriage and test specimen mass, the shape of the plunger and the size of the cylinder orifice. A rubber bumper is used to absorb the final impact as the carriage stops.

For these tests, plunger Number 102 was mounted under the carriage. Drop height varied depending on the test cell requirements, which ranged from 5′9″ to 11′9″.

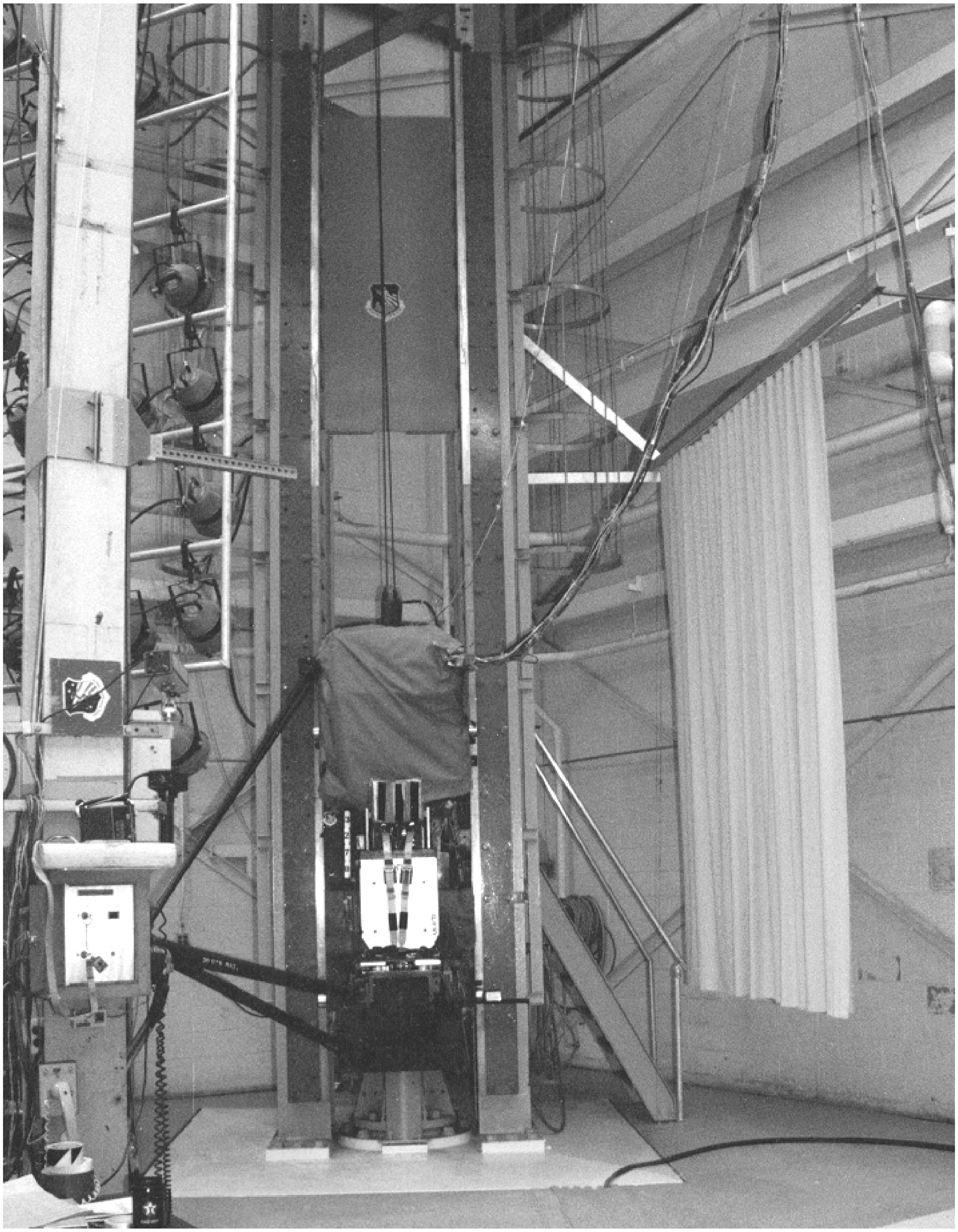

Figure A-1: Vertical Deceleration Tower

2. SEAT FIXTURE

The VIP seat fixture (Figure A-2) was used for all of the tests. The seat was designed to withstand vertical impact accelerations up to 50 G. The seat pan and seat back are adjustable.

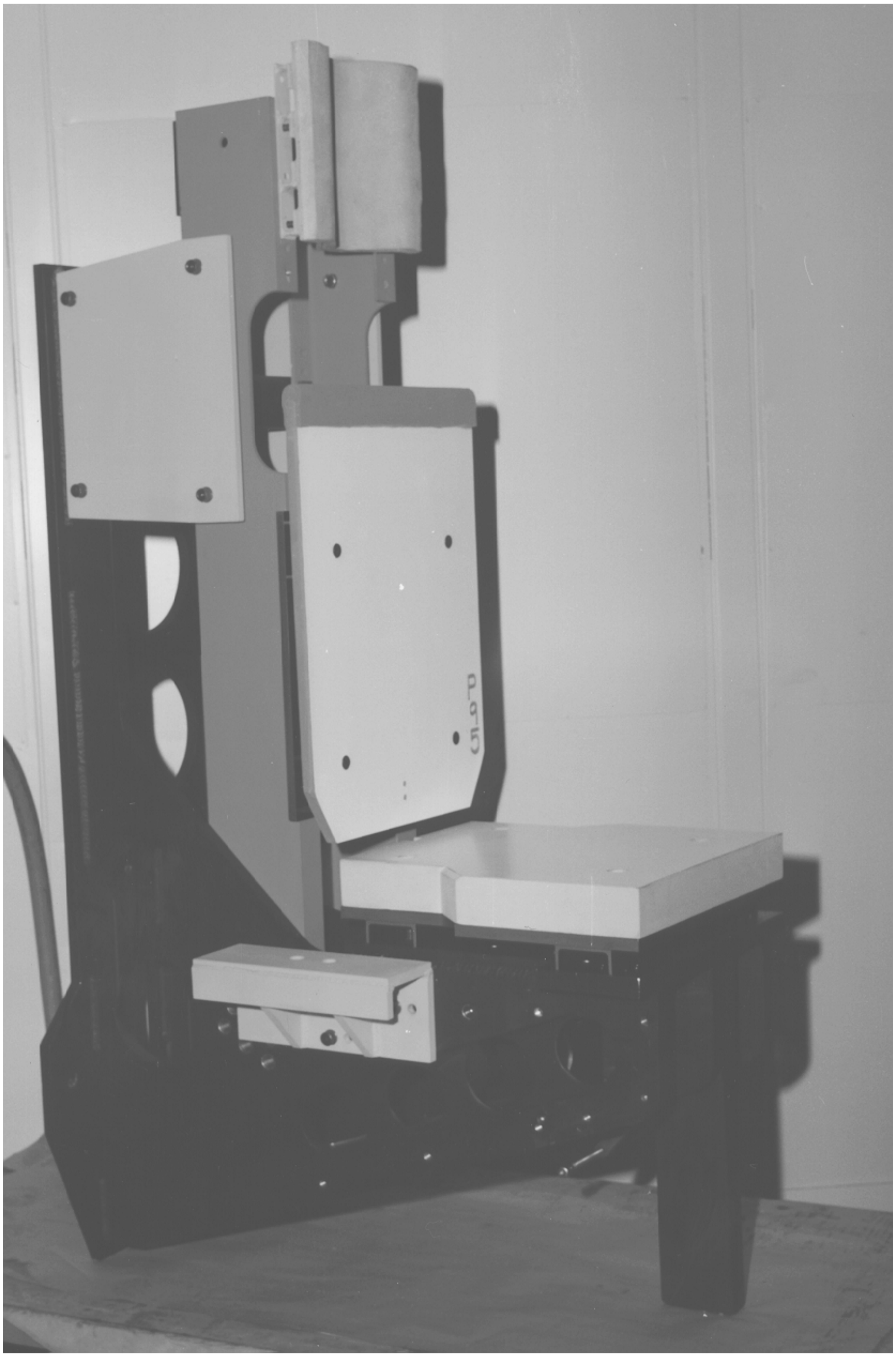

Figure A-2: Basic VIP Seat

For this study, the seat back and headrest were exactly vertical to be in line with the impact vector. The seat pan was perpendicular to the seat back. The subjects were secured in the seat with a standard USAF double shoulder strap restraint harness and lap belt configuration. The lap belt and shoulder strap were preloaded to 20 ±5 pounds, as required in the test plan.

3. TEST SUBJECT

The CT Study used human volunteer subjects from the AFRL/HEPA Impact Panel. A Hybrid III manikin was used only for a safety check at the beginning of each day's testing. All the subjects wore cutoff long john underwear with cutouts for attaching sensors. A typical subject in position for testing is shown in Figure A-3.

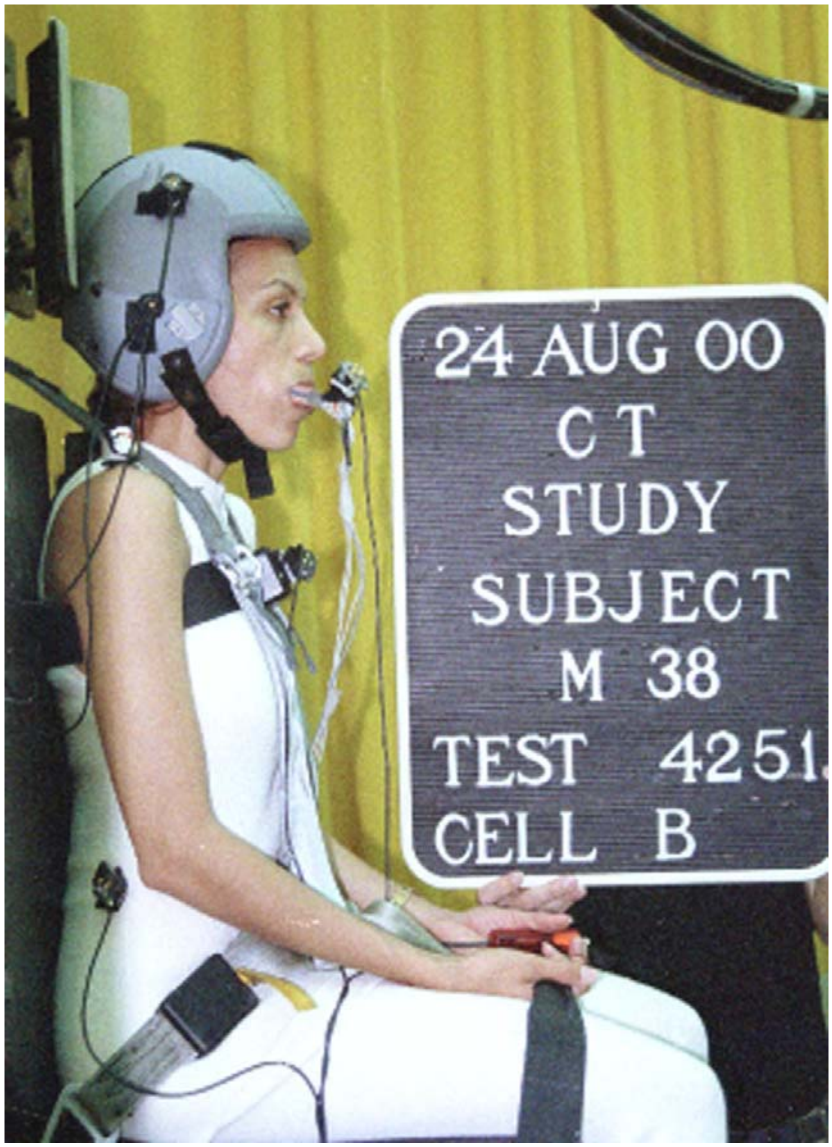

Figure A-3: CT Test Subject

The RSC addendum used only a 158-lb HYBRID III (50th percentile) manikin for testing. The manikin was dressed in full flight gear for this testing. The manikin positioned for testing is shown in Figure A-4.

Figure A-4: Manikin In Position For RSC Test

The primary test articles for the RSC study were the various seat cushions. One of the cushions from Oregon Aero is pictured in Figure A-5, and it shows the positioning of the Ride Quality Meter used for this study. The complete list of cushions tested is shown in the RSC Test Conditions Matrix (Table A-3).

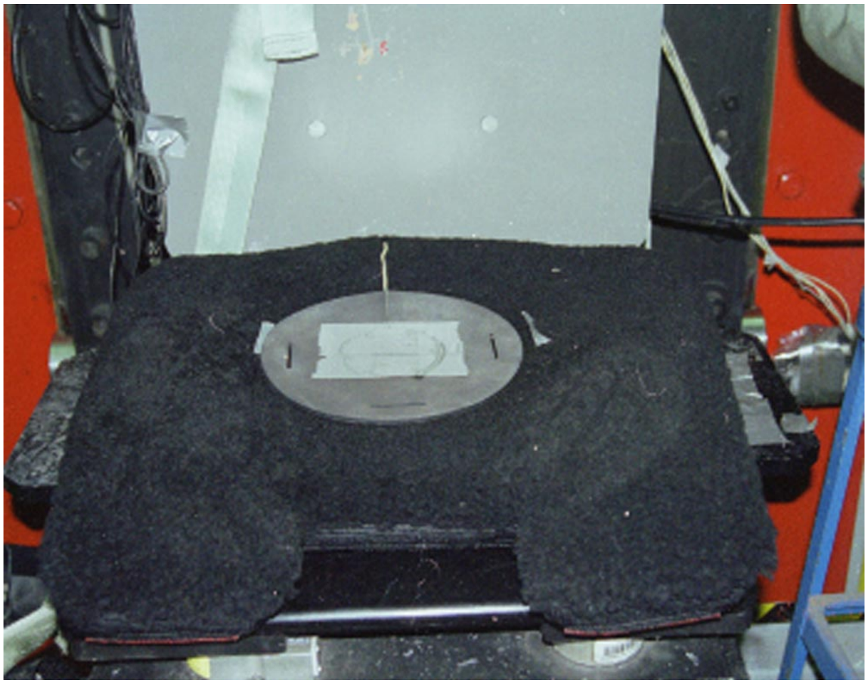

Figure A-5: Oregon Aero Seat Cushion w/ Ride Quality Meter

Table A-1 summarizes the facilities and equipment used for this study.

Equipment	ID
Facility	VDT
Pin Number	102
Seat Fixture	VIP
Seat Cushion	None
Harness	PCU-15/P
Helmet	HGU-55/P
Inertial Reel	None
Lap Belt	MA5
Oxygen Mask	None
NVG/HMD	None
Neg-G Strap	None
Head Rest Position	See Test Matrix
Seat Pan Position	Horizontal
Seat Back Position	Vertical

Table A-1: Test Equipment Summary

4. TEST CONFIGURATIONS

CT STUDY VARIABLE CONDITIONS			
CELL	**G LEVEL**	**HEADREST POSITION (inches)**	**HELMET TYPE**
A	6	0	HGU-55/P
B	8	0	HGU-55/P
C	10	0	HGU-55/P
G	10	1	VWI No added weight

Table A-2: CT Test Conditions Matrix

EJECTION SEAT CUSHION VARIABLE CONDITIONS	
Cell	**Cushion Configuration**
A	None
B	ACES II
C	Oregon Aero APECS I (Confor)
D	Oregon Aero APECS I (PORON)
E	DYN SYS 1
F	C47 w/ STIMULITE

Table A-3: RSC Test Conditions Matrix

5. INSTRUMENTATION

Accelerometers and load transducers were chosen to provide the optimum resolution over the expected test load range. Full scale data ranges were chosen to provide the expected full scale range plus 50% to assure the capture of peak signals. All transducer bridges were balanced for optimum output prior to the start of the program. The accelerometers were adjusted for the effect of gravity in software by adding the component of a 1 G vector in line with the force of gravity that lies along the accelerometer axis.

The accelerometer and load transducer coordinate systems are shown in Figure A-6. The seat coordinate system is right-handed with the z-axis parallel to the seat back and positive upward. The x-axis is perpendicular to the z-axis and positive eyes forward from the subject. The y-axis is perpendicular to the x and z-axes according to the right-hand rule.

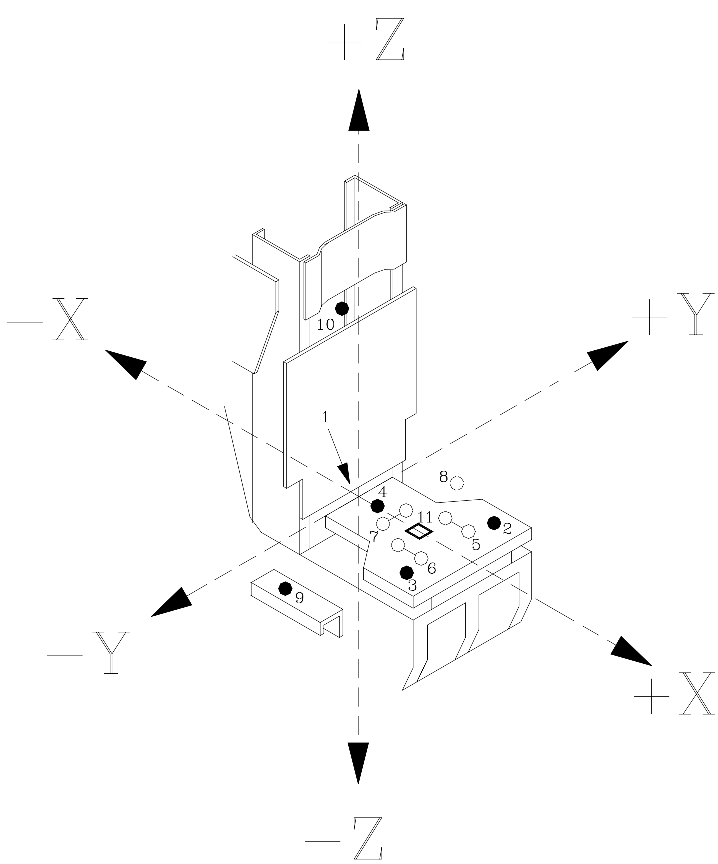

Figure A-6: VDT Coordinate Diagram

TRANSDUCER CONTACT POINT LOCATIONS IN INCHES (CM)

NO.	X	Y	Z	DESCRIPTION
1	0.00 (0.00)	0.00 (0.00)	0.00 (0.00)	SEAT REFERENCE POINT
2	17.90 (45.46)	5.00 (12.70)	-1.22 (-3.10)	LEFT SEAT Z FORCE
3	17.90 (45.46)	-5.00 (-12.70)	-1.22 (-3.10)	RIGHT SEAT Z FORCE
4	6.68 (16.96)	0.00 (0.00)	-1.22 (-3.10)	CENTER SEAT Z FORCE
5	10.00 (25.41)	6.00 (15.25)	-1.85 (-4.70)	LEFT SEAT X FORCE
6	10.00 (25.41)	-6.00 (-15.25)	-1.85 (- 4.70)	RIGHT SEAT X FORCE
7	9.26 (23.51)	1.99 (5.05)	-1.85 (-4.70)	CENTER SEAT Y FORCE
8	0.81 (2.06)	9.00 (22.86)	-1.61 (-4.10)	LEFT LAP BELT FORCE
9	0.81 (2.06)	-9.00 (-22.86)	-1.61 (-4.10)	RIGHT LAP BELT FORCE
10	-5.47 (-13.90)	0.00 (0.00)	27.39 (69.58)	SHOULDER FORCE
11	12.33 (31.31)	0.00 (0.00)	-1.69 (-4.30)	X, Y, Z ACCELERATION

Table A-4: VDT Transducer System

The origin of the seat coordinate system is designated as the seat reference point (SRP). The SRP is at the midpoint of the line segment formed by the intersection of the seat pan and seat back. All vector components (for accelerations, angular accelerations, forces, moments, etc.) were positive when the vector component (x, y and z) was in the direction of the positive axis.

The linear accelerometers were wired to provide a positive output voltage when the acceleration experienced by the accelerometer was applied in the +x, +y and +z directions. The load cells and load links were wired to provide a positive output voltage when the force exerted by the load cell on the subject was applied in the +x, +y or +z direction. All transducers, except the carriage accelerometers and the carriage velocity tachometer, were referenced to the seat coordinate system. The carriage tachometer was wired to provide a positive output voltage during freefall. The carriage accelerometers were referenced to the carriage coordinate system. The measurement instrumentation used in this test program is listed in Table A-5 for the CT study and Table A-6 for the RSC study.

Carriage velocity was measured using a Globe Industries tachometer (Model 22A672-2). The rotor of the tachometer was attached to an aluminum wheel with a rubber "O" ring around its circumference to assure good rail contact. The wheel contacted the track rail and rotated as the carriage moved, producing an output voltage proportional to the velocity.

5.1 Accelerometers

Human subject's head accelerations were measured by a bite block fitted with three linear and one angular accelerometer. Internal accelerometer packages were mounted in the manikin chest and head. They were arranged to measure linear acceleration of the chest and head in all three axes, and angular acceleration of the head about all three axes. Also, for the RSC study, a Ride Quality Meter was used. It is a thin disk with small accelerometers, which is placed under the subject. For this study there was only one accelerometer installed in the z-axis. The specific transducers used are listed by channel in Table A- 5 for the CT study and Table A-6 for the RSC study.

Carriage z acceleration was measured using one Endevco Model 2262A-200 linear accelerometer. The accelerometer was mounted on a small acrylic block and located behind the seat on the VIP seat structure. Additional linear accelerometers were used to measure acceleration at the seat pan. They were attached to a 1 x 1 x ¾-inch acrylic block and were mounted near the center of the load cell mounting plate.

5.2 Load Transducers

Shoulder/anchor forces were measured using a mix of available load cells. Specific sensors are listed by channel in Table A-5 for the CT study and Table A-6 for the RSC study. The load parameters measured are indicated below:

Shoulder x, y and z force
Seat Pan x, y, and z force
Head Rest x force
Left lap belt x, y and z force
Right lap belt x, y and z force.

The lap/vertical anchor force triaxial load cells were located on separate brackets mounted on the side of the seat frame parallel to the seat pan. The shoulder strap force triaxial load cell was mounted on the seat frame between the seat back support plate and the headrest. The load transducer locations are shown in Figure A-6.

Left, right and center seat forces were measured using three load cells and three load links. The three load cells included three Strainsert Model FL2.5U-2SPKT load cells. DynCorp fabricated the three load links (Figure A-7) using Micro Measurement Model EA-06-062TJ-350 strain gages. All measurement devices were located under the seat pan support plate. The load links were used for measuring loads in the x and y directions, two in the x direction and one in the y direction. Each load link housed a swivel ball, which acted as a coupler between the seat pan and load cell mounting plate. The Strainsert load cells were used for measuring loads in the z direction.

Figure A-7: DynCorp Load Link Diagram

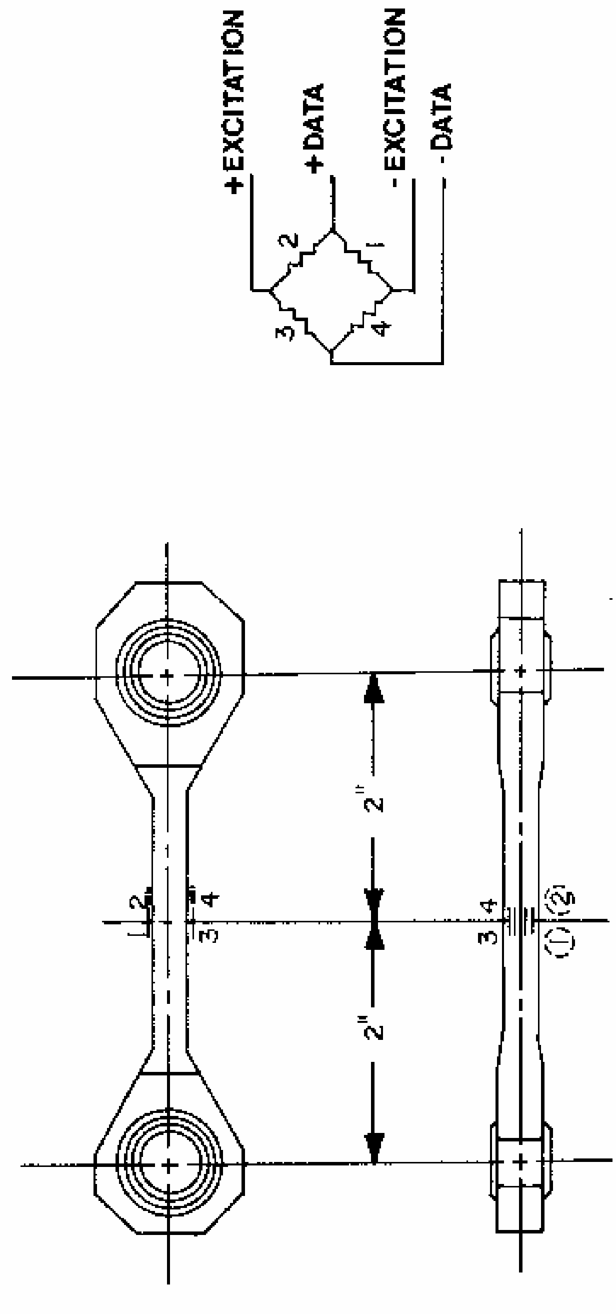

5.3 Calibration

Calibrations were performed before and after testing to confirm the accuracy and functional characteristics of the transducers. Pre-program and post-program calibrations are given in Table A-5 for the CT study and Table A-6 for the RSC study. The Precision Measurement Equipment Laboratories (PMEL) at Wright-Patterson Air Force Base calibrated all Strainsert load cells. PMEL calibrated these devices on a regular basis and provided current sensitivity and linearity data.

DynCorp used the comparison method (Ensor, 1970) to calibrate the laboratory accelerometers. A laboratory standard accelerometer, calibrated on a yearly basis by Endevco with standards traceable to the National Bureau of Standards, and a test accelerometer were mounted on a shaker table. A random noise generator drove the shaker table and the accelerometer output was collected. The frequency response and phase shift of the test accelerometer was determined by using Fourier analysis on an MS-DOS PC computer. The natural frequency and the damping factor of the test accelerometer were determined, recorded and compared to previous calibration data for that test accelerometer. Sensitivities were calculated at 40 G and 100 Hertz. The sensitivity of the test accelerometer was determined by comparing its output to the output of the standard accelerometer.

DynCorp calibrated the shoulder/lap triaxial load cells and load links. These transducers were calibrated to a laboratory standard load cell in a special test fixture. The sensitivity and linearity of each test load cell were obtained by comparing the output of the test load cell to the output of the laboratory standard under identical loading conditions. The laboratory standard load cell, in turn, is calibrated by PMEL on a regular basis.

The angular accelerometers are calibrated on a pre- and post-study basis by comparing their output to the output of a linear standard accelerometer. The angular sensors are mounted parallel to the axis of rotation of a Honeywell low inertia D.C. motor. The linear sensor is mounted perpendicular to the axis of rotation. An alternating current is supplied to the motor, which drives a constant sinusoidal angular acceleration of 100 Hertz. The sensitivity of the angular accelerometer is calculated from the RMS output voltage to match the angular value computed from the linear standard.

DynCorp regularly calibrates the velocity wheel by rotating it at approximately 2000, 4000 and 6000 revolutions per minute (RPM) and recording both the output voltage and the RPM.

6. DATA ACQUISITION

The Master Instrumentation Control Unit in the Instrumentation Station controls data acquisition. Using a comparator, a test was initiated when the countdown clock reaches zero. The comparator is set to start data collection at a pre-selected time. All data was collected at 1000 samples per second and filtered at 120 Hz cutoff frequency using a 8-pole Butterworth filter.

Prior to placing a subject in the seat, data was recorded to establish a zero reference for all transducers. The reference data was stored separately from the test data and was used in the processing of the test data. A reference mark pulse was generated to mark the Model 5600A electronic data and Selspot optical motion data at a pre-selected time after test initiation to place the reference mark close to the impact point. The reference mark time was used as the start time for data processing of the electronic and Selspot optical motion data.

6.1 Model 5600 Portable Data Acquisition System

The Model 5600A Portable Data Acquisition System (DAS), manufactured by Pacific Instruments, was used for this test program. The Model 5600A DAS is a ruggedized, DC powered, fully programmable signal conditioning and recording system for transducers and events. The Model 5600A DAS is designed to withstand a 50G shock in any direction. The Model 5600A DAS is housed in two units and its installation on top of the seat carriage is shown in Figure A-8.

Each of the two units can accommodate up to 28 transducer channels and 32 events. The signal conditioning accepts a variety of transducers including full and partial bridges, voltage, and piezoresistive. Transducer signals are amplified, filtered, digitized and recorded in onboard solid state memory. The data acquisition system is controlled through an IEEE-488.1 interface using the GPIB instruction language.

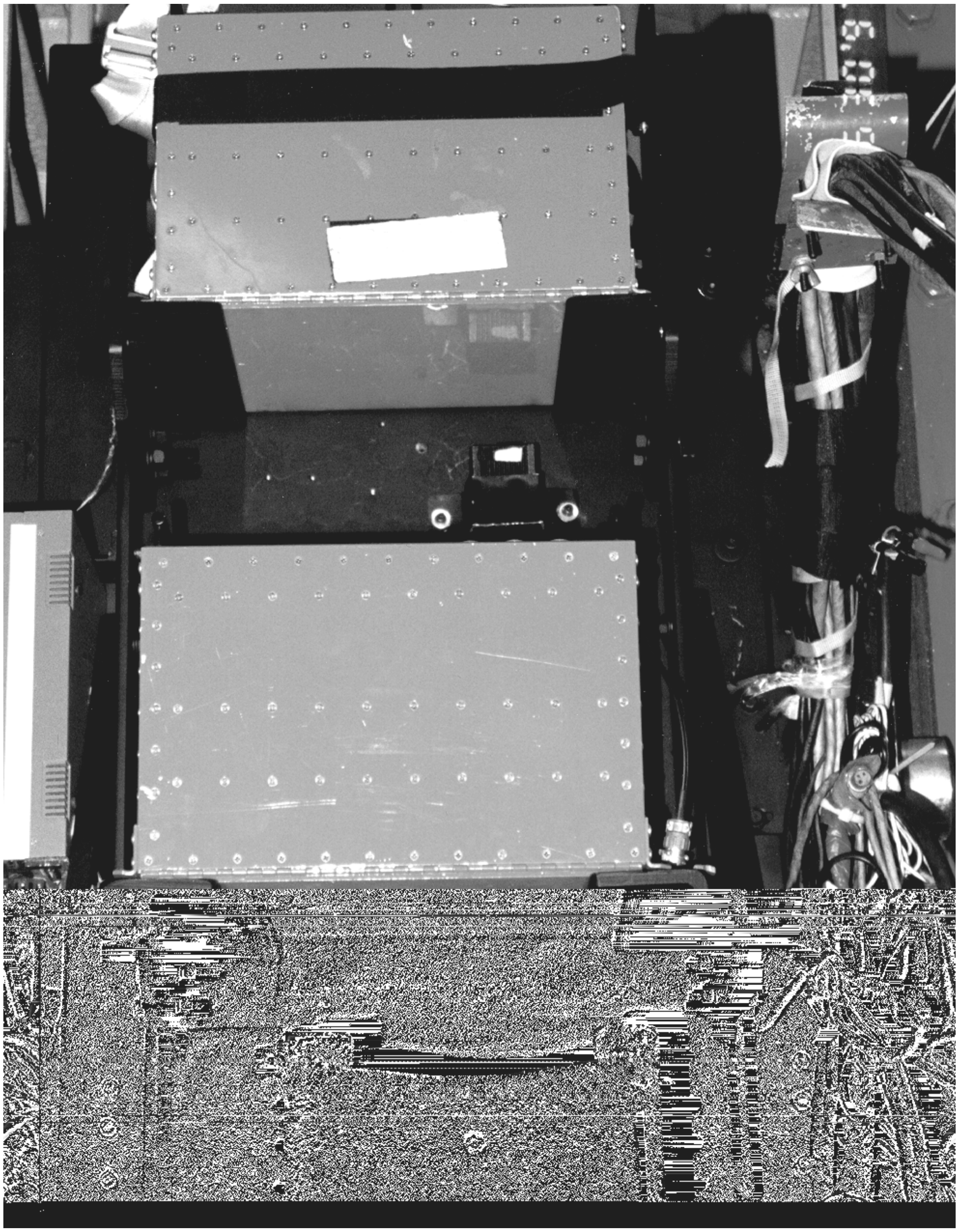

Figure A-8: Pacific Instruments 5600A

An MS Windows PC with an AT-GPIB board configures the 5600A before testing and retrieves the data after each test. The PC stores the raw data and then passes it on to the laboratory server for processing and output to permanent storage and printouts.

The DynCorp program 'TDR5600' on the PC handles the interface with the Model 5600A DAS. It includes options to compute and store zero reference voltage values; collect and store a binary zero reference data file; compute and display preload values; and collect and store binary test data. The program communicates over the GPIB interface.

Test data could be reviewed after it was converted to digital format using the "quick look" ScanEME routine. ScanEME produced a plot of the data stored for each channel as a function of time. The routine determined the minimum and maximum values of each data plot. It also calculated the rise time, pulse duration, and carriage acceleration, and created a disk file containing significant test parameters.

6.2 Selspot Motion Analysis System

The Selspot Motion Analysis System utilizes photosensitive cameras to track the motion of infrared LED targets attached to different points on the test fixture. The three-dimensional motion of the LEDs was determined by combining the images from two different Selspot cameras. The two Selspot cameras were mounted onboard the carriage. The side camera was a Selspot Model 412 (S/N 457) and the oblique camera was a Selspot Model 412 (S/N 458). Both cameras had 24mm lenses. A Motorola 68030 VME based microcomputer in the camera interface unit handles camera control and photogrammetric data collection. An MS DOS PC, running Selspot MULTILAB System software, is used to trigger the Selspot system, process the data, generate printouts, and temporarily store the data.

The Selspot System was calibrated by determining the camera locations and orientations prior to the start of the test program. The camera locations and orientations were referenced to the coordinate system of the Position Reference Structure (PRS). The PRS is shaped as a tetrahedron with reference LEDs 1, 2, 3 and 4 located at the vertices. The PRS is shown in Figure A-9.

Motion of the subjects' helmet, head, shoulder, and chest were quantified by tracking the motion of subject-mounted LEDs. Four reference LEDs were placed on the test fixture. The locations of the LEDs generally followed the guidelines provided in "Film Analysis Guides for Dynamic Studies of Test Subjects, Recommended Practice (SAE J138, March 1980)." Figure A-10 identifies the LED target locations.

Photogrammetric data was collected from the six moving and four reference LEDs at a 500 Hz sample rate during the impact. Data collection started at T = -3 seconds for 5 seconds. The data was processed starting at the reference mark time for 600 milliseconds on the Selspot Motion Analysis System. The camera image coordinates were corrected for camera vibration, converted into three-dimensional coordinates, and transformed into the seat coordinate seat.

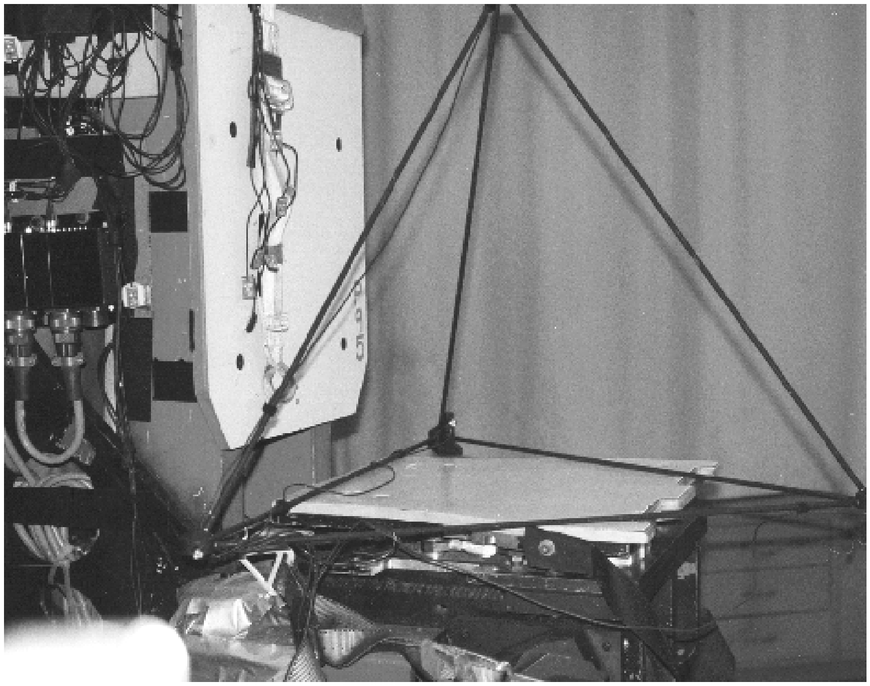

Figure A-9: SELSPOT Position Reference Structure

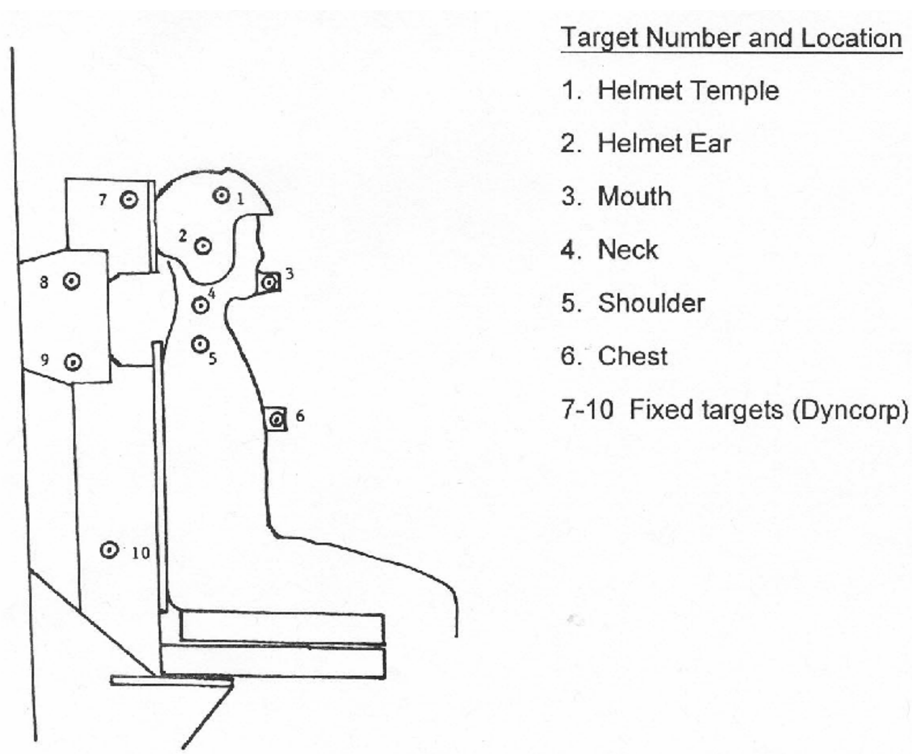

Figure A-10: SELSPOT Target Locations

6.3 Kodak High Speed Video

A Kodak Ektapro 1000 video system was also used to provide onboard coverage of each test. This video recorder and display unit is capable of recording high-speed motion up to a rate of 1000 frames per second. Immediate replay of the impact is possible in real time or in slow motion.

7. PROCESSING PROGRAMS

The Excel 2000 Workbook CtVdt.xls is used to analyze the TDR5600 DAS test data from the CT Study (Vertical Deceleration Tower Facility). CtVdt.xls contains the Visual Basic module Module1 and the forms UserForm1 and UserForm2. Module1 contains one main subroutine that calls numerous other subroutines and functions. CtVdt.xls calls the DLL functions in the Dynamic Link Libraries Scandll and Mathdll. The shortcut ctrl+r can be used to execute the Visual Basic module. The Visual Basic module displays the two user forms.

UserForm1 requests the user to enter the system acronym, study description, impact channel number, magnitude of the impact start level, start time, processing time, T0 bit number and reference mark bit number. The user has the option to find the Kodak start time, start at the reference mark time, and use the processing time as the impact window time. The user has the option to plot the channels, print out the summary sheet, print out the plots, create a test summary file for the Biodynamic Data Bank, and create a time history file for the Biodynamic Data Bank. Default values are displayed based on the last test that was analyzed. The default values are stored in worksheet “Defaults” inside the workbook.

UserForm2 requests the user to enter the test number for each test to be processed. The default test parameters are retrieved from the test sensitivity file and displayed on the form. The user may specify new values for any of the displayed test parameters. The test parameters include the subject id, weight, age, height and sitting height. Additional parameters include the cell type, nominal g level, subject type (manikin or human) and belt preload status (computed or not computed).

The workbook contains worksheets named “Channels”, “Formulas”, “Preloads”, “Plots”, “Time History File”, “Plot Pages” and “Defaults”. The “Channels” worksheet contains the channel number, channel name, database ID number, channel description, and summary sheet description for each channel. The “Formulas” worksheet contains Excel formulas and Excel functions. The “Preloads” worksheet contains the preload numbers and descriptions. The “Plots” worksheet contains the channel name, the plot description, and the plot vertical axis minimum, maximum and increment for each channel to be plotted. The "Time History File" worksheet defines the channel names for the time history files (the database time history files do not use this worksheet). The "Plot Pages" worksheet allows the user to print out selected plot pages (by default, all plot pages are printed).

CtVdt generates time histories for the carriage x, y and z axis accelerations; the carriage velocity; the seat pan x, y and z axis accelerations; the seat pan z dynamic response; the head x, y, z, Ry and resultant accelerations; the chest x, y, z, Ry and resultant accelerations; the T1 x, y, z and resultant accelerations; the angle corrected T1 x, y, z and resultant accelerations; the upper and lower headrest x axis forces and their sum; and the shoulder x, y, z and resultant forces. Time histories are also generated for the left and right lap x, y and z axis forces and resultants; the left, right and center seat back x axis forces and their sum; the seat back y force; the left and right seat back z axis forces and their sum; the tare corrected seat back z sum; the seat back resultant force; the tare corrected seat back resultant force; the left and right seat pan x axis forces and their sum; the seat pan y force; the left, right and center seat pan z axis forces and their sum; the tare corrected seat pan z sum; the seat pan resultant force; the tare corrected seat pan resultant force; and the total body x, y, z and resultant forces.

A slightly modified version of the Excel workbook CtVdt.xls was created named CtVdtCellG. The CtVdt.xls workbook was designed to calculate corrected values for the T1 x, y and z-axis accelerations that take into account the tilt angle. However, the information about the angle was not available at the time when the first processed data was requested. Consequently, the corrected T1 acceleration calculations were dropped from the CtVdtCellG workbook. CtVdtCellG was modified later to correct the chest x and z axis accelerations for the chest angle. A worksheet was added to CtVdtCellG that contains the chest angle that was measured for each cell C test. The revised version of CtVdtCellG was used to create Excel workbooks containing time histories and plots for the cell C tests.

The RSC Study was conducted during the Ct Study. The Excel workbook RscVdt.xls is used to analyze the TDR5600 DAS test data from the RSC Study. RscVdt generates time histories for the carriage x, y and z axis accelerations; the carriage velocity; the seat pan x, y and z axis accelerations; the seat pan z dynamic response; the seat cushion z and lumbar z accelerations; the chest x, y, z, Ry and resultant accelerations; the upper and lower headrest x axis forces and their sum; and the shoulder x, y, z and resultant forces. Time histories are also generated for the left and right lap x, y and z axis forces and resultants; the left, right and center seat back x axis forces and their sum; the seat back y force; the left and right seat back z axis forces and their sum; the tare corrected seat back z sum; the seat back resultant force; the tare corrected seat back resultant force; the left and right seat pan x axis forces and their sum; the seat pan y force; the left, right and center seat pan z axis forces and their sum; the tare corrected seat pan z sum; the seat pan resultant force; the tare corrected seat pan resultant force; the total body x, y, z and resultant forces; the lumbar x, y, z and resultant forces; and the lumbar x, y, z and resultant torques. The lumbar z, seat cushion z and seat pan z accelerations are filtered at 60 Hz using the IIR Butterworth filter algorithm contained in SAE J211. The DRI for the seat cushion z accelerometer is also calculated.

Values for the preimpact level and the extrema for each time history are stored in the Excel worksheet summary file and printed out as a summary sheet for each test. The retraction time is calculated and printed out on the summary sheet. The time histories are also plotted with up to six plots per page. The user has the option to create test summary information and Excel workbooks containing the time histories for the Biodynamic Data Bank.

Table A-5: CT Instrumentation Setup and Calibration Log

DYNCORP PROGRAM SETUP AND CALIBRATION LOG

PROGRAM: AN INVESTIGATION OF GENDER DIFFERENCES IN VERTEBRAL BODY SIZE AND LUMBAR LOADING DURING +GZ IMPACT ACCELERATION (CT STUDY)

TEST DATES: 13 SEPT 1999 - 2 Feb 2001

TEST NUMBERS: 3902 - 4048, 4071-4318

STUDY NUMBER: 199906

SAMPLE RATE: 1K

FACILITY: VERTICAL DROP TOWER

FILTER FREQUENCY: 120 Hz

DATA COLLECTION SYSTEM: PACIFIC INSTRUMENTS

TRANSDUCER RANGE (VOLTS): 10 v

DATA CHANNEL	DATA POINT	TRANSDUCER MFG. & MODEL	SERIAL NUMBER	PRE-CAL DATE	PRE-CAL SENS	POST-CAL DATE	POST-CAL SENS	% Δ	EXC. VOL.	AMP GAIN	FULL SCALE	NOTES
0	VELOCITY	GLOBE 22A672-2	4	13-Nov-98	.158 v/ft/sec	1-Dec-99	.153 v/ft/sec	-3.2	10 V	1	63.3 FT/SEC	Raw sensitivity=.1857 v/rev/sec: (12in/ft / 4.56 in/rev) x .1857 v/r/s = .4887 rev/ft; Atten @ 3.094; .4887 v/ft x (1 / 3.094)=.158v/ft/sec Due for calibration
0	VELOCITY	GLOBE 22A672-2	4	1-Dec-99	.153 v/ft/sec	14-Mar-01	.152 v/ft/sec	-0.7	10V	1	65.4 FT/SEC	Raw sensitivity=.1755 v/rev/sec; (12in/ft / 4.44 in/rev) x .1755 v/r/s = .4743 rev/ft; Atten @ 3.094: .4743 v/ft x (1 / 3.094)=. 1533v/ft/sec
1	CARRIAGE X ACCEL (G)	ENDEVCO 7264-200	CC99H	12-Aug-99	3.0344 mv/g	8-Mar-01	2.9949 mv/g	-1.3	10V	100	33 G	
2	CARRIAGE Y ACCEL (G)	ENDEVCO 2262A-200	CC86H	12-Aug-99	2.8407 mv/g	8-Mar-01	2.8054 mv/g	-1.2	10V	200	17.6 G	
3	CARRIAGE Z ACCEL (G)	ENDEVCO 2262A-200	MH82	3-Feb-99	2.0616 mv/g	8-Mar-01	2.0644 mv/g	.1	10V	200	24.3 G	

DYNCORP PROGRAM SETUP AND CALIBRATION LOG

DATA CHANNEL	DATA POINT	TRANSDUCER MFG. & MODEL	SERIAL NUMBER	PRE-CAL		POST-CAL		%Δ	EXC. VOL.	AMP GAIN	FULL SCALE	NOTES
				DATE	SENS	DATE	SENS					
4	SEAT PAN X ACCEL (G)	ENDEVCO 7264-200	BH81H	12-Aug-99	3.3031 mv/g	7-Mar-01	3.2423 mv/g	-1.8	10V	100	30.3 G	
5	SEAT PAN Y ACCEL (G)	ENDEVCO 7264-200	BH87H	12-Aug-99	3.0472 mv/g	7-Mar-01	2.9884 mv/g	-2	10V	100	32.8 G	
6	SEAT PAN Z ACCEL (G)	ENDEVCO 7264-200	BY77H	12-Aug-99	3.3837 mv/g	7-Mar-01	3.3271 mv/g	1.7	10V	100	29.8 G	
7	HEAD X ACCEL (G)	ENDEVCO 2264-200	BW10	27-Aug-99	2.5523 mv/g	23-Dec-99	2.5707 mv/g	.7	10 V	200	19.6 G	Channel went bad on test 3935. Moved to channel 45
45	HEAD X ACCEL (G)	ENDEVCO 2264-200	BW10	27-Aug-99	2.5523 mv/g		NA		10V	200	19.6 G	Was channel 8 until it went bad. Used on test 3936 and after. Went bad on test 3981. Moved to channel 48
48	HEADX ACCEL (G)	ENDEVCO 2264-200	BW10	27-Aug-99	2.5523 mv/g		NA		10 V	200	19.6 G	Was channel 45 until it went bad. Used on test 3982 and after. Broke on 3982.Replaced with CM18H. New sens 3.248 mv/g.
48	HEAD X ACCEL (G)	ENDEVCO 2264-200	CM18H	15-Sep-99	3.248 mv/g		NA		10V	200	15.4 G	Used on test 3963 and after. Channel went bad on test 4087.
49	HEAD X ACCEL (G)	ENDEVCO 2264-200	CM18H	15-Sep-99	3.248 mv/g	8-Mar-01	3.214 mv/g	-.9	10V	200	15.4 G	Used on test 4088 and after.
8	HEAD Y ACCEL (G)	ENDEVCO 2264-200	BP10	27-Aug-99	2.5141 mv/g		NA		10V	200	19.9 G	Channel went bad on test 3908. Moved to channel 43

DYNCORP PROGRAM SETUP AND CALIBRATION LOG

DATA CHANNEL	DATA POINT	TRANSDUCER MFG. & MODEL	SERIAL NUMBER	PRE-CAL DATE	PRE-CAL SENS	POST-CAL DATE	POST-CAL SENS	% Δ	EXC. VOL.	AMP GAIN	FULL SCALE	NOTES
43	HEAD Y ACCEL (G)	ENDEVCO 2264-200	BP10	27-Aug-99	2.5141 mv/g	8-Mar-OI	2.4773 mv/g	-1.5	10V	200	19.9 G	Was channel 8 until it went bad. Used on test 3909 and after.
9	HEADZACCEL (G)	ENDEVCO 2264-200	BN38	27-Aug-99	3.3102 mv/g	8-Mar-OI	3.2777 mv/g	-1	10V	50	60.4 G	
10	HEAD RYANG ACCEL (RAD/SEC2)	ENDEVCO 7302BM2	10016	23-Aug-99	45.34 uv/rad/sec2		NA		10V	50	4411.1 RAD/SEC2	Broke on test 3991. Replaced with 10024 and new sens 45.73 uv/rad/sec2
10	HEAD RYANG ACCEL (RAD/SEC2)	ENDEVCO 7302BM2	10024	14-Jun-99	45.73 uv/rad/sec2	8-Mar-OI	45.24 uv/rad/sec2	-1.1	10 V	50	4373.5 RAD/SEC2	Used on test 3992 and after.
11	CHEST X ACCEL (G)	ENDEVCO 7264-200	CF48H	24-Aug-99	-2.3091 mv/g	8-Mar-OI	2.2737 mv/g	-1.5	10V	200	21.7 G	USE NEGATIVE SENSITIVITY
12	CHESTY ACCEL (G)	ENTRAN EGE-72-200	95195106-002	23-Aug-99	2.7064 mv/g	8-Mar-OI	2.6569 mv/g	-1.8	10V	100	36.9 G	
13	CHESTZ ACCEL (G)	ENTRAN EGE-72-200	95H95H14-A07	23-Aug-99	2.6018 mv/g	8-Mar-OI	2.5494 mv/g	-2	10 V	50	78.9 G	
14	CHEST RY ANG ACCEL (RAD/SEC2)	ENDEVCO 7302BM2	10018	23-Aug-99	58.33 uv/rad/sec2		NA		10V	50	3428.8 RAD/SEC2	Broke on test 4036. Replaced with 10022 and new sens of 48.07 uv/rad/sec2
14	CHEST RY ANG ACCEL (RAD/SEC2)	ENDEVCO 7302BM2	10022	10-Mar-00	48.07 uv/rad/sec2	8-Mar-01	46.6 uv/rad/sec2	-3.1	10 V	50	4160.9 RAD/SEC2	Used on test 4037 and after.

DYNCORP PROGRAM SETUP AND CALIBRATION LOG

DATA CHANNEL	DATA POINT	TRANSDUCER MFG. & MODEL	SERIAL NUMBER	PRE-CAL		POST-CAL		%Δ	EXC. VOL.	AMP GAIN	FULL SCALE	NOTES
				DATE	SENS	DATE	SENS					
15	T1 X ACCEL (G)	ENTRAN EGAXT-.100	87E87D29-V11	13-Aug-99	-.9940 mv/g	7-Mar-01	.9714 mv/g	-1.6	10 V	500	20.1 G	Use negative sensitivity. BROKE ON TEST 4036. Replaced with 21M3T4-v23-3 and new sens of 1.3772 mv/g.
15	T1 X ACCEL (G)	ENTRAN EGAXT-100	21M3T4-V23-3	24-Feb-00	1.3772 mv/g	7-Mar-01	1.4027 mv/g	1.9	10 V	500	15G	Used on test 4037 and after.
16	T1 Y ACCEL (G)	ENTRAN EGAXT-100	87E87D29-V12	13-Aug-99	1.0054 mv/g	7-Mar-01	.97 mv/g	-1.9	10V	200	49.7 G	
17	T1 Z ACCEL (G)	ENTRAN EGAXT-100	87E87D29-V13	13-Aug-99	.9884 mv/g	7-Mar-01	.9884 mv/g	0	10V	200	50.6 G	
18	LEFT SEAT PAN Z FORCE (LB)	STRAINCERT FL2.5U-2SPKT	Q-3294-3	3-May-99	-7.99 uv/lb	12-Mar-01	7.94 uv/lb	-.6	10 V	200	6257.8 LB	USE NEGATIVE SENSITIVITY
19	RIGHT SEAT PAN Z FORCE (LB)	STRAINCERT FL2.5U-2SPKT	Q-3294-6	4-Feb-99	-7.94 uv/lb	12-Mar-01	7.88 uv/lb	-.8	10V	200	6297.2 LB	USE NEGATIVE SENSITIVITY
20	CENTER SEAT PAN Z FORCE (LB)	STRAINCERT FL2.5U-2SPKT	Q-3294-4	3-May-99	-8.00 uv/lb	12-Mar-01	7.87 uv/lb	-1.7	10V	200	6250 LB	USE NEGATIVE SENSITIVITY
21	LEFT SEAT PAN X FORCE (LB)	AAMRL/ DYN LOAD LINK	3A	4-Nov-99	10.90 uv/lb	13-Mar-01	10.62 uv/lb	-2.6	10 V	1000	917.4 LB	
22	RIGHT SEAT PAN X FORCE (LB)	AAMRL/ DYN LOAD LINK	1	4-Nov-98	11.44 uv/lb	13-Mar-01	11.16 uv/lb	-2.5	10V	1000	874.1 LB	

DYNCORP PROGRAM SETUP AND CALIBRATION LOG

DATA CHANNEL	DATA POINT	TRANSDUCER MFG. & MODEL	SERIAL NUMBER	PRE-CAL		POST-CAL		% Δ	EXC. VOL.	AMP GAIN	FULL SCALE	NOTES
				DATE	SENS	DATE	SENS					
23	SEAT PAN Y FORCE (LB)	AAMRL/DYN LOAD LINK	2	4-Nov-98	-11.25 uv/lb	13-Mar-01	10.91 uv/lb	-3.1	10 V	1000	888.9 LB	USE NEGATIVE SENSITIVITY
24	LEFT SEAT BACK X FORCE (LB)	STRAINCERT FL1U-2SGKT	Q-8415-1	10-Apr-99	-19.85 uv/lb	12-Mar-01	19.75 uv/lb	-.5	10V	1000	503.8 LB	USE NEGATIVE SENSITIVITY
25	RIGHT SEAT BACK X FORCE (LB)	SRTAINCERT FL 1 U-2SGKT	Q-8415-2	10-Apr-99	-19.85 uv/lb	12-Mar-01	19.65 uv/lb	-1	10 V	1000	503.8 LB	USE NEGATIVE SENSITIVITY
26	CENTER BACK X FORCE (LB)	STRAINCERT FL 1 U-2SGKT	Q-8415-3	12-Apr-99	-19.86 uv/lb		NA		10V	1000	503.5 LB	USE NEGATIVE SENSITIVITY Channel went bad on test 3938. Moved to channel 46
46	CENTER BACK X FORCE (LB)	STRAINCERT FL 1 U-2SGKT	Q-8415-3	12-Apr-99	-19.86 uv/lb	12-Mar-01	19.75 uv/lb	-.6	10V	1000	503.5 LB	USE NEGATIVE SENSITIVITY
27	LEFT SEAT BACKZ FORCE (LB)	AAMRL/DYN LOAD LINK	8	26-Aug-98	-10.99 uv/lb	12-Mar-01	10.9 uv/lb	-.8	10 V	1000	909.9 LB	USE NEGATIVE SENSITIVITY
28	EVENT /T=O								0	1		Bit 0 is Event Bit 1 is T=O
29	RIGHT SEAT BACKZ FORCE (LB)	AAMRL/ DYN LOAD LINK	9	24-Aug-98	-11.54 uv/lb		NA		10 V	1000	866.6 LB	USE NEGATIVE SENSITIVITY Channel went bad on test 3908. Moved to channel 44.
44	RIGHT SEAT BACKZ FORCE (LB)	AAMRL/ DYN LOAD LINK	9	24-Aug-98	-11.54 uv/lb	12-Mar-01	11.21 uv/lb	-2.9	10V	1000	866.6 LB	USE NEGATIVE SENSITIVITY

DYNCORP PROGRAM SETUP AND CALIBRATION LOG

DATA CHANNEL	DATA POINT	TRANSDUCER MFG. & MODEL	SERIAL NUMBER	PRE-CAL		POST-CAL		% Δ	EXC. VOL.	AMP GAIN	FULL SCALE	NOTES
				DATE	SENS	DATE	SENS					
30	SEAT BACK Y FORCE (LB)	AAMRL/ DYN LOAD LINK	10	24-Aug-98	-10.69 uv/lb	12-Mar-01	10.41 uv/lb	-2.7	10 V	1000	935.5 LB	USE NEGATIVE SENSITIVITY
31	LEFT LAP X FORCE (LB)	MICH-SCI4000	2	26-Aug-99	-13.87 uv/lb	13-Mar-01	14.05 uv/lb	1.3	10V	500	1442 LB	USE NEGATIVE SENSITIVITY
32	LEFT LAP Y FORCE (LB)	MICH-SCI 4000	2	26-Aug-99	-13.32 uv/lb	13-Mar-01	13.43 uv/lb	.8	10V	500	1501.6 LB	USE NEGATIVE SENSITIVITY
33	LEFT LAP Z FORCE (LB)	MICH-SCI 4000	2	26-Aug-99	13.24 uv/lb	13-Mar-01	13.6 uv/lb	2.6	10V	500	1510.6 LB	
34	RIGHTLAP X FORCE (LB)	MICH-SCI 4000	5	16-Dec-98	-14.08 uv/lb	13-Mar-01	13.71 uv/lb	-2.7	10V	500	1420.4 LB	USE NEGATIVE SENSITIVITY
35	RIGHT LAP Y FORCE (LB)	MICH-SCI4000	5	16-Dec-98	14.52 uv/lb	13-Mar-01	14.23 uv/lb	-2	10V	500	1377.48 LB	
36	RIGHTLAP Z FORCE (LB)	MICH-SCI4000	5	16-Dec-98	14.15 uv/lb	13-Mar-01	13.81 uv/lb	-2.5	10V	500	1413.4 LB	
37	SHOULDER X FORCE (LB)	MICH-SCI4000	4	16-Dec-98	13.77 uv/lb		NA		10V	500	1452.4 LB	Channel went bad on test 3938. Moved to channel47.
47	SHOULDER X FORCE (LB)	MICH-SCI 4000	4	16-Dec-98	13.77 uv/lb	13-Mar-01	13.5 uv/lb	-2	10V	500	1452.4 LB	

DYNCORP PROGRAM SETUP AND CALIBRATION LOG

DATA CHANNEL	DATA POINT	TRANSDUCER MFG. & MODEL	SERIAL NUMBER	PRE-CAL		POST-CAL		% Δ	EXC. VOL.	AMP GAIN	FULL SCALE	NOTES
				DATE	SENS	DATE	SENS					
38	SHOULDER Y FORCE (LB)	MICH-SCI4000	4	16-Dec-98	-14.25 uv/lb	13-Mar-01	13.69 uv/lb	-2.6	10V	1000	701.8 LB	USE NEGATIVE SENSITIVITY
39	SHOULDER Z FORCE (LB)	MICH-SCI 4000	4	16-Dec-98	-13.76 uv/lb	13-Mar-01	13.46 uv/lb	2.2	10V	500	1453.5 LB	USE NEGATIVE SENSITIVITY
41	LOWER HEADREST X FORCE (LB)	STRAINCERT FL 1 U-2SPKT	0-5297-3	6-Feb-99	-19.91 uv/lb	12-Mar-01	19.53 uv/lb	-1.9	10V	1000	502.3 LB	USE NEGATIVE SENSITIVITY
42	UPPER HEADREST X FORCE (LB)	STRAINCERT FL 1 U-2SPKT	0-5297-4	16-Feb-99	-20.13 uv/lb	12-Mar-01	19.64 uv/lb	-2.5	10V	1000	496.6 LB	USE NEGATIVE SENSITIVITY
50	HEAD X ACCEL (G)	ENTRAN EGE-72-200	93C93C19-R08	7-Sep-00	2.1959 mv/g	8-Mar-01	2.1719 mv/g	-1.1	10V	200	22.8 G	Used on test 4287 and after. To be used only for subj C-25.
51	HEAD Y ACCEL (G)	ENTRAN EGE-72-200	93C93C19-R09	26-Sep-00	2.3204 mv/g	8-Mar-01	2.302 mv/g	-.8	10V	200	21.5 g	Used on test 4287 and after. To be used only for subj C-25
52	HEAD Z ACCEL (G)	ENTRAN EGE-72-200	93C93C19-R10	26-Sep-00	2.1917 mv/g		NA		10V	50	91.3 G	Used on teat 4287 and after. To be used only for subj C-25. Channel bad on test 4291. Moved to channel 55
55	HEAD Z ACCEL (G)	ENTRAN EGE-72-200	93C93C19-R10	26-Sep-00	2.1917 mv/g	8-Mar-01	2.1634 mv/g	-1.3	10V	50	91.3G	Used on teat 4292 and after. To be used only for subj C-25.
54	HEAD RY ANG ACCEL (RAD/SEC2)	ENDEVCO 7302B	F93M	23-Aug-99	-4.727 uv/rad/sec2	8-Mar-01	4.703 mv/g	-.5	10V	500	4231 RAD/SEC2	USE NEGATIVE SENSITIVITY Used on test 4287 and after. To be used only for subj C-25.

Table A-6: RSC Instrumentation Setup and Calibration Log

DYNCORP PROGRAM SETUP AND CALIBRATION LOG

PROGRAM: AN INVESTIGATION OF GENDER DIFFERENCES IN VERTEBRAL BODY SIZE AND LUMBAR LOADING DURING +GZ IMPACT ACCELERATION (RSC ADDENDUM)

TEST DATES: 29 FEB 2000 - 1 MAR 2000

TEST NUMBERS: 4049 - 4070

STUDY NUMBER: 200001

SAMPLE RATE: 1K

FACILITY: VERTICAL DROP TOWER

FILTER FREQUENCY: 120 Hz

DATA COLLECTION SYSTEM: PACIFIC INSTRUMENTS

TRANSDUCER RANGE (VOLTS): 10 v

DATA CHANNEL	DATA POINT	TRANSDUCER MFG. & MODEL	SERIAL NUMBER	PRE-CAL DATE	PRE-CAL SENS	POST-CAL DATE	POST-CAL SENS	%Δ	EXC. VOL.	AMP GAIN	FULL SCALE	NOTES
0	VELOCITY	GLOBE 22A672-2	4	1-Dec-99	.153 v/ft/sec	14-Mar-01	.152 v/ft/sec	-0.7	10V	1	65.4 FT/SEC	Raw sensitivity=.1755 v/rev/sec; (12in/ft / 4.44 in/rev) x .1755 v/r/s = .4743 rev/ft; Allen @ 3.094; .4743 v/ft x (1 / 3.094)= .1533v/ft/sec
1	CARRIAGE X ACCEL (G)	ENDEVCO 7264-200	CC99H	12-Aug-99	3.0344 mv/g	6-Mar-01	2.9949 mv/g	-1.3	10V	100	33 G	
2	CARRIAGE Y ACCEL(G)	ENDEVCO 2262A-200	CC66H	12-Aug-99	2.8407 mv/g	6-Mar-01	2.8054 mv/g	-1.2	10 V	200	17.6 G	
3	CARRIAGE Z ACCEL (G)	ENDEVCO 2262A-200	MH82	3-Feb-99	2.0616 mv/g	8-Mar-01	2.0644 mv/g	.1	10V	200	24.3 G	
4	SEAT PAN X ACCEL (G)	ENDEVCO 7264-200	BH81H	12-Aug-99	3.3031 mv/g	7-Mar-01	3.2423 mv/g	-1.8	10V	100	30.3G	
5	SEAT PAN Y ACCEL (G)	ENDEVCO 7264-200	BH87H	12-Aug-99	3.0472 mv/g	7-Mar-01	2.9864 mv/g	-2	10 V	100	32.8 G	

DYNCORP PROGRAM SETUP AND CALIBRATION LOG

DATA CHANNEL	DATA POINT	TRANSDUCER MFG. & MODEL	SERIAL NUMBER	PRE-CAL		POST-CAL		%Δ	EXC. VOL.	AMP GAIN	FULL SCALE	NOTES
				DATE	SENS	DATE	SENS					
6	SEAT PAN Z ACCEL (G)	ENDEVCO 7264-200	BY77H	12-Aug-99	3.3837 mv/g	7-Mar-01	3.3271 mv/g	1.7	10V	100	29.6 G	
48	HEAD X ACCEL (G)	ENDEVCO 2264-200	CM18H	15-Sep-99	3.248 mv/g		NA		10V	200	15.4G	Broke on test 3962. Used on test 3963 and after. Channel went bad on test 4087.
49	HEAD X ACCEL (G)	ENDEVCO 2264-200	CM18H	15-Sep-99	3.248 mv/g	8-Mar-01	3.214 mv/g	-.9	10V	200	15.4 G	Used on test 4088 and after.
7	SEAT CUSHION Z ACCEL (G)	ENDEVCO 2264-200	BW10	23-Dec-99	-2.5707 mv/g	2-Mar-00	2.5686 mv/g	.7	10 V	200	19.4 G	Channel repaired. This test point inserted on test 4049. Used on test 4049 thru 4070 on RSC study. Use negative sensitivity
43	HEAD Y ACCEL (G)	ENDEVCO 2264-200	BP10	27-Aug-99	2.5141 mv/g	8-Mar-01	2.4773 mv/g	11.5	10V	200	19.9 G	Was channel 8 until it went bad. Used on test 3909 and after.
8	INT LUMBAR Z ACCEL (G)	ENTRAN EGE-72-200	93C93C19-R14	15-Sep-99	2.2822 mv/g	2-Mar-00	2.2836 mv/g	.1	10V	200	21.9 G	Channel repaired. This test point inserted on test 4049. Used on test 4049 thru 4070 on RSC study.
9	HEAD Z ACCEL (G)	ENDEVCO 2264-200	BN36	27-Aug-99	3.3102 mv/g	8-Mar-01	3.2777 mv/g	-1	10 V	50	60.4 G	
10	HEAD RY ANG ACCEL (RAD/SEC2)	ENDEVCO 7302BM2	10024	14-Jun-99	45.73 uv/rad/sec2	8-Mar-01	45.24 uv/rad/sec2	-1.1	10V	50	4373.5 RAD/SEC2	Used on test 3992 and after.
11	CHEST X ACCEL (G)	ENDEVCO 7264-200	CF46H	24-Aug-99	-2.3091 mv/g	8-Mar-01	2.2737 mv/g	-1.5	10V	200	21.7 G	USE NEGATIVE SENSITIVITY

DYNCORP PROGRAM SETUP AND CALIBRATION LOG

DATA CHANNEL	DATA POINT	TRANSDUCER MFG. & MODEL	SERIAL NUMBER	PRE-CAL		POST-CAL		%Δ	EXC. VOL.	AMP GAIN	FULL SCALE	NOTES
				DATE	SENS	DATE	SENS					
12	CHEST Y ACCEL (G)	ENTRAN EGE-72-200	95195106-D02	23-Aug-99	2.7064 mv/g	8-Mar-01	2.6569 mv/g	-1.8	10V	100	36.9 G	
13	CHEST Z ACCEL (G)	ENTRAN EGE-72-200	95H95H14-A07	23-Aug-99	2.6018 mv/g	8-Mar-01	2.5494 mv/g	-2	10V	50	78.9 G	
14	CHEST RY ANG ACCEL (RAD/SEC2)	ENDEVCO 7302BM2	10022	10-Mar-00	48.07 uv/rad/sec2	8-Mar-01	46.6 uv/rad/sec2	-3.1	10V	50	4160.9 RAD/SEC2	Used on test 4037 and after.
18	LEFT SEAT PAN Z FORCE (LB)	STRAINCERT FL2.5U-2SPKT	Q-3294-3	3-May-99	-7.99 uv/lb	12-Mar-01	7.94 uv/lb	-.6	10V	200	6257.8 LB	USE NEGATIVE SENSITIVITY
19	RIGHT SEAT PAN Z FORCE (LB)	STRAINCERT FL2.5U-2SPKT	Q-3294-6	4-Feb-99	-7.94 uv/lb	12-Mar-01	7.88 uv/lb	-.8	10V	200	6297.2 LB	USE NEGATIVE SENSITIVITY
20	CENTER SEAT PAN Z FORCE (LB)	STRAINCERT FL2.5U-2SPKT	Q-3294-4	3-May-99	-8.00 uv/lb	12-Mar-01	7.87 uv/lb	-1.7	10V	200	6250 LB	USE NEGATIVE SENSITIVITY
21	LEFT SEAT PAN X FORCE (LB)	AAMRL/ DYN LOAD LINK	3A	4-Nov-99	10.90 uv/lb	13-Mar-01	10.62 uv/lb	-2.6	10V	1000	917.4 LB	
22	RIGHT SEAT PAN X FORCE (LB)	AAMRL/ DYN LOAD LINK	1	4-Nov-98	11.44 uv/lb	13-Mar-01	11.16 uv/lb	-2.5	10V	1000	874.1 LB	
23	SEAT PAN Y FORCE (LB)	AAMRL/ DYN LOAD LINK	2	4-Nov-98	-11.25 uv/lb	13-Mar-01	10.91 uv/lb	-3.1	10V	1000	888.9 LB	USE NEGATIVE SENSITIVITY

DYNCORP PROGRAM SETUP AND CALIBRATION LOG

DATA CHANNEL	DATA POINT	TRANSDUCER MFG. & MODEL	SERIAL NUMBER	PRE-CAL		POST-CAL		%Δ	EXC. VOL.	AMP GAIN	FULL SCALE	NOTES
				DATE	SENS	DATE	SENS					
24	LEFT SEAT BACK X FORCE (LB)	STRAINCERT FL 1U-2SGKT	Q-8415-1	10-Apr-99	-19.85 uv/lb	12-Mar-01	19.75 uv/lb	-.5	10V	1000	503.8 LB	USE NEGATIVE SENSITIVITY
25	RIGHT SEAT BACK X FORCE (LB)	SRTAINCERT FL 1 U-2SGKT	Q-8415-2	10-Apr-99	-19.85 uv/lb	12-Mar-01	19.65 uv/lb	-1	10V	1000	503.8 LB	USE NEGATIVE SENSITIVITY
46	CENTER BACK X FORCE (LB)	STRAINCERT FL 1 U-2SGKT	Q-8415-3	12-Apr-99	-19.86 uv/lb	12-Mar-01	19.75 uv/lb	-.6	10V	1000	503.5 LB	USE NEGATIVE SENSITIVITY
27	LEFT SEAT BACK Z FORCE (LB)	AAMRL/ DYN LOAD LINK	8	26-Aug-98	-10.99 uv/lb	12-Mar-01	10.9 uv/lb	-.8	10 V	1000	909.9 LB	USE NEGATIVE SENSITIVITY
28	EVENT / T=O								0	1		Bit 0 Is Event Bit 1 Is T=O
44	RIGHT SEAT BACK Z FORCE (LB)	AAMRL/ DYN LOAD LINK	9	24-Aug-98	-11.54 uv/lb	12-Mar-01	11.21 uv.lb	-2.9	10V	1000	866.6 LB	USE NEGATIVE SENSITIVITY
30	SEAT BACK Y FORCE (LB)	AAMRL/ DYN LOAD LINK	10	24-Aug-98	-10.69 uv/lb	12-Mar-01	10.41 uv/lb	-2.7	10V	1000	935.5 LB	USE NEGATIVE SENSITIVITY
31	LEFT LAP X FORCE (LB)	MICH-SCI4000	2	26-Aug-99	-13.87 uv/lb	12-Mar-01	14.05 uv/lb	1.3	10V	500	1442 LB	USE NEGATIVE SENSITIVITY
32	LEFT LAP Y FORCE (LB)	MICH-SCI4000	2	26-Aug-99	-13.32 uv/lb	13-Mar-01	13.43 uv/lb	.8	10V	500	1501.6 LB	USE NEGATIVE SENSITIVITY

DYNCORP PROGRAM SETUP AND CALIBRATION LOG

DATA CHANNEL	DATA POINT	TRANSDUCER MFG. & MODEL	SERIAL NUMBER	PRE-CAL		POST-CAL		%Δ	EXC. VOL.	AMP GAIN	FULL SCALE	NOTES
				DATE	SENS	DATE	SENS					
33	LEFT LAP Z FORCE (LB)	MICH-SCI4000	2	26-Aug-99	13.24 uv/lb	13-Mar-01	13.6 uv.lb	2.6	10 V	500	1510.6 LB	
34	RIGHT LAP X FORCE (LB)	MICH-SCI 4000	5	16-Dec-98	-14.08 uv/lb	13-Mar-01	13.71 uv/lb	-2.7	10V	500	1420.4 LB	USE NEGATIVE SENSITIVITY
35	RIGHT LAP Y FORCE (LB)	MICH-SCI4000	5	16-Dec-98	14.52 uv/lb	13-Mar-01	14.23 uv/lb	-2	10V	500	1377.48 LB	
36	RIGHT LAP Z FORCE (LB)	MICH-SCI4000	5	16-Dec-98	14.15 uv/lb	13-Mar-01	13.81 uv/lb	-2.5	10V	500	1413.4 LB	
47	SHOULDER X FORCE (LB)	MICH-SCI 4000	4	16-Dec-98	13.77 uv/lb	13-Mar-01	13.5 uv/lb	-2	10V	500	1452.4 LB	Moved to this channel on test 3939.
38	SHOULDER Y FORCE (LB)	MICH-SCI 4000	4	16-Dec-98	-14.25 uv/lb	13-Mar-01	13.89 uv/lb	-2.6	10V	1000	701.8 LB	USE NEGATIVE SENSITIVITY
39	SHOULDER Z FORCE (LB)	MICH-SCI 4000	4	16-Dec-98	-13.76 uv/lb	13-Mar-01	13.46 uv/lb	-2.2	10V	500	1453.5 LB	USE NEGATIVE SENSITIVITY
41	LOWER HEADREST X FORCE (LB)	STRAINCERT FL 1 U-2SPKT	Q-5297-3	6-Feb-99	-19.91 uv/lb	12-Mar-01	19.53 uv/lb	-1.9	10 V	1000	502.3 LB	USE NEGATIVE SENSITIVITY
42	UPPER HEADREST X FORCE (LB)	STRAINCERT FL1U-2SPKT	Q-5297-4	16-Feb-99	-20.13 uv/lb	12-Mar-01	19.64 uv/lb	-2.5	10V	1000	496.8 LB	USE NEGATIVE SENSITIVITY

DYNCORP PROGRAM SETUP AND CALIBRATION LOG

DATA CHANNEL	DATA POINT	TRANSDUCER MFG. & MODEL	SERIAL NUMBER	PRE-CAL		POST-CAL		%Δ	EXC. VOL.	AMP GAIN	FULL SCALE	NOTES
				DATE	SENS	DATE	SENS					
49	INT LUMBAR Mx TORQUE (IN-LB)	DENTON 1914A	365	8-Jun-99	-4.98 uv/in-lb	7-Mar-00	5.08 uv/in-lb	2	10V	1000	2008IN-LB	Channel repaired. This test point inserted on test 4049. Used on test 4049 thru 4070 on RSC study. Use negative sensitivity
50	INT LUMBAR X FORCE	DENTON 1914A	365	8-Jun-99	-6.41 uv/lb	7-Mar-00	6.41 uv/lb	0	10V	1000	1560.1 LB	Used on test 4049 thru 4070 on RSC study. Use negative sensitivity.
51	INT LUMBAR Y FORCE (LB)	DENTON 1914A	365	8-Jun-99	-6.37 uv/lb	7-Mar-00	6.38 uv/lb	.2	10V	1000	1569.9 LB	Used on test 4049 thru 4070 on RSC study. Use negative sensitivity.
52	INT LUMBAR Z FORCE (LB)	DENTON 1914A	365	8-Jun-99	-2.66 uv/lb	7-Mar-00	2.66 uv/lb	0	10V	1000	3759.3 LB	Used on test 4049 thru 4070 on RSC study. Use negative sensitivity.
55	INT LUMBAR My TORQUE (IN-LB)	DENTON 1914A	365	8-Jun-99	4.99 uv/in-lb	7-Mar-00	5.02 uv/in-lb	.6	10V	1000	2004IN-LB	Used on test 4049 thru 4070 on RSC study.
56	INT LUMBAR Mz	DENTON 1914A	365	8-Jun-99	8.42 uv/in-lb	7-Mar-00	8.67 uv/in-lb	2.9	10V	500	2375.3 IN-LB	Used on test 4049 thru 4070 on RSC study.

APPENDIX D: SAMPLE ACCELERATION DATA SHEETS

CT Study Test: 4083 Test Date: 000330 Subj: B-23 Wt: 193.0
Nom G: 10.0 Cell: C

Data ID	Immediate Preimpact	Maximum Value	Minimum Value	Time Of Maximum	Time Of Minimum
Kodak Start Time (Ms)				-2894.0	
Reference Mark Time (Ms)				-146.0	
Impact Rise Time (Ms)				74.1	
Impact Duration (Ms)				147.0	
Velocity Change (Ft/Sec)		30.10			
Carriage Acceleration (G)					
X Axis	-0.02	4.74	-2.94	18.0	23.0
Y Axis	0.02	1.12	-0.76	19.0	44.0
Z Axis	0.04	9.98	0.46	67.0	0.0
Carriage Velocity (Ft/Sec)	-26.76	-1.21	-27.56	437.0	4.0
Seat Pan Acceleration (G)					
X Axis	-0.01	3.86	-2.30	18.0	23.0
Y Axis	0.08	1.74	-2.22	29.0	49.0
Z Axis	0.03	9.91	-0.43	69.0	23.0
Z Axis DRI	0.05	11.95	-1.52	98.0	166.0
Head Acceleration (G)					
X Axis	-0.06	0.71	-1.48	37.0	108.0
Y Axis	0.04	2.05	-1.06	79.0	235.0
Z Axis	-0.24	12.37	-0.11	80.0	0.0
Resultant	0.27	12.53	0.05	80.0	1.0
Ry (Rad/Sec2)	-10.75	162.63	-287.96	62.0	98.0
Chest Acceleration (G)					
X Axis	-0.04	4.30	-0.86	86.0	24.0
Y Axis	0.02	1.48	-0.67	101.0	191.0
Z Axis	-0.06	12.34	0.03	91.0	0.0
Resultant	0.11	12.76	0.06	90.0	2.0
Ry (Rad/Sec2)	-1.69	511.67	-1202.95	29.0	24.0
Corrected Chest Acceleration (G)					
X Axis	-0.02	1.98	-1.23	74.0	24.0
Z Axis	-0.07	12.73	0.02	90.0	2.0
Resultant	0.11	12.76	0.06	90.0	2.0
T1 Acceleration (G)					
X Axis	0.04	7.43	-4.72	68.0	60.0
Y Axis	-0.02	2.28	-2.58	65.0	54.0
Z Axis	-0.09	23.47	-2.20	60.0	67.0
Resultant	0.15	23.94	0.09	60.0	22.0

D-1

CT Study Test: 4083 Test Date: 000330 Subj: B-23 Wt: 193.0
Nom G: 10.0 Cell: C

Data ID	Immediate Preimpact	Maximum Value	Minimum Value	Time Of Maximum	Time Of Minimum
Headrest Force (Lb)					
Upper X Axis	8.36	7.38	-16.15	0.0	57.0
Lower X Axis	24.29	34.52	1.17	29.0	135.0
X Axis Sum	32.64	33.16	-3.02	28.0	92.0
Shoulder Force (Lb)					
X Axis	-104.66	-68.02	-155.25	171.0	76.0
Y Axis	0.25	8.60	-7.84	91.0	208.0
Z Axis	4.24	50.16	4.02	92.0	1.0
Resultant	104.74	162.96	68.69	82.0	172.0
Left Lap Force (Lb)					
X Axis	-86.02	-41.58	-100.02	176.0	85.0
Y Axis	44.21	45.70	20.78	12.0	183.0
Z Axis	-100.41	-43.55	-101.82	184.0	2.0
Resultant	139.41	141.93	64.69	2.0	176.0
Right Lap Force (Lb)					
X Axis	-59.23	-28.18	-71.18	41.0	81.0
Y Axis	-26.47	-10.43	-27.25	40.0	88.0
Z Axis	-64.60	-23.90	-65.31	43.0	0.0
Resultant	91.55	92.64	39.42	0.0	43.0
Seat Back Force (Lb)					
Left X Axis	65.37	84.78	38.29	86.0	134.0
Right X Axis	61.13	102.21	29.40	85.0	139.0
Center X Axis	66.82	156.28	11.96	144.0	381.0
X Axis Sum	193.33	285.98	133.99	19.0	123.0
Y Axis	4.81	50.19	-10.56	63.0	125.0
Left Z Axis	-9.54	74.56	-9.42	71.0	0.0
Right Z Axis	-8.19	126.20	-6.24	87.0	0.0
Z Axis Sum	-17.73	199.91	-15.66	72.0	0.0
Z Axis Minus Tare	0.77	54.70	-26.73	99.0	40.0
Resultant	194.21	315.19	143.40	78.0	434.0
Resultant Minus Tare	193.40	286.22	135.82	19.0	123.0

CT Study Test: 4083 Test Date: 000330 Subj: B-23 Wt: 193.0
Nom G: 10.0 Cell: C

Data ID	Immediate Preimpact	Maximum Value	Minimum Value	Time Of Maximum	Time Of Minimum
Seat Pan Force (Lb)					
Left X Axis	31.29	51.18	-41.55	33.0	93.0
Right X Axis	0.97	15.17	-1.90	437.0	64.0
X Axis Sum	32.27	53.05	-40.46	18.0	93.0
Y Axis	-43.66	19.64	-70.64	94.0	23.0
Left Z Axis	41.34	525.53	30.53	82.0	24.0
Right Z Axis	44.27	530.68	41.79	75.0	1.0
Center Z Axis	138.22	1617.26	152.42	74.0	1.0
Z Axis Sum	223.83	2633.76	236.95	75.0	1.0
Z Axis Minus Tare	246.83	2429.81	248.44	75.0	1.0
Resultant	230.34	2633.85	242.20	75.0	1.0
Resultant Minus Tare	252.75	2429.91	253.44	75.0	1.0
Total Body Force (Lb)					
X Axis	0.00	150.67	-153.54	19.0	93.0
Y Axis	0.00	101.54	-23.86	92.0	139.0
Z Axis	0.00	2302.26	-6.07	75.0	1.0
Resultant	6.90	2305.89	8.02	75.0	0.0

CT Study Test: 4083 Test Date: 000330 Subj: B-23 Cell: C

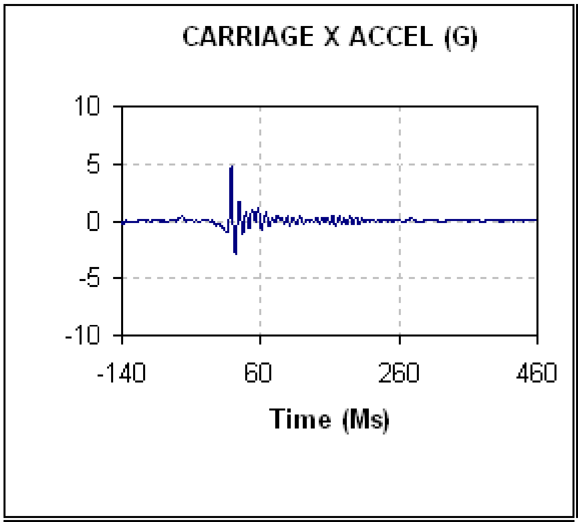

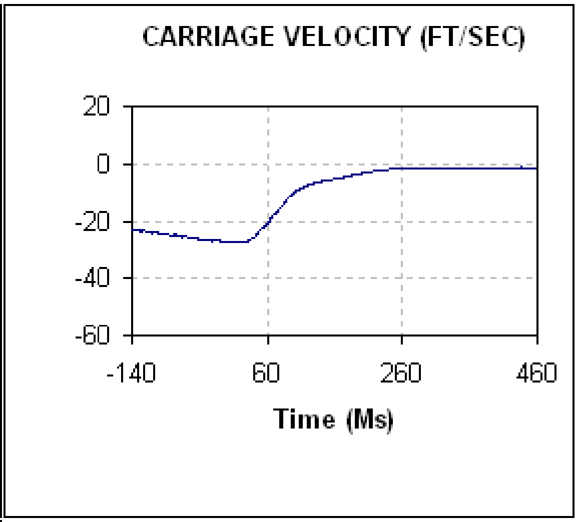

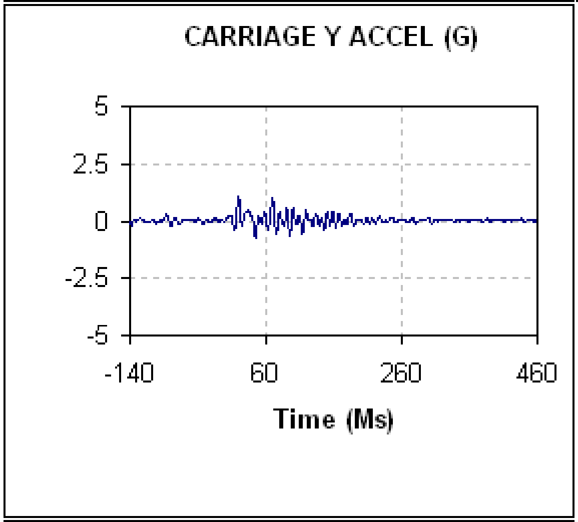

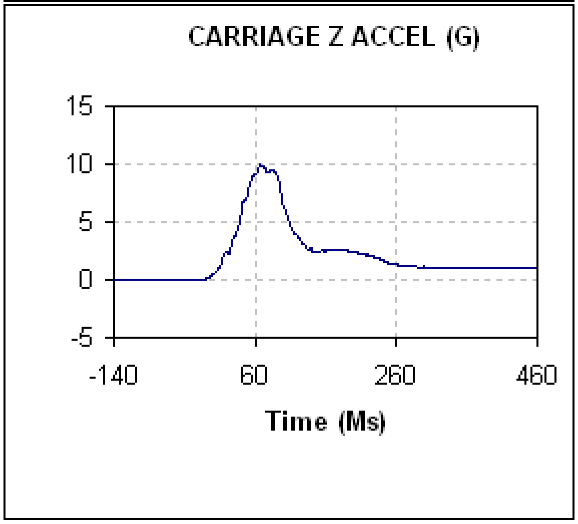

D-4

CT Study Test: 4083 Test Date: 000330 Subj: B-23 Cell: C

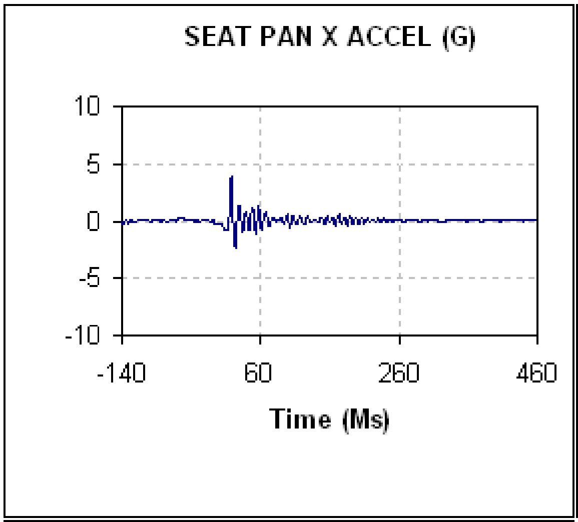

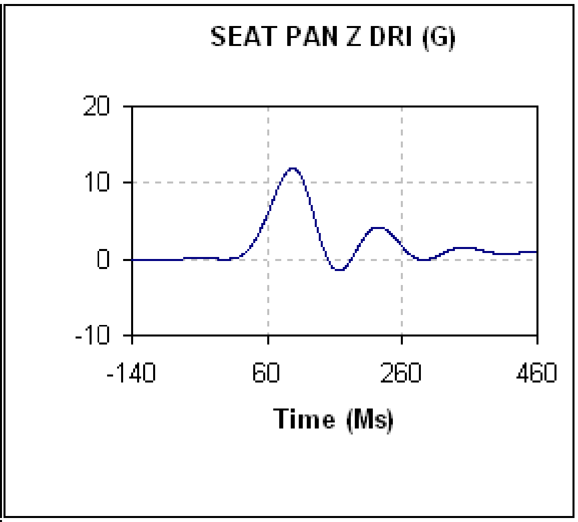

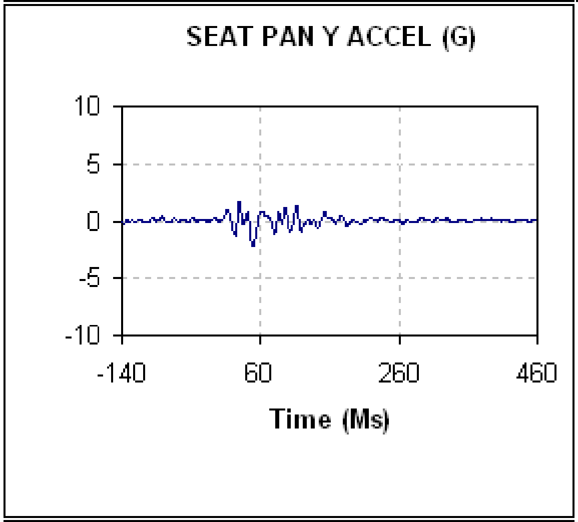

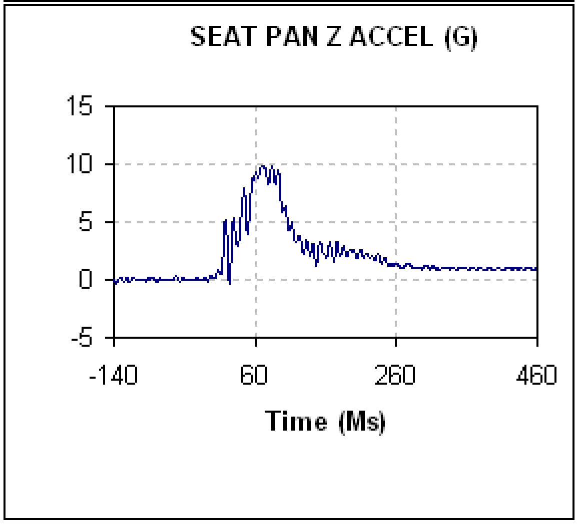

D-5

CT Study Test: 4083 Test Date: 000330 Subj: B-23 Cell: C

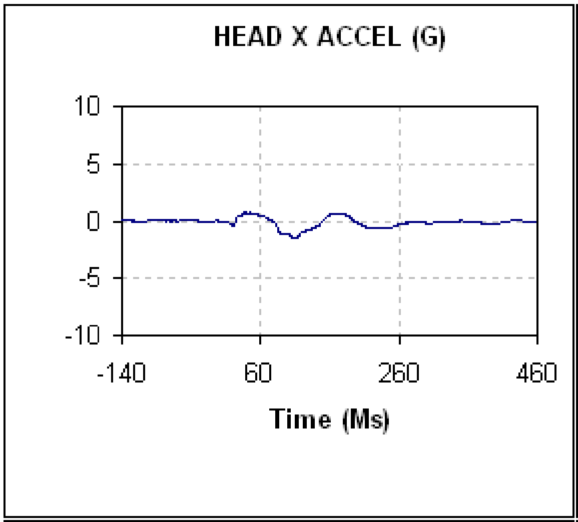

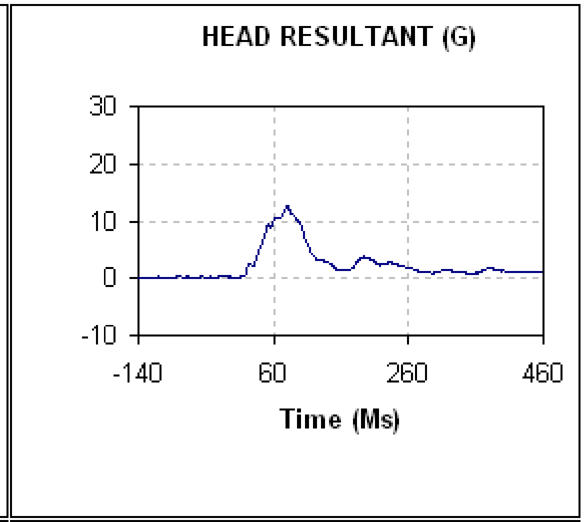

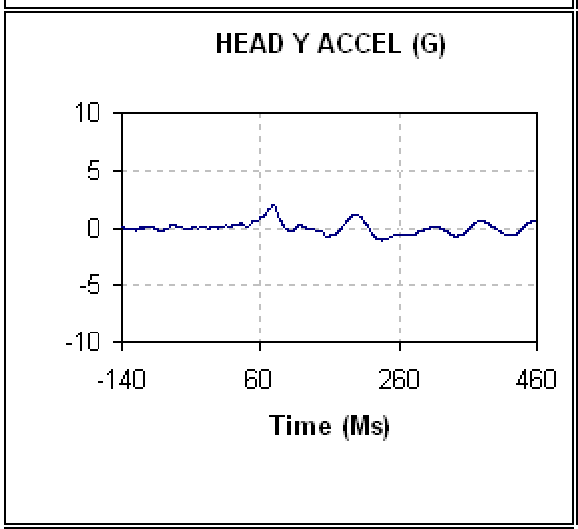

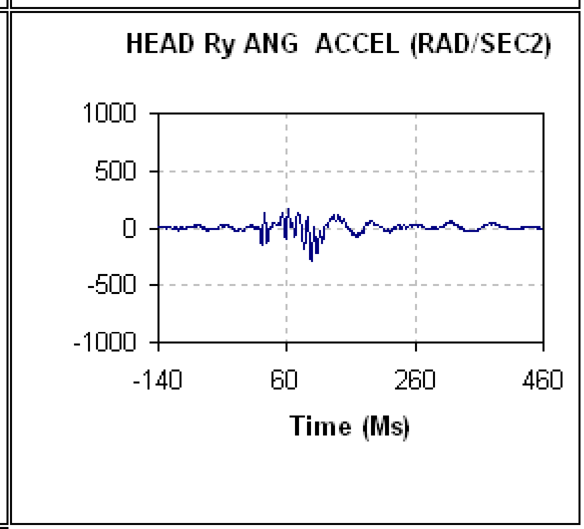

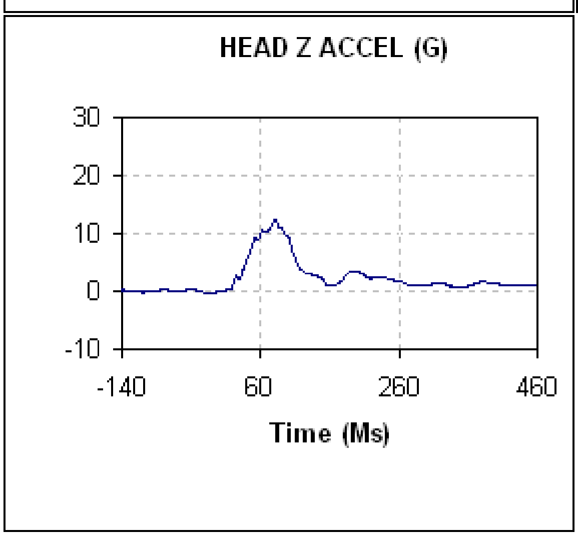

D-6

CT Study Test: 4083 Test Date: 000330 Subj: B-23 Cell: C

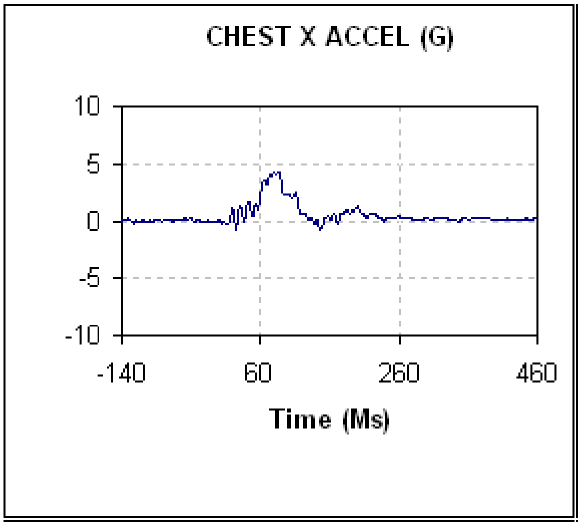

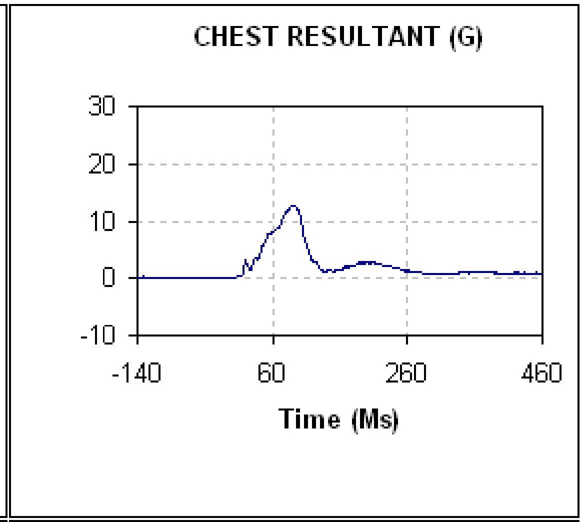

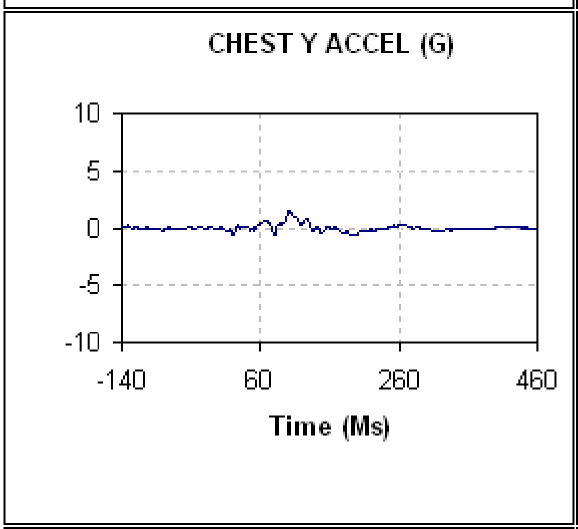

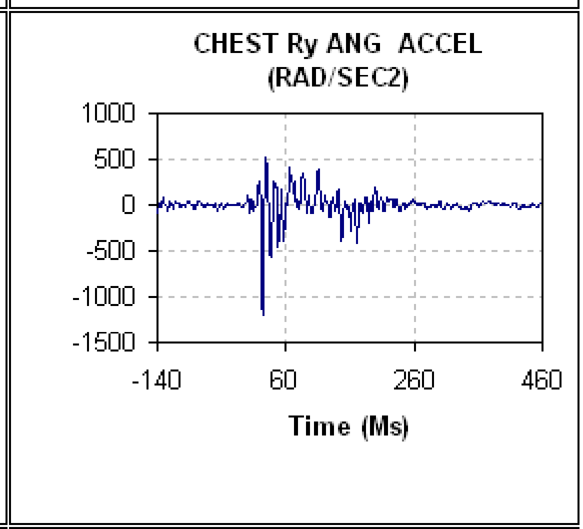

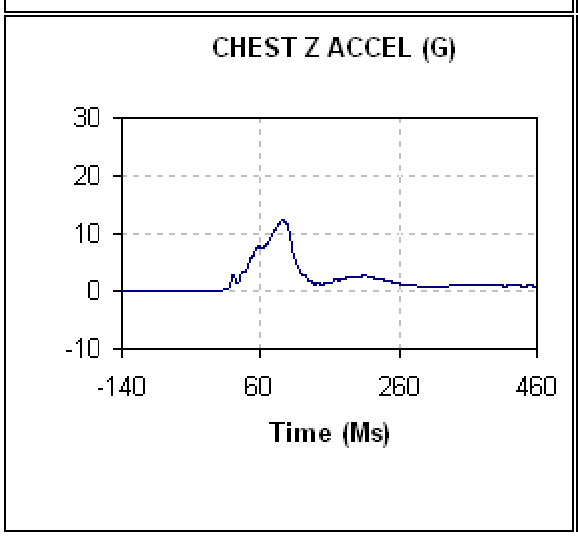

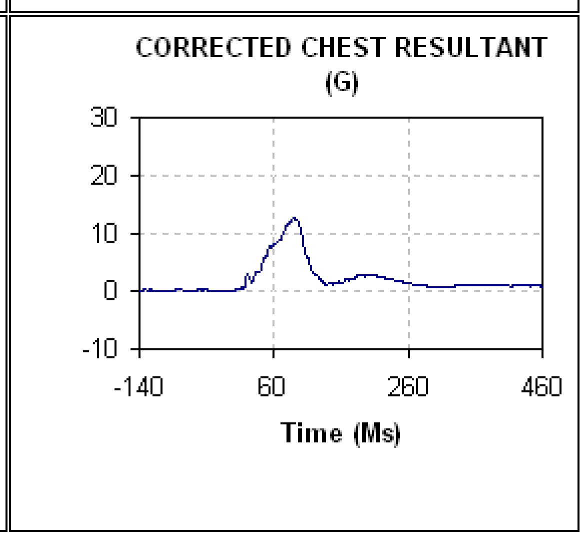

D-7

CT Study Test: 4083 Test Date: 000330 Subj: B-23 Cell: C

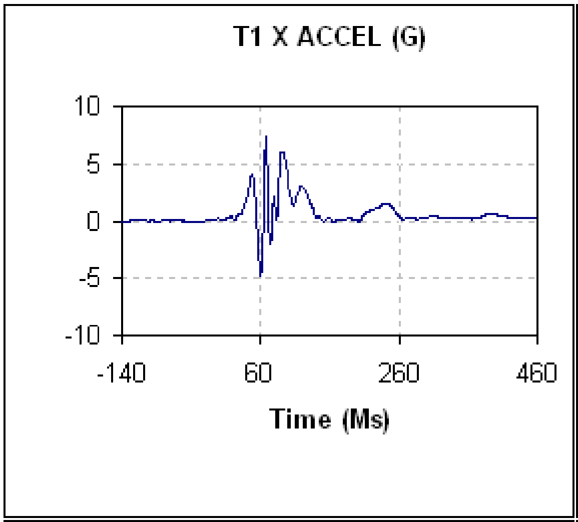

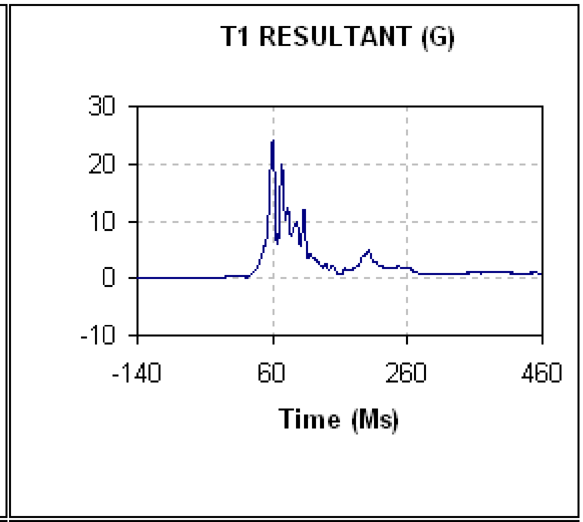

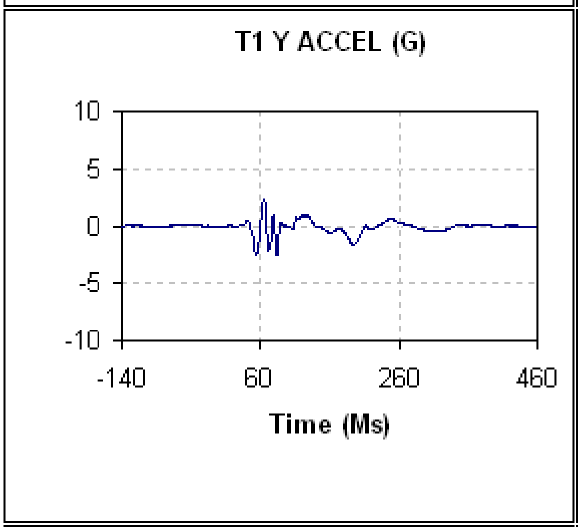

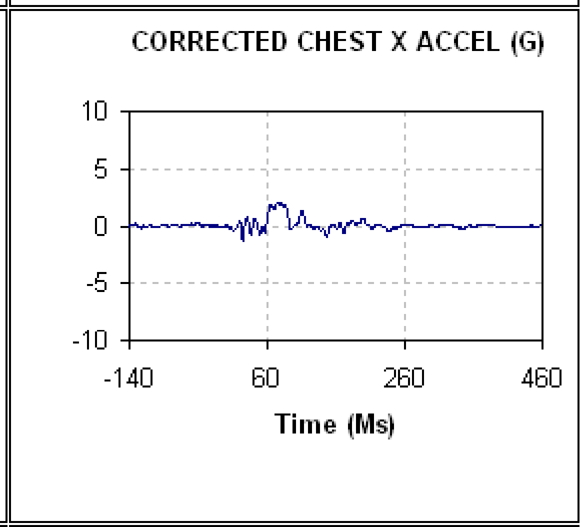

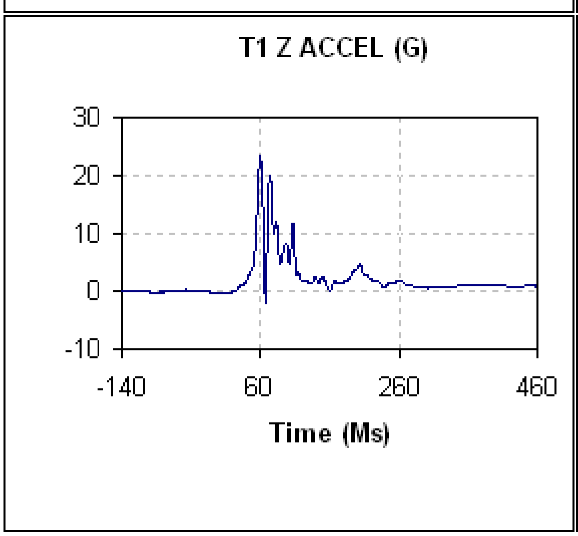

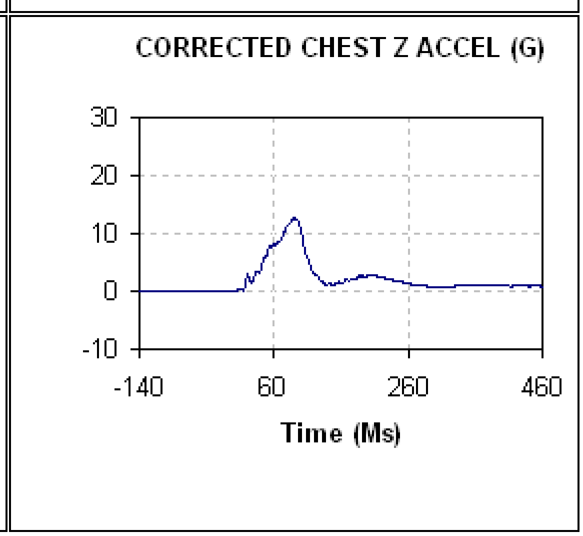

D-8

CT Study Test: 4083 Test Date: 000330 Subj: B-23 Cell: C

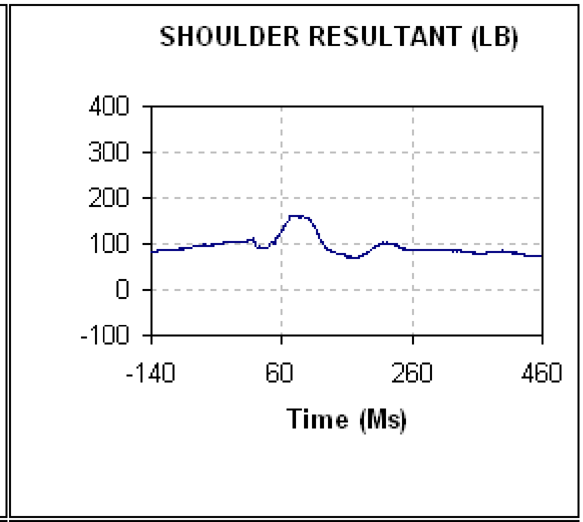

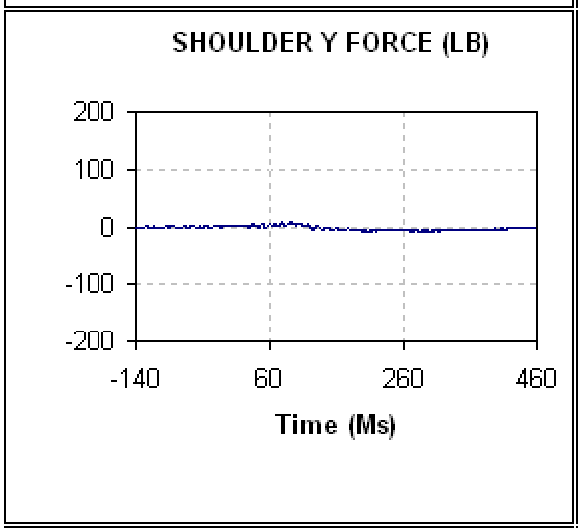

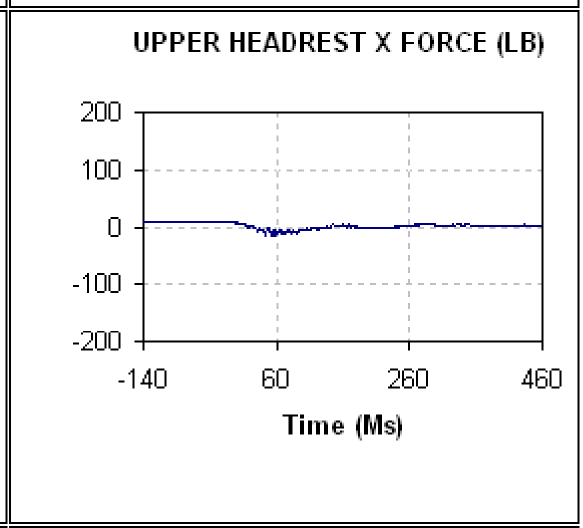

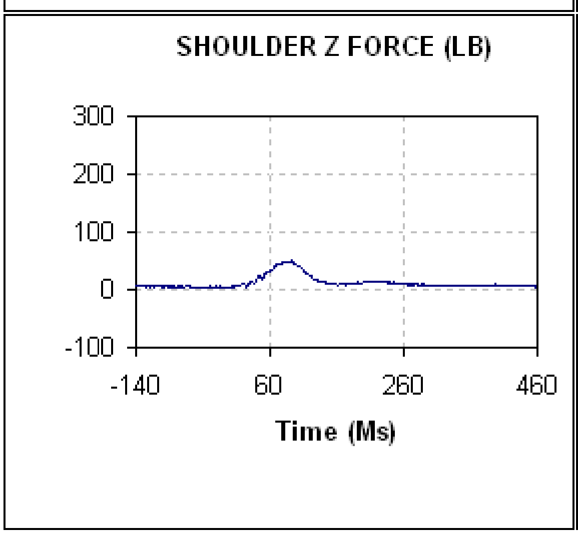

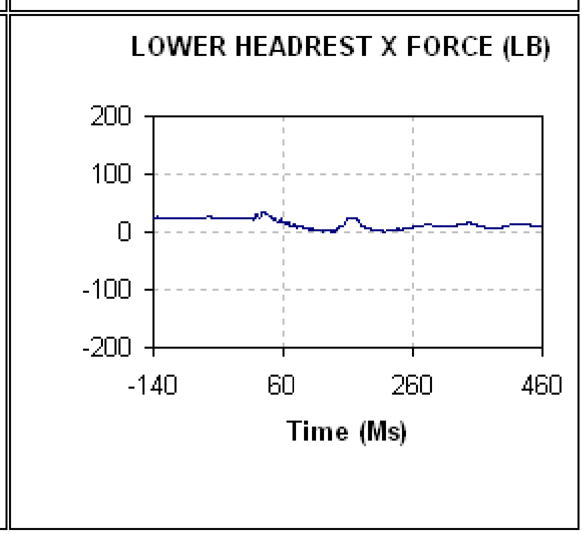

CT Study Test: 4083 Test Date: 000330 Subj: B-23 Cell: C

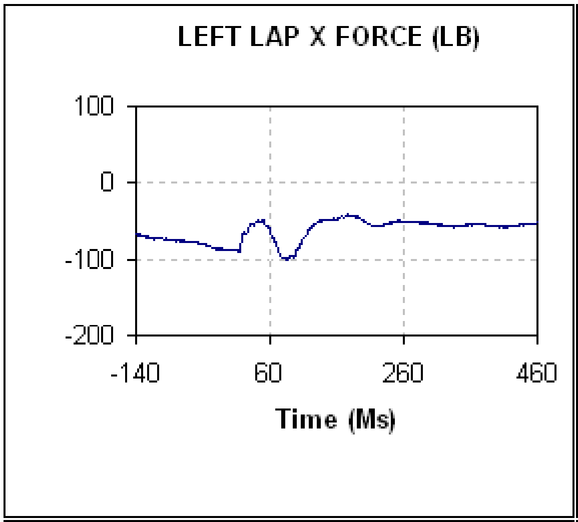

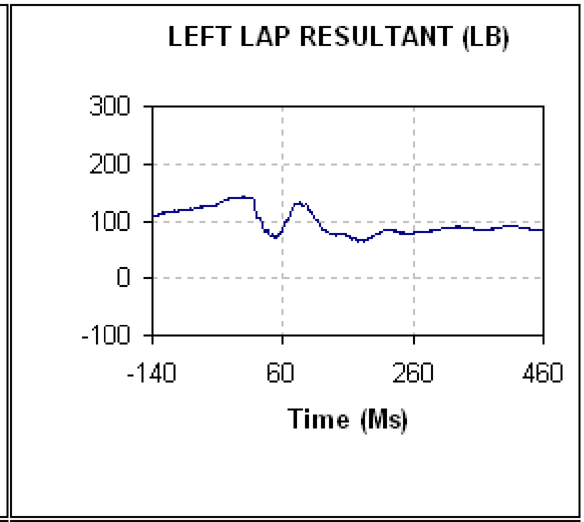

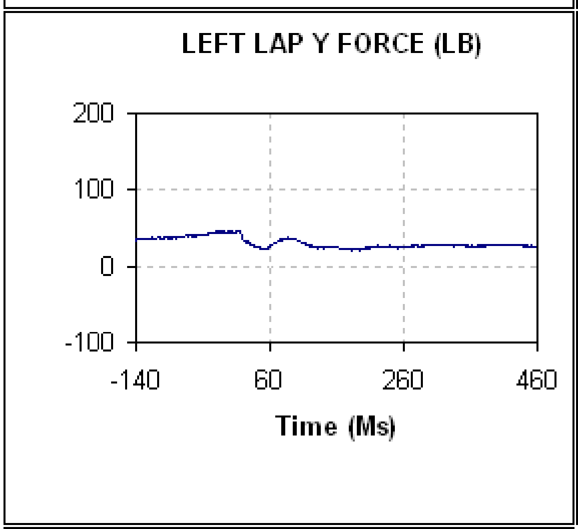

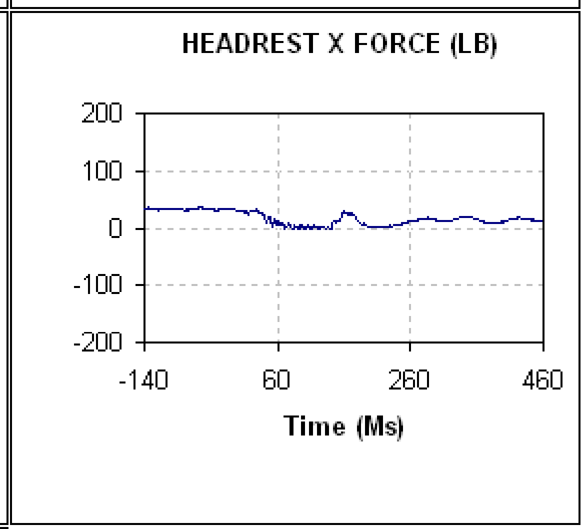

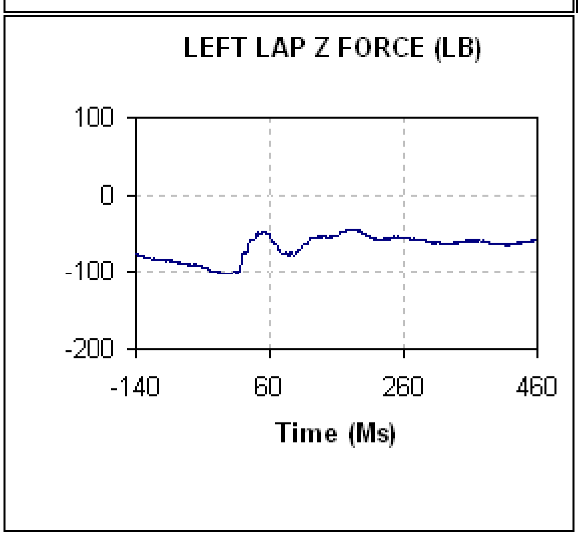

D-10

CT Study Test: 4083 Test Date: 000330 Subj: B-23 Cell: C

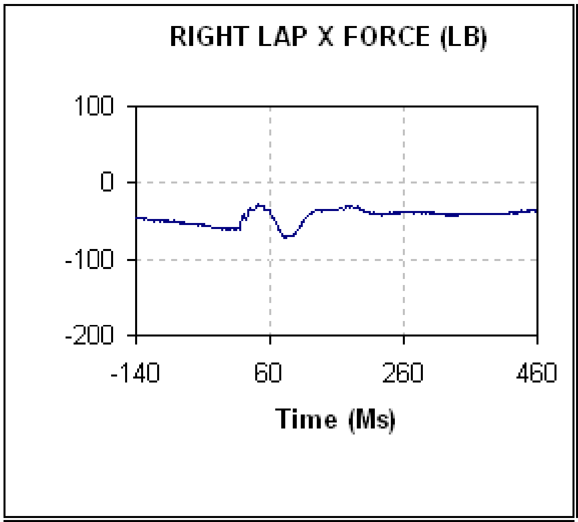

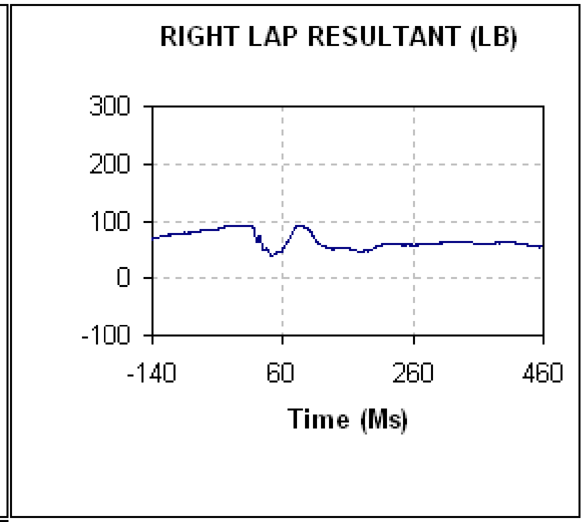

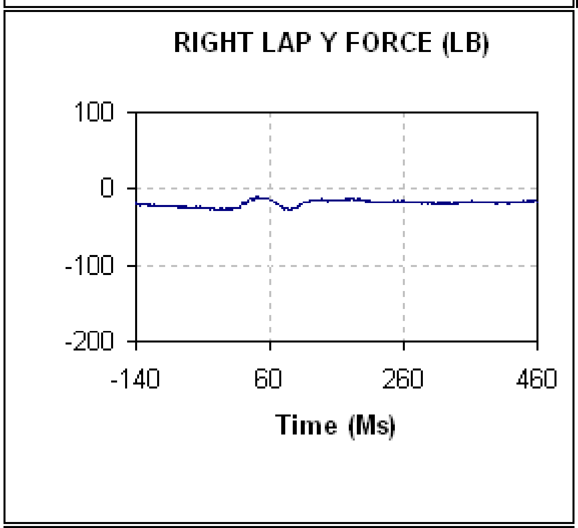

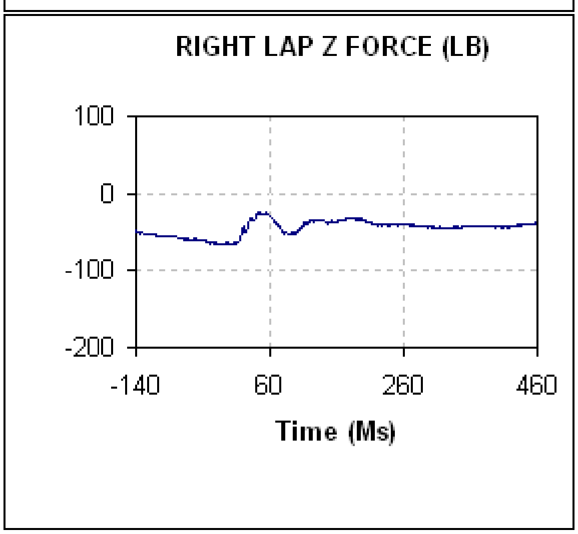

D-11

CT Study Test: 4083 Test Date: 000330 Subj: B-23 Cell: C

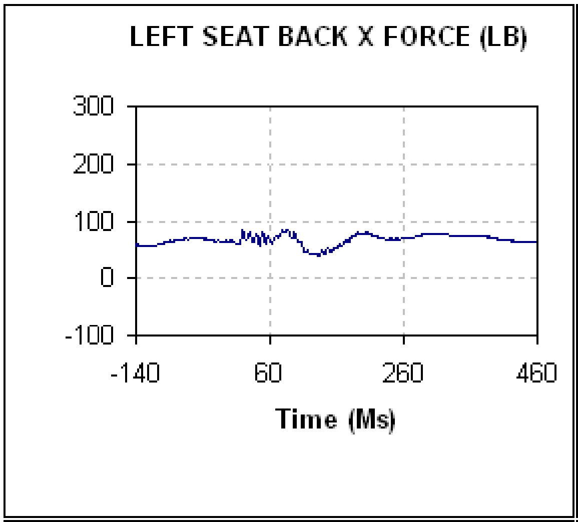

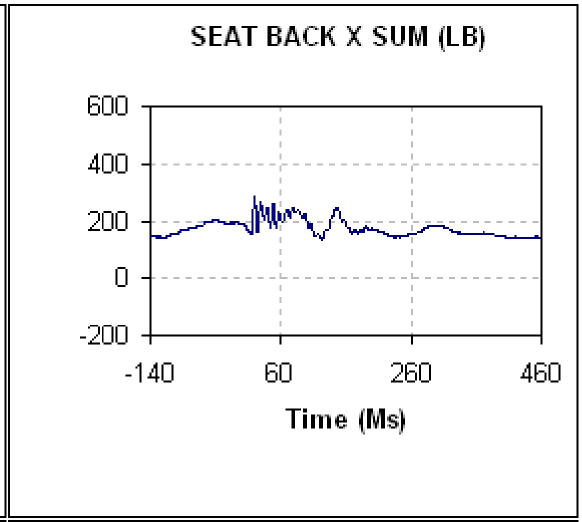

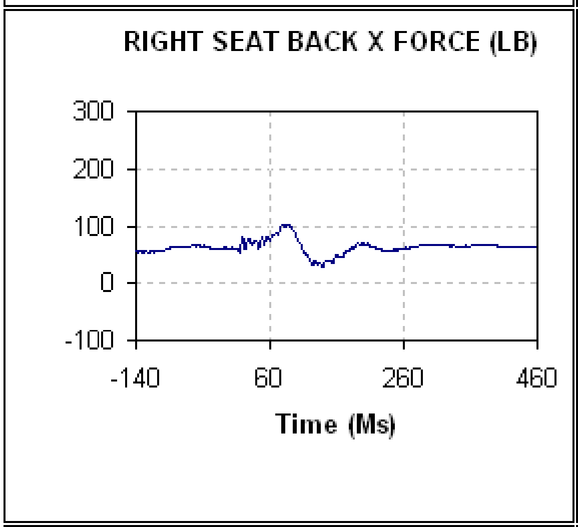

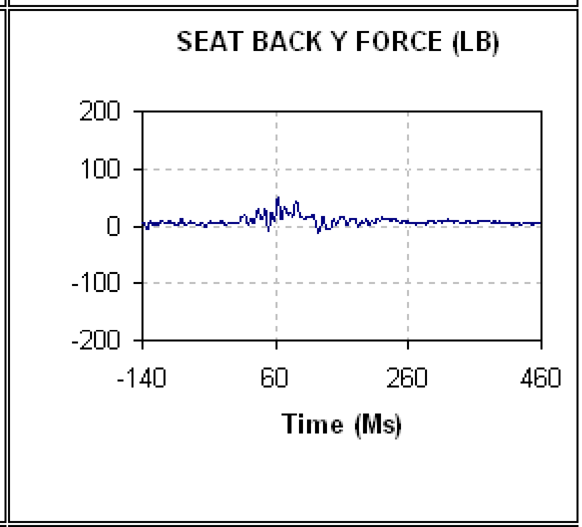

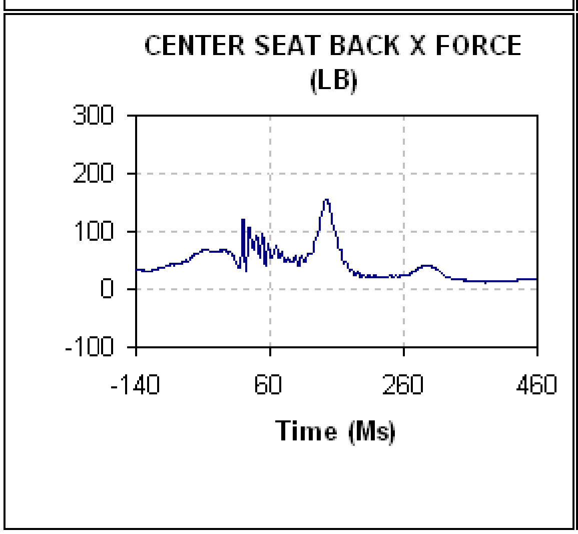

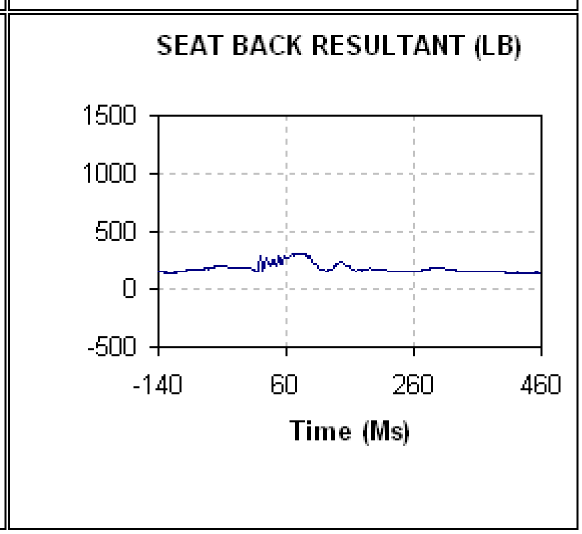

D-12

CT Study Test: 4083 Test Date: 000330 Subj: B-23 Cell: C

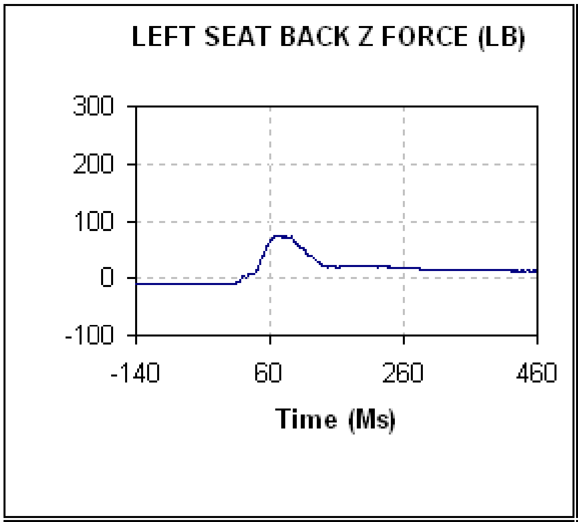

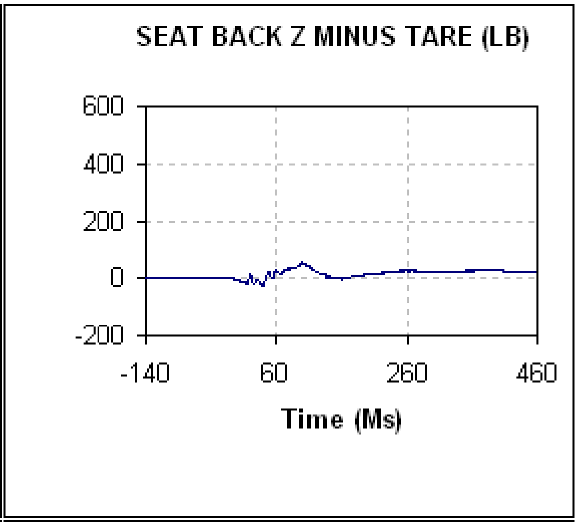

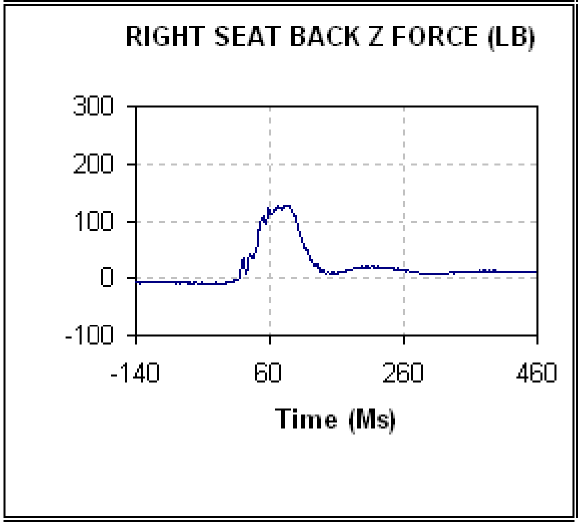

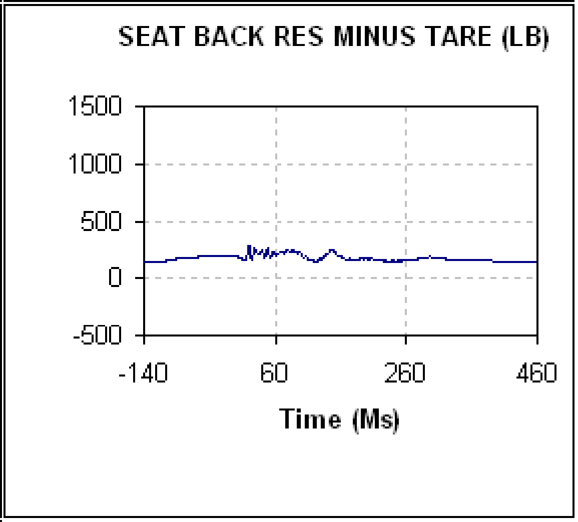

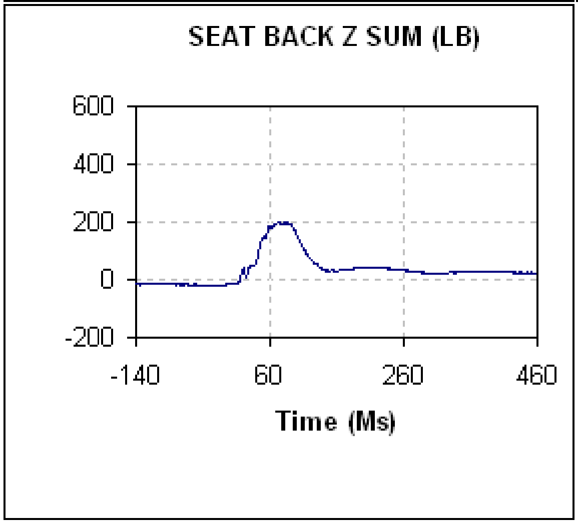

D-13

CT Study Test: 4083 Test Date: 000330 Subj: B-23 Cell: C

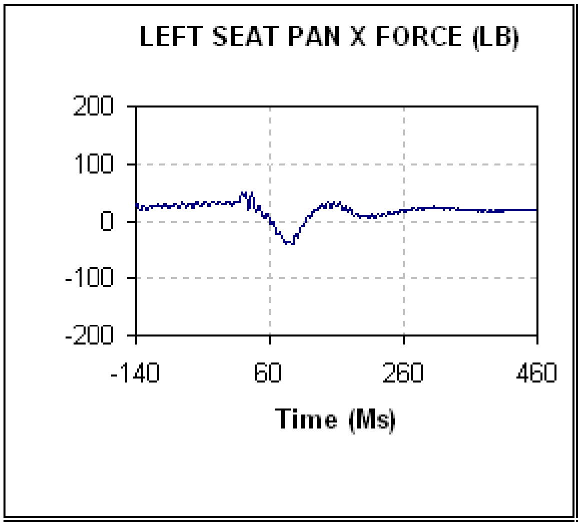

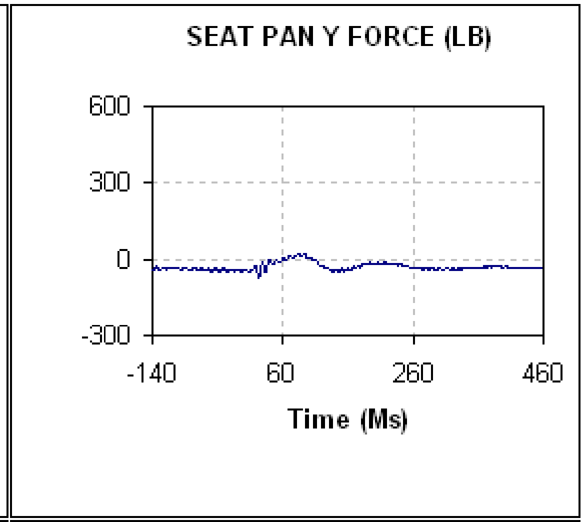

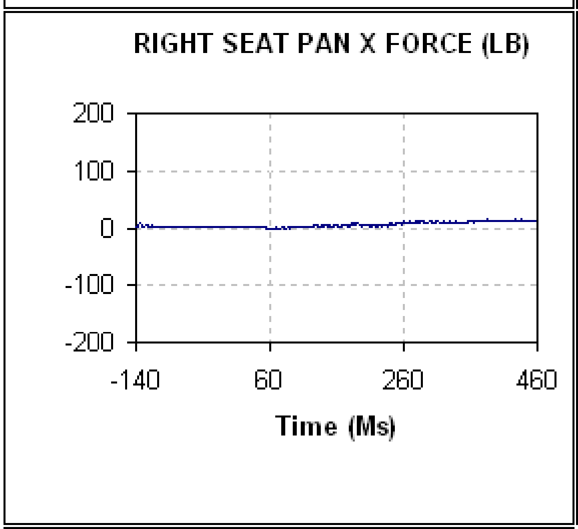

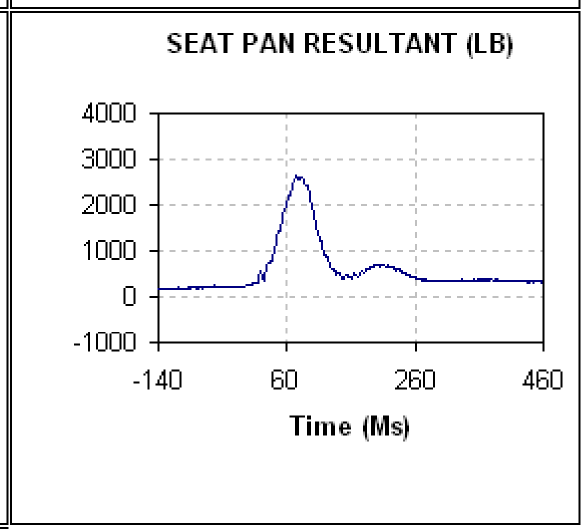

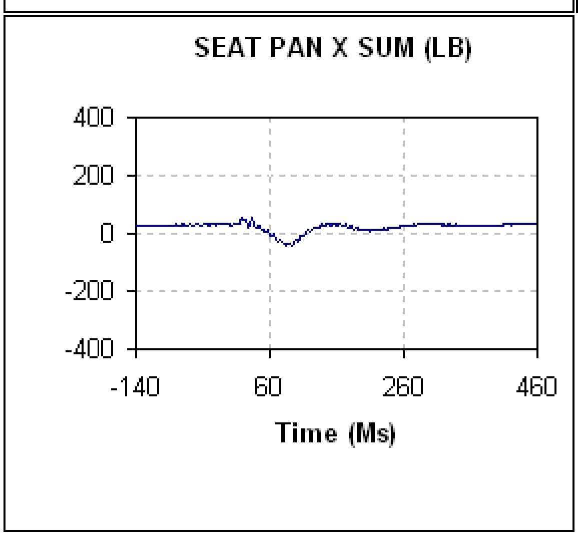

CT Study Test: 4083 Test Date: 000330 Subj: B-23 Cell: C

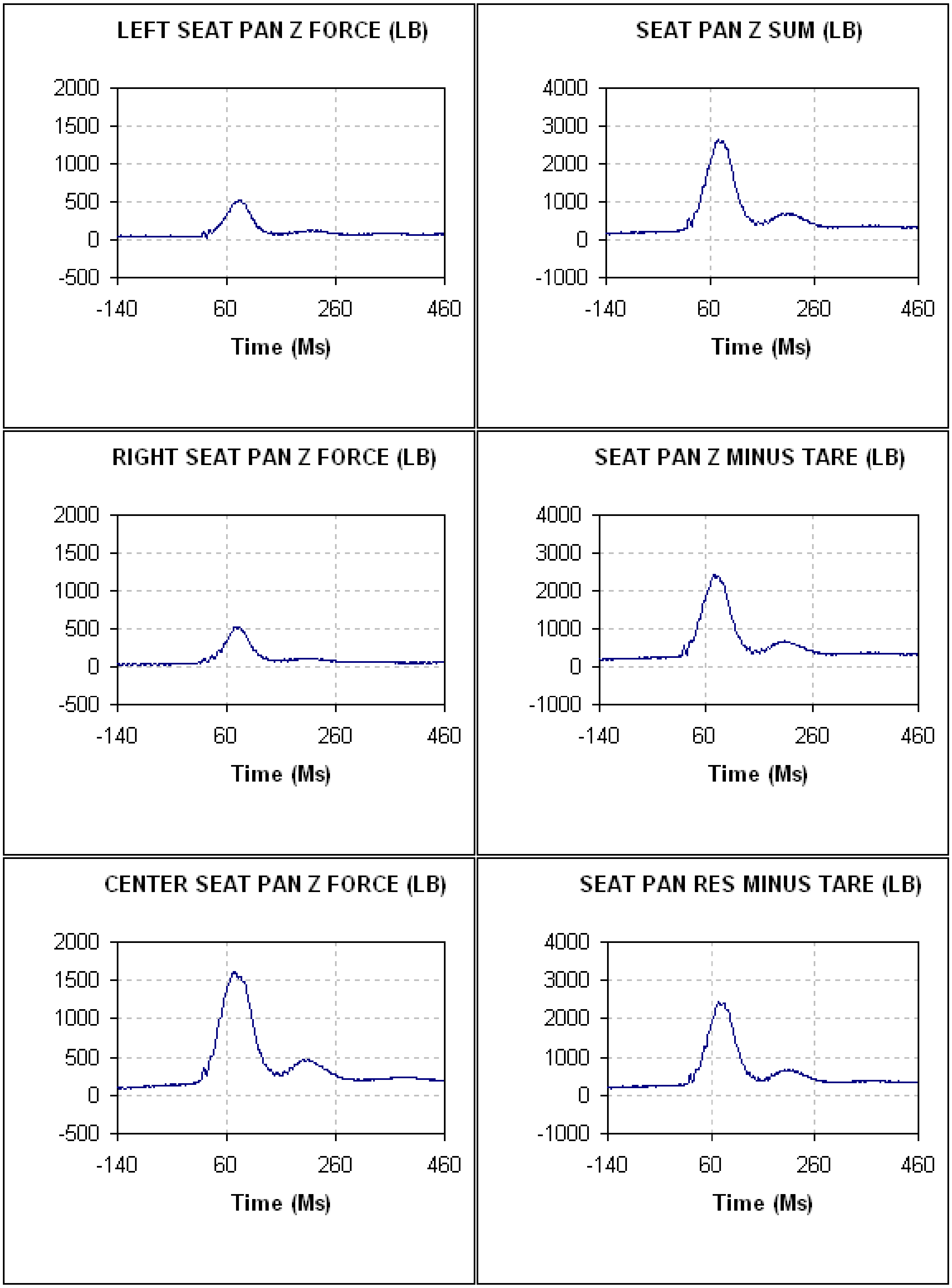

D-15

CT Study Test: 4083 Test Date: 000330 Subj: B-23 Cell: C

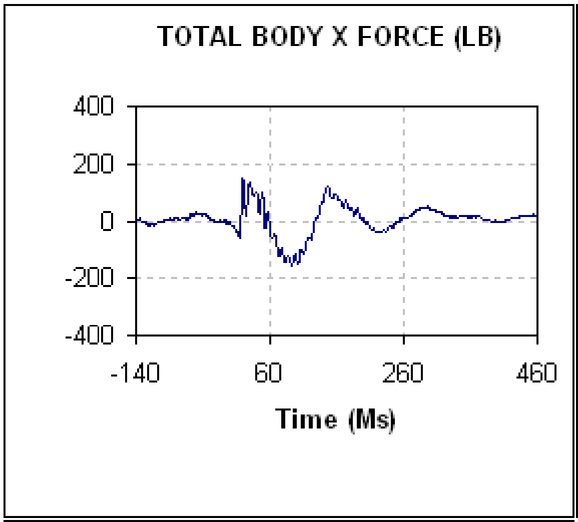

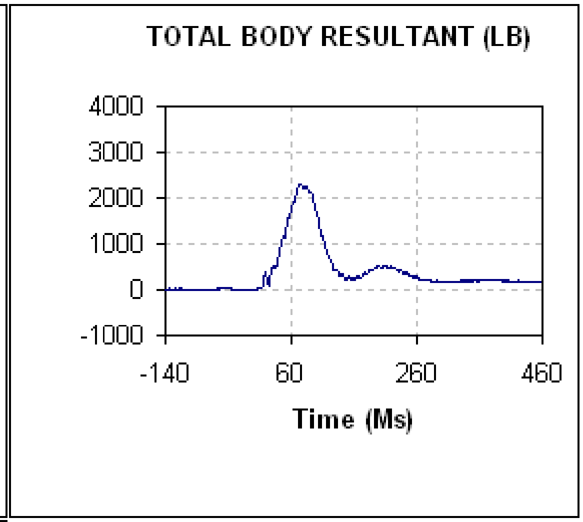

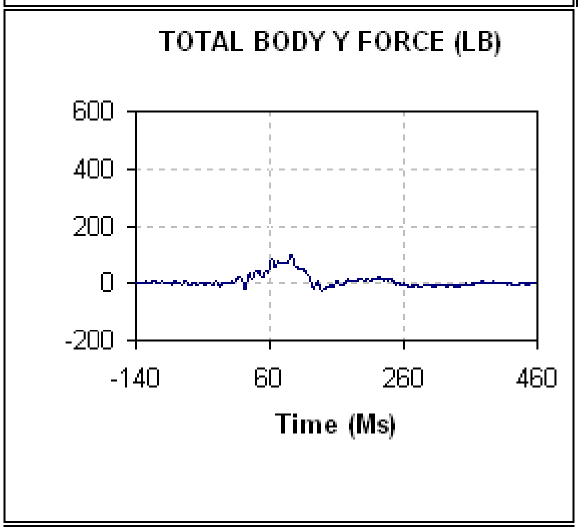

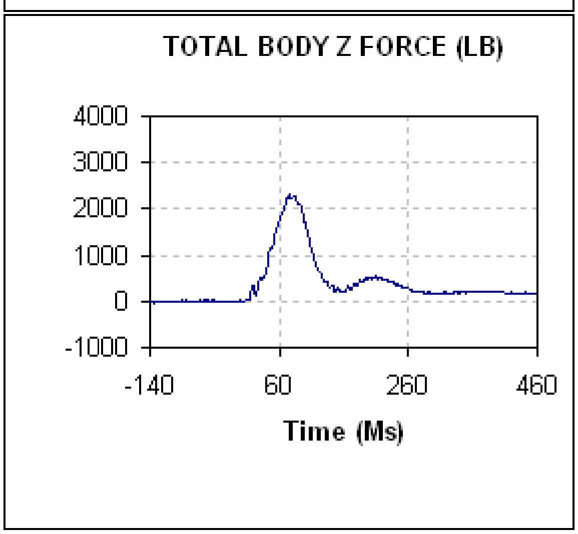

D-16

APPENDIX E: SAMPLE SELSPOT DATA

CT STUDY TEST: 4083 DATE: 30MAR00 SUBJ: B-23 CELL: C
NOMINAL G LEVEL: 10

Data ID	Preimpact	Maximum Value	Minimum Value	Time Of Max (ms)	Time Of Min (ms)
HELMET TEMPLE					
POSITION (IN)					
X AXIS	5.37	7.50	5.37	254.0	0.0
Y AXIS	-4.74	-2.21	-5.09	272.0	12.0
Z AXIS	35.84	36.20	34.71	286.0	92.0
VELOCITY (IN/SEC)	8.14	43.13	5.92	112.0	356.0
ACCELERATION (G)	0.87	6.49	0.29	154.0	406.0
DISPLACEMENT (IN)					
X AXIS	0.00	2.12	0.00	254.0	0.0
Y AXIS	0.00	2.53	-0.35	272.0	12.0
Z AXIS	0.00	0.36	-1.13	286.0	92.0
RESULTANT	0.00	3.30	0.00	260.0	0.0
HELMET EAR					
POSITION (IN)					
X AXIS	5.71	7.58	5.63	276.0	20.0
Y AXIS	-4.77	-2.96	-4.85	260.0	12.0
Z AXIS	31.73	32.15	30.72	268.0	82.0
VELOCITY (IN/SEC)	10.02	34.23	3.20	112.0	276.0
ACCELERATION (G)	0.59	4.25	0.21	94.0	346.0
DISPLACEMENT (IN)					
X AXIS	0.00	1.86	-0.08	276.0	20.0
Y AXIS	0.00	1.81	-0.08	260.0	12.0
Z AXIS	0.00	0.42	-1.00	268.0	82.0
RESULTANT	0.00	2.58	0.00	260.0	0.0
MOUTH					
POSITION (IN)					
X AXIS	11.15	12.47	11.15	244.0	0.0
Y AXIS	-0.32	1.61	-0.63	264.0	54.0
Z AXIS	30.88	30.88	29.64	0.0	246.0
VELOCITY (IN/SEC)	4.25	29.34	1.27	44.0	242.0
ACCELERATION (G)	0.32	3.93	0.20	158.0	316.0
DISPLACEMENT (IN)					
X AXIS	0.00	1.32	0.00	244.0	0.0
Y AXIS	0.00	1.93	-0.31	264.0	54.0
Z AXIS	0.00	0.00	-1.24	0.0	246.0
RESULTANT	0.00	2.52	0.00	262.0	0.0
HIP					
POSITION (IN)					
X AXIS	4.43	4.86	4.21	100.0	326.0
Y AXIS	-7.58	-7.34	-8.08	322.0	66.0
Z AXIS	8.29	8.29	6.93	0.0	82.0
VELOCITY (IN/SEC)	2.91	35.64	0.63	62.0	454.0
ACCELERATION (G)	0.66	4.85	0.11	82.0	332.0

E-1

CT STUDY TEST: 4083 DATE: 30MAR00 SUBJ: B-23 CELL: C
NOMINAL G LEVEL: 10

Data ID	Preimpact	Maximum Value	Minimum Value	Time Of Max (ms)	Time Of Min (ms)
HIP					
DISPLACEMENT (IN)					
X AXIS	0.00	0.43	-0.22	100.0	326.0
Y AXIS	0.00	0.24	-0.50	322.0	66.0
Z AXIS	0.00	0.00	-1.36	0.0	82.0
RESULTANT	0.00	1.43	0.00	98.0	0.0
SHOULDER					
POSITION (IN)					
X AXIS	5.38	6.10	5.29	140.0	44.0
Y AXIS	-5.84	-4.19	-7.27	180.0	102.0
Z AXIS	27.96	28.24	26.13	320.0	90.0
VELOCITY (IN/SEC)	10.22	100.26	1.15	148.0	398.0
ACCELERATION (G)	3.96	18.03	0.10	172.0	290.0
DISPLACEMENT (IN)					
X AXIS	0.00	0.73	-0.09	140.0	44.0
Y AXIS	0.00	1.64	-1.44	180.0	102.0
Z AXIS	0.00	0.28	-1.83	320.0	90.0
RESULTANT	0.00	2.28	0.00	98.0	0.0
CHEST					
POSITION (IN)					
X AXIS	11.89	12.16	11.83	134.0	52.0
Y AXIS	0.12	0.35	-0.54	248.0	102.0
Z AXIS	20.39	20.41	19.27	8.0	94.0
VELOCITY (IN/SEC)	8.30	25.87	0.88	70.0	194.0
ACCELERATION (G)	1.11	4.40	0.17	90.0	212.0
DISPLACEMENT (IN)					
X AXIS	0.00	0.28	-0.05	134.0	52.0
Y AXIS	0.00	0.23	-0.66	248.0	102.0
Z AXIS	0.00	0.02	-1.12	8.0	94.0
RESULTANT	0.00	1.28	0.00	98.0	0.0

CT STUDY TEST: 4083 DATE: 30MAR00 SUBJ: B-23 CELL: C

Reliability Factors (In)

TARGET DESCRIPTION	Maximum	Minimum	Average	Standard Deviation	At Max Displacement
HELMET TEMPLE	0.0972	0.0002	0.0385	0.0278	0.0198
HELMET EAR	0.0806	0.0001	0.0255	0.0168	0.0250
MOUTH	0.1207	0.0081	0.0619	0.0255	0.0467
HIP	0.1634	0.0003	0.0736	0.0311	0.0724
SHOULDER	0.8530	0.0015	0.4478	0.1986	0.0609
CHEST	0.1004	0.0003	0.0470	0.0238	0.0829

E-3

CT STUDY TEST: 4083 DATE: 30MAR00 SUBJ: B-23 CELL: C

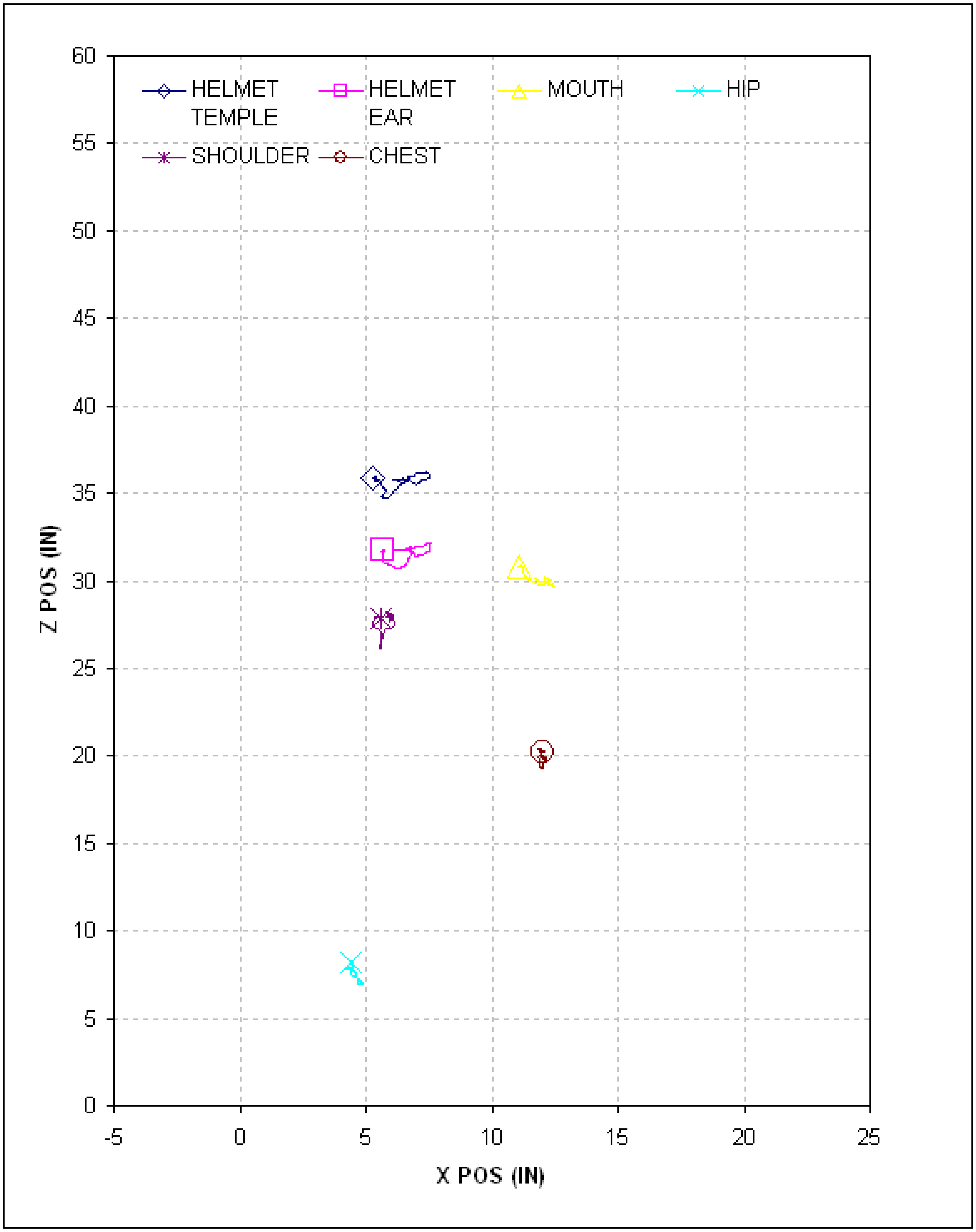

E-4

CT STUDY TEST: 4083 DATE: 30MAR00 SUBJ: B-23 CELL: C

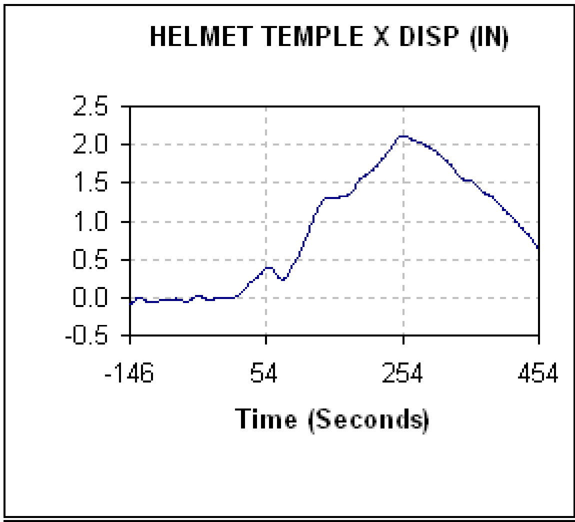

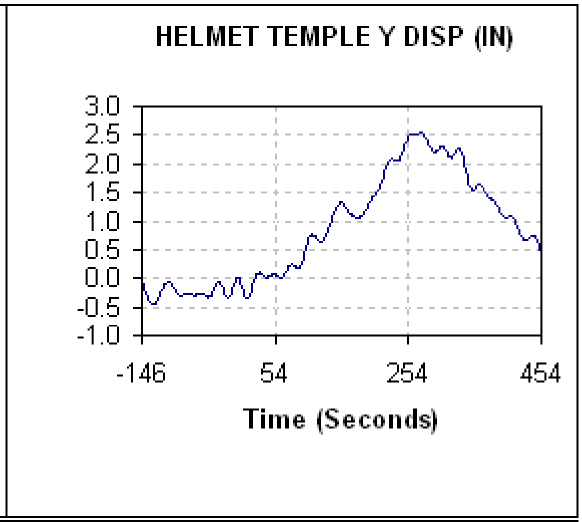

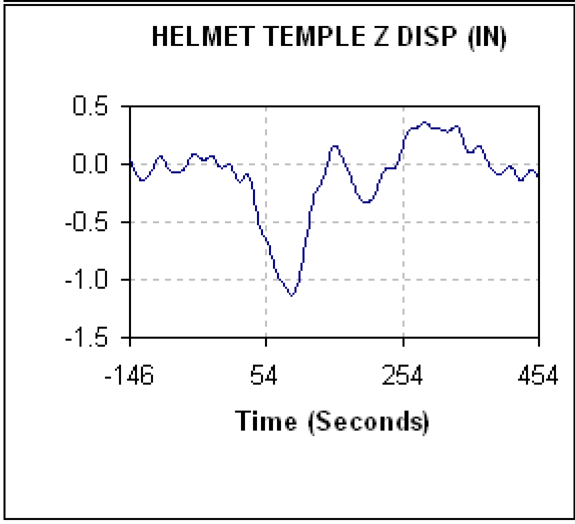

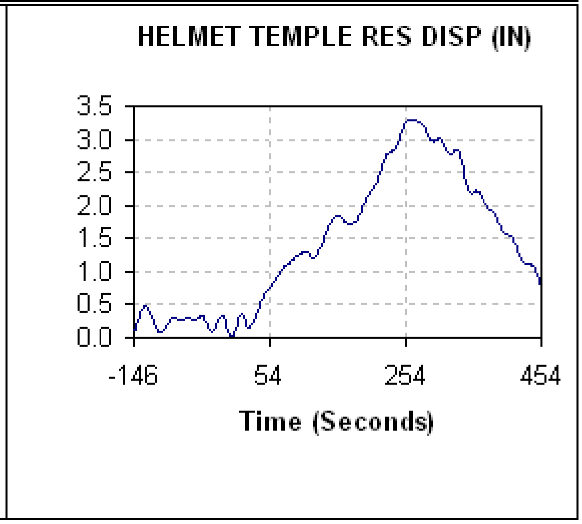

E-5

CT STUDY TEST: 4083 DATE: 30MAR00 SUBJ: B-23 CELL: C

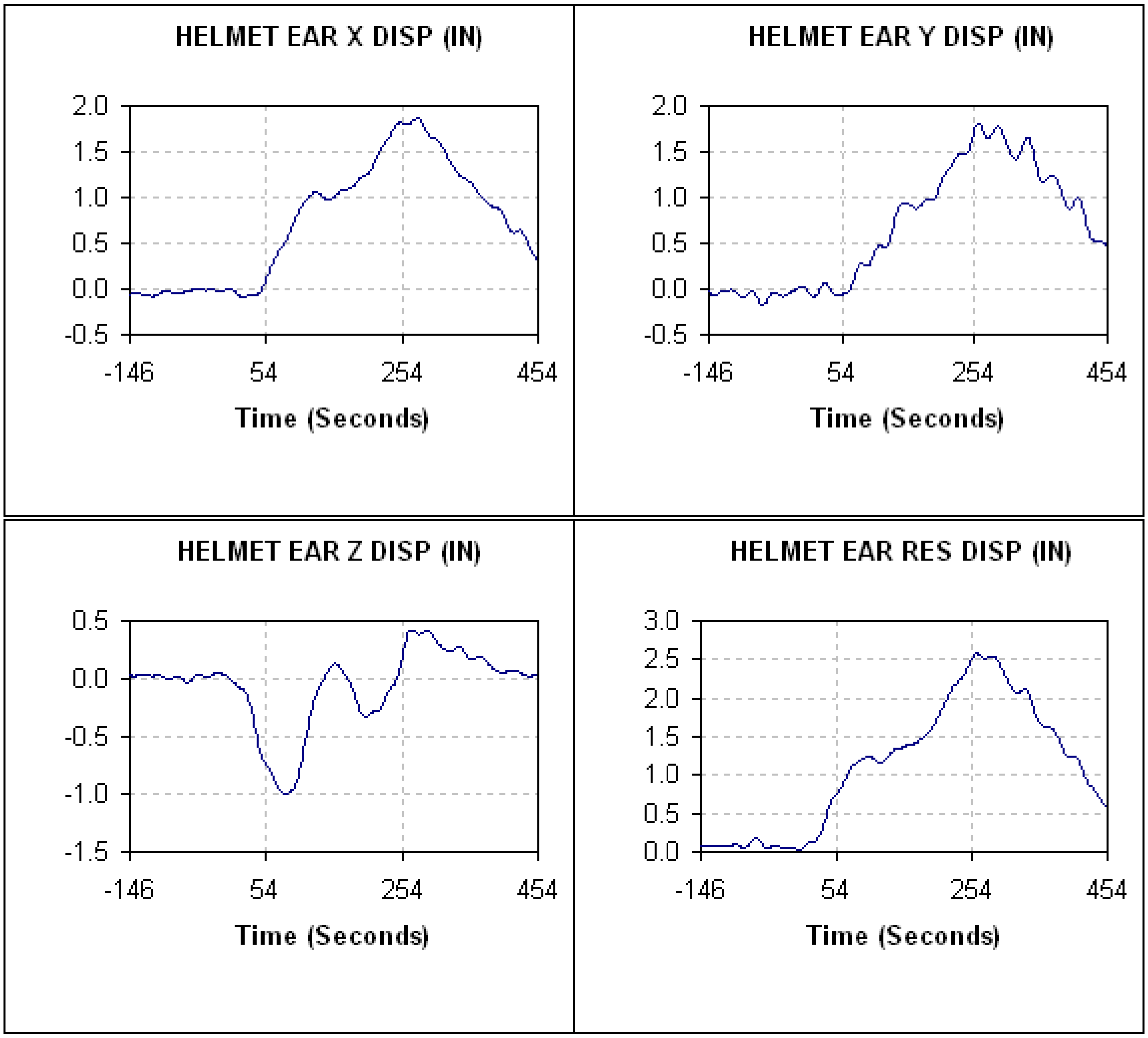

E-6

CT STUDY TEST: 4083 DATE: 30MAR00 SUBJ: B-23 CELL: C

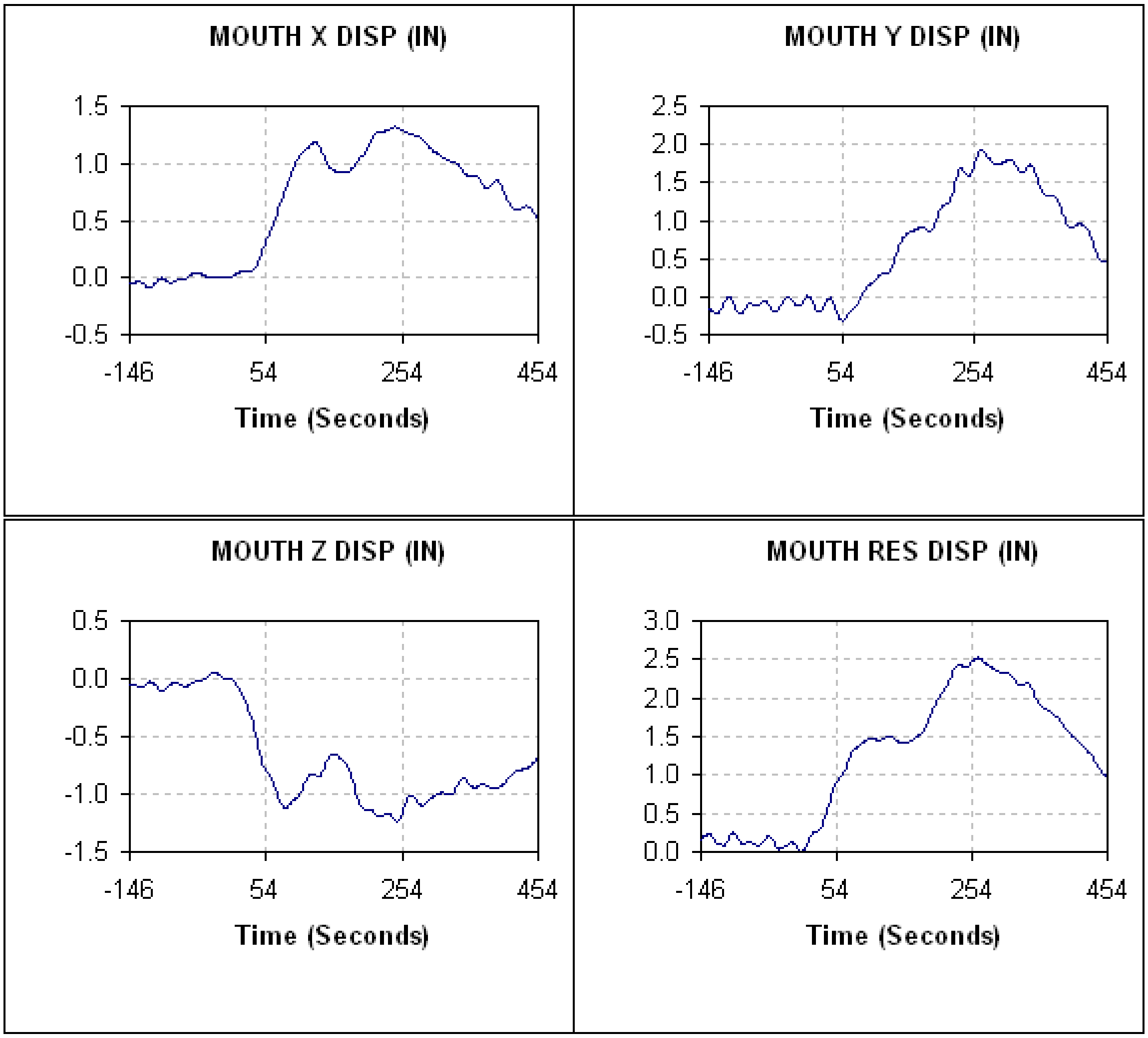

E-7

CT STUDY TEST: 4083 DATE: 30MAR00 SUBJ: B-23 CELL: C

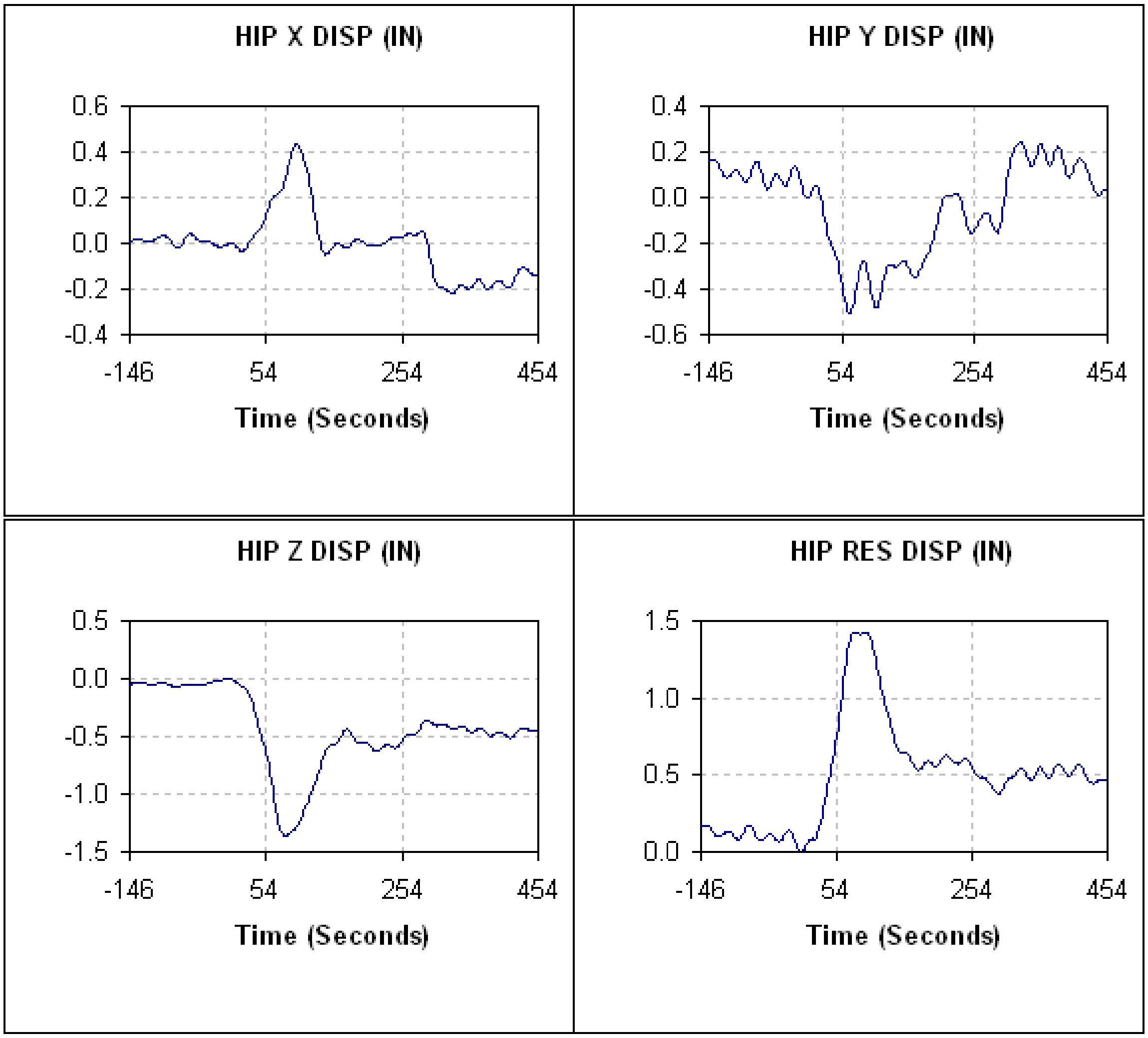

CT STUDY TEST: 4083 DATE: 30MAR00 SUBJ: B-23 CELL: C

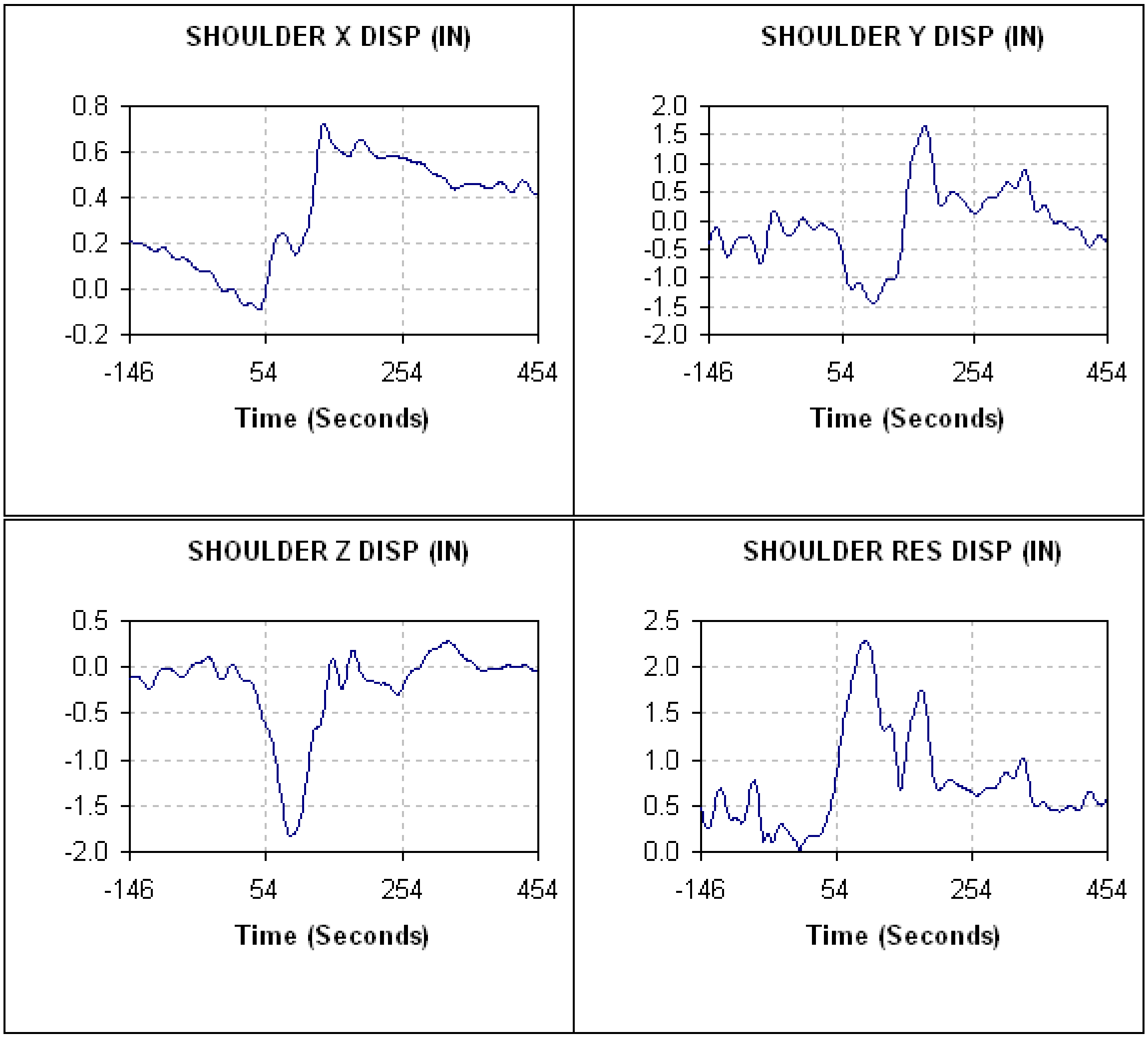

E-9

CT STUDY TEST: 4083 DATE: 30MAR00 SUBJ: B-23 CELL: C

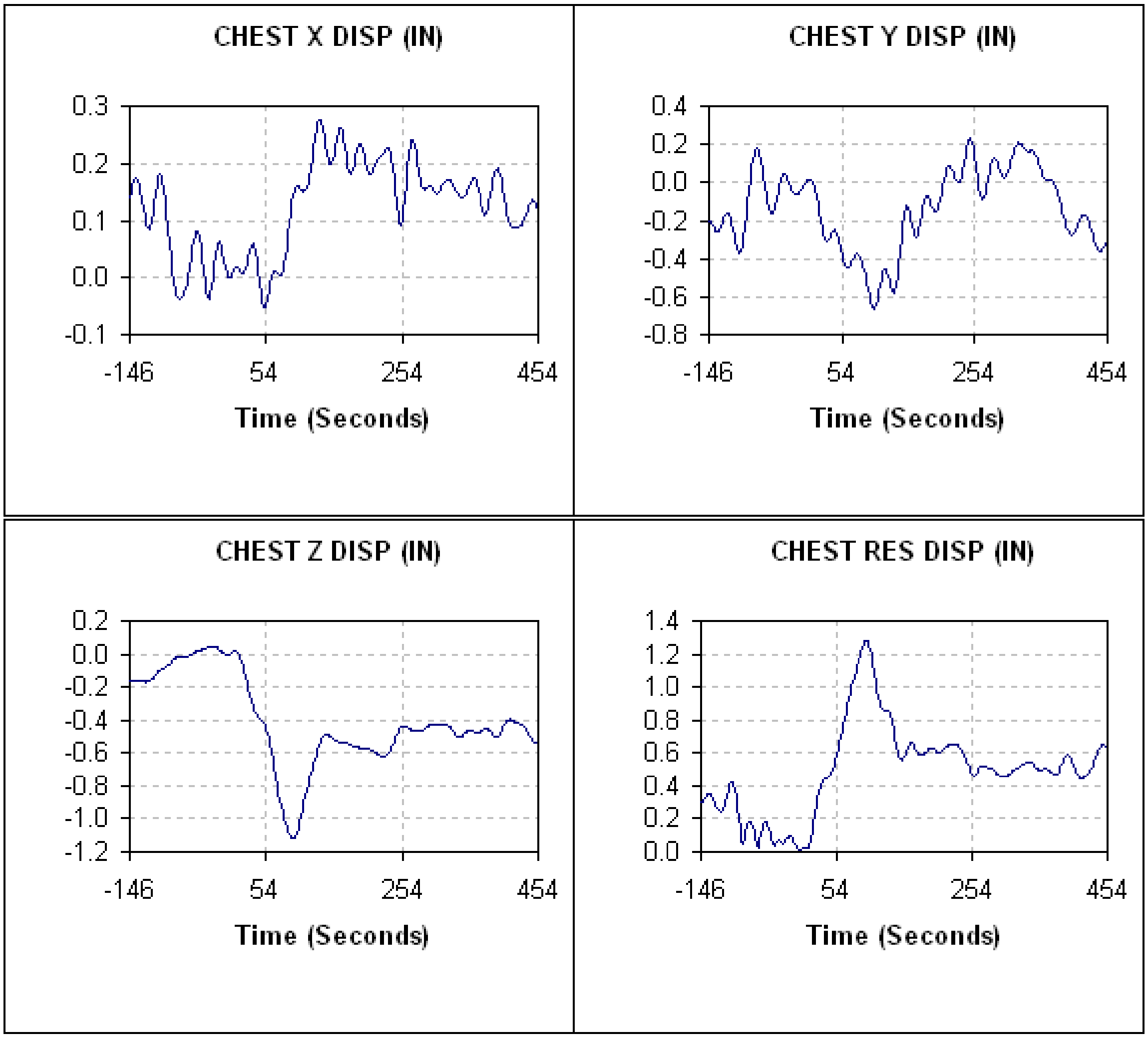

CT STUDY TEST: 4083 DATE: 30MAR00 SUBJ: B-23 CELL: C

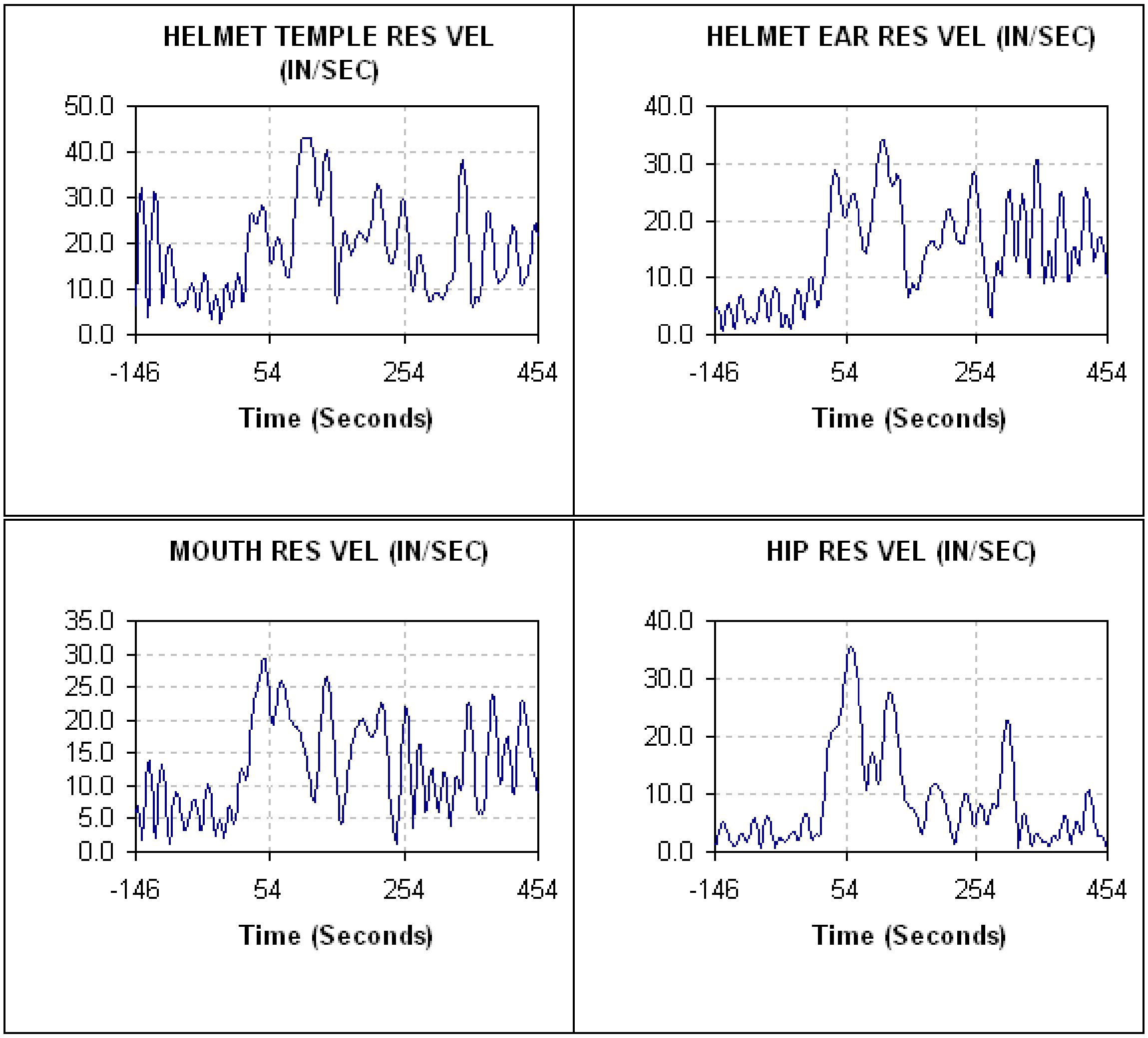

E-11

CT STUDY TEST: 4083 DATE: 30MAR00 SUBJ: B-23 CELL: C

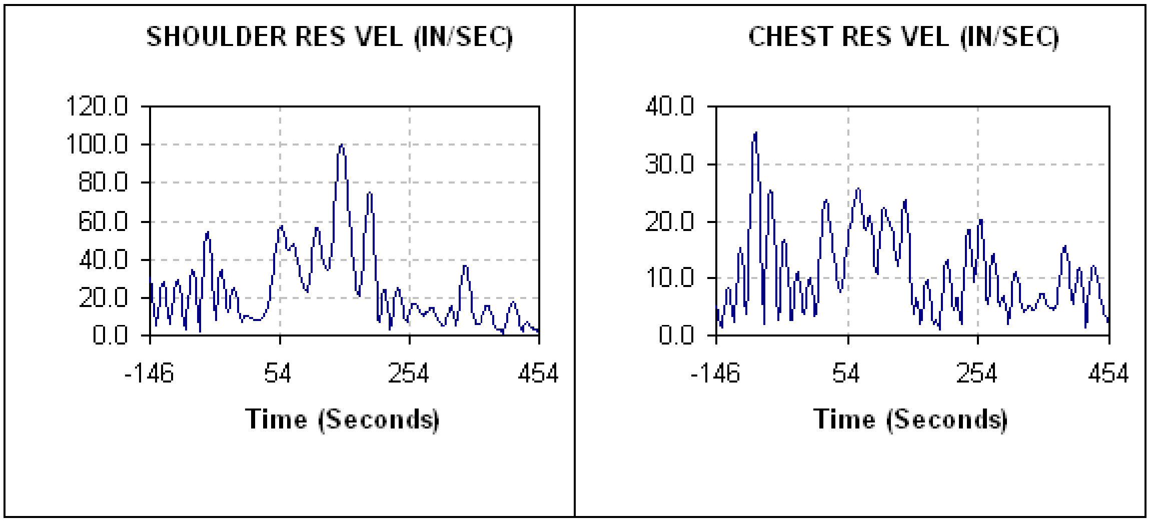

E-12